10-2019

EVALUATION OF A NEW APPROACH FOR QUALITATIVE GAS ANALYSIS BASED ON DIFFUSION PROPERTIES

Abdalla Jamal Muhammad Abunamous

United Arab Emirates University

College of Science

Department of Chemistry

EVALUATION OF A NEW APPROACH FOR QUALITATIVE GAS ANALYSIS BASED ON DIFFUSION PROPERTIES

Abdalla Jamal Muhammad Abunamous

This thesis is submitted in partial fulfillment of the requirements for the degree of Master of Science in Chemistry

Under the Supervision of Professor Sayed Marzouk

October 2019

Declaration of Original Work

I, Abdalla Jamal Muhammad Abunamous, the undersigned, a graduate student at the United Arab Emirates University (UAEU), and the author of this thesis entitled *"Evaluation of a New Approach for Qualitative Gas Analysis Based on Diffusion properties"*, hereby, solemnly declare that this thesis is my own original research work that has been done and prepared by me under the supervision of Professor Sayed Marzouk, in the College of Science at UAEU. This work has not previously been presented or published, or formed the basis for the award of any academic degree, diploma or a similar title at this or any other university. Any materials borrowed from other sources (whether published or unpublished) and relied upon or included in my thesis have been properly cited and acknowledged in accordance with appropriate academic conventions. I further declare that there is no potential conflict of interest with respect to the research, data collection, authorship, presentation and/or publication of this thesis.

Student's Signature: _____ Date: 6/2/2020

Approval of the Master Thesis

This Master Thesis is approved by the following Examining Committee Members:

1) Advisor (Committee Chair): Dr. Sayed Marzouk
   Title: Professor
   Department of Chemistry
   College of Science
   Signature Sayed Marzouk Date 9/10/2019

2) Member: Dr. Ahmed S. Alshamsi
   Title: Assistant Professor
   Department of Chemistry
   College of Science
   Signature _____ Date 9/10/2019

3) Member (External Examiner): Dr. Maguy Abi Jaoude
   Title: Assistant Professor
   Department of Chemistry
   Institution: Khalifa University
   Signature _____ Date 09/10/2019

This Master Thesis is accepted by:

Dean of the College of Science: Professor Ahmed Murad

Signature _____ Date 06/02/2020

Dean of the College of Graduate Studies: Professor Ali H. Al-Marzouqi

Signature _____ Date 06/2/2020

Copy 1 of 3

Advisory Committee

1) Advisor: Sayed Marzouk

Title: Professor

Department of Chemistry

College of Science

2) Co-advisor: Mohamed H. Al-Marzouqi

Title: Professor

Department of Chemical and Petroleum Engineering

College of Engineering

3) Co-advisor: Muna Al Falasi

Title: Associate Professor

Department of Chemistry

College of Science

Abstract

The design and construction of a 6-channel parallel gas diffusion system and its application to evaluate the proposed novel approach for gas fingerprinting are described. The present gas diffusion system allows the simultaneous recording of the pressure accumulation of the permeating test gas behind six different gas permeable membranes, respectively. The obtained simultaneous diffusion rates through different membranes demonstrated clear potential as a new technique for qualitative gas identification of the ten test gases used in the present work. The test gases were helium, neon, argon hydrogen, nitrogen, carbon dioxide, methane, ethane, propane, and ethylene, which are representative examples of mono-, di-, tri- and polyatomic gases. The utilized membranes included Teflon AF, Silicone Rubber, track-etch hydrophilic polycarbonate, track-etch hydrophobic polycarbonate, track-etch polyimide, nano-porous anodic alumina, Zeolite ZSM-5, and Zeolite Nay. Preliminary investigation of the possibility of applying the developed gas diffusion system in semi-quantitative analysis of N_2-CO_2 binary mixture is also reported. Finally, the proposed analogy between the rate of pressure accumulation of the permeating gas into the confined space behind the membrane and the charging of a capacitor in an RC circuit is thoroughly validated both theoretically and experimentally.

Keywords: Gas diffusion system, Gas permeable membranes, Qualitative gas fingerprint, Membrane

Title and Abstract (in Arabic)

تقييم طريقة جديدة للتحليل النوعي للغازات بالاعتماد على خصائص الانتشار

الملخص

تم تصميم ووصف تصنيع نظام لقياس سرعة انتشار الغازات وهو ذو ستة قنوات متوازية وكذلك تطبيقه في تقويم تقنية جديدة تم اقتراحها للحصول على بصمة مميزة لكل غاز تستخدم في التحديد النوعي. يسمح نظام انتشار الغازات بالتسجيل المتزامن لتراكم ضغط عينة غاز الاختبار المتغلغل خلف ستة أغشية. أظهرت معدلات الانتشار المتزامنة التي تم الحصول عليها من خلال أغشية مختلفة بوضوح امكانية استخدام هذه الطريقة الجديدة في التحديد النوعي للغازات التي تم استخدامها. واشتملت قائمة غازات الاختبار المستخدمة في هذا البحث على غازات الهيليوم والنيون والأرجون والهيدروجين والنيتروجين وثاني أكسيد الكربون والميثان والإيثان والبروبان والإيثيلين وهي أمثلة للغازات الأحادية والثنائية والثلاثية ومتعددة الذرات. واشتملت الأغشية المستخدمة على التيفلون إيه أف ومطاط السيليكون والبولي كاربونات المحب للماء والبولي كاربونات الكاره للماء والبولي أميد والألومينا الأنودية ذات المسامية النانومترية والزيوليت ZSM-5 والزيوليت ناي. هذا وتم وصف استخدام النظام الذي تم استحداثه في تجارب أولية للتحليل شبه الكمي لمخاليط ثنائية من غازي ثاني أكسيد الكربون والنيتروجين. كذلك تم التحقق بشكل كامل من الناحية النظرية والمعملية للاقتراح الذي تم استحداثه أثناء هذه الدراسة بخصوص التناظر بين معدل تراكم ضغط الغاز المتغلغل في الحجم المحصور خلف غشاء الانتشار وشحن المكثف في الدوائر الكهربية التي تحتوي علي مكثف كهربائي ومقاومة كهربية والمعروفة بدوائر الـ RC.

مفاهيم البحث الرئيسية: نظام قياس انتشار الغاز، أغشية الغاز القابلة للنفاذ، بصمة الغاز النوعية، تناظر مقاومة الأغشية المنفذة والمقاومة الكهربية.

Acknowledgements

To commence with, I pay my obeisance to Allah, the almighty to have bestowed upon me good health, courage, inspiration, zeal and the light. After Allah, I express my sincere and deepest gratitude to my supervisor Dr. Sayed Marzouk, Professor. Department of Chemistry, United Arab Emirates University, from the core of my heart for his deep sense of gratitude, reverence, logical criticism, timely admiration, keen interest, constructive and invaluable suggestions in planning and execution of this research and in preparation of this manuscript. I deem myself fortunate to work under his guidance and for providing me conductive atmosphere for my research work.

I would be failing in my duty if I do not express my sincere thanks to my co-advisors Dr**.** Muna Al Falasi**,** Assistant Professor, Department of Chemistry, United Arab Emirates University, for her suggestions and moral support.

It is matter of diligence to convey my heartiest thanks to my co-advisors Dr. Mohamed H. Al-Marzouqi, Professor, Department of Engineering, United Arab Emirates University, for his valuable suggestions and moral support.

I also thankful my committee for their guidance, support, and assistance throughout my preparation of this thesis, I would like to express my special thanks to my academic advisor Prof. Abbas Khalil. It is a pleasure as well to thank all members of the Chemistry Department at the United Arab Emirates University for assisting me all over my studies and research.

I am very much thankful to my lab-mates for their all-time cooperation in the laboratory. And my all research mates for providing me cooperation throughout my research work.

Last but not the least, I would like to grab this opportunity to express my deep sense of gratitude to my Family Members for their love, constant inspiration and encouragement, without their cooperation I would never been successful in achieving this goal.

Dedication

To my beloved parents, who taught me the value of hard work

Table of Contents

List of Tables

List of Figures

List of Abbreviations

8-CH DAQ	8-Channel Data Acquisition Card
A_m	Active Area of Membranes
C_m	Volume Behind Membranes
CNC	Computer Numerical Control
MFC-4	4-Channel Computer Controlled Gas Mixer
NBR O-ring	Nitrile Rubber
P_m	Pressure Behind Membranes
R_m	Membranes Resistance
SS	Stainless Steel
NPT thread	National Pipe Taper
MFC	Mass Flow Controller
P_i	Initial Pressure
σ_m	Resistivity of Membranes
τ_m	Time Constant For Membranes

Chapter 1: Introduction

1.1 Overview

1.1.1 Membrane definition

Membrane is defined as a barrier material between two phases and it allows some components to diffuse through it according to some properties. Figure 1 shows the fundamentals of membranes. Moreover, the definition of membrane can also fit with "conventional filter", however thefilter is limited to separate particulate suspensions within 1-10 μm [1, 2].

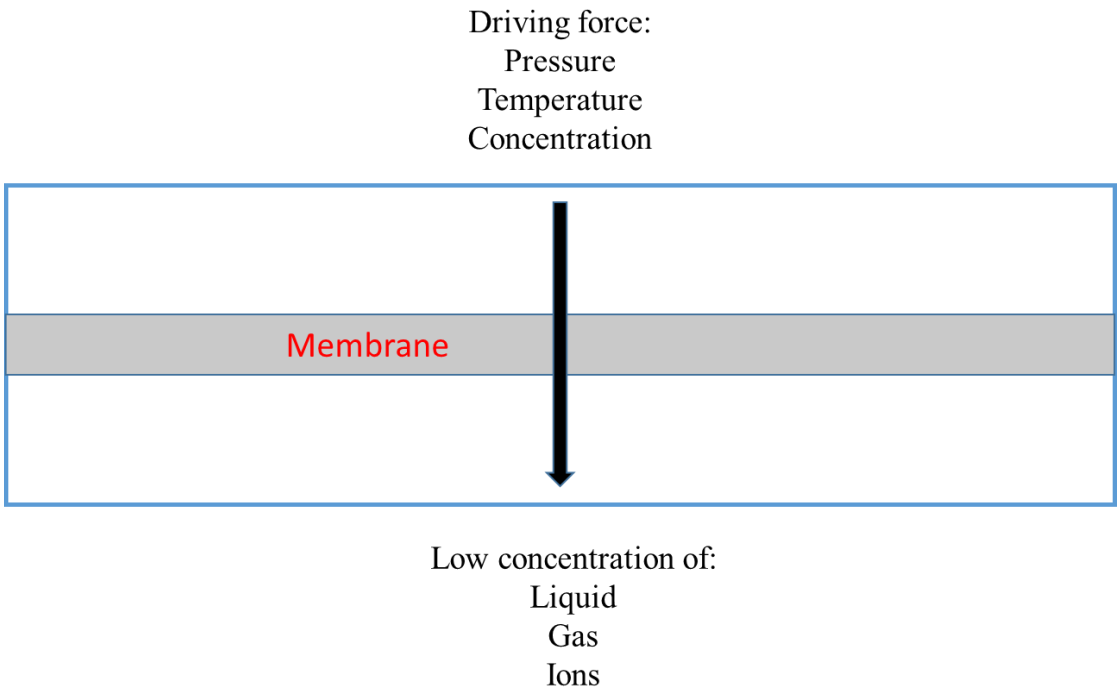

Figure 1: Fundamental of membrane processes

Nowadays, membranes based on different material types found different novel applications. So, membranes can be classified based on different points such as nature and material, structure and morphology, geometry and configuration, etc. Literature review will spot the light on classification according to natural and material.

1.2 Purpose of this work

The present work aims at testing the hypothesis of measuring simultaneously gas diffusion rates through different multiple membranes as a new method for gas identification. To achieve this main aim, the following milestones are rationalized: (i) Design of 6-chanell parallel gas diffusion system, (ii) custom fabrication of the 6-channel gas diffusion system, (iii) construction of the complete experimental setup which also contains gas cylinders, controllers, and data acquisition, (iv) Characterization of the gas diffusion system using nitrogen as a test gas and one permeable gas membrane, (v) selecting a total of 10 different test gases, (vi) selecting and testing several gas permeable membranes for their ability to show somehow different gas permeation rates for the test gases, (vi) testing the simultaneous permeation rates of the each of the test gas through the selected membranes, (vii) comparing the obtained diffusion patterns for all test gases to prove the hypothesis. As a secondary aim of this work, the potential of the gas diffusion system to achieve semi-quantitative analysis of binary gas mixtures will be attempted.

1.3 Relevant literature

1.3.1 Classification of membranes based on natural and material

Materials that used to fabricate membranes depend on several things like separation task, structure, operating condition, coast of material, and the chemical stability. Normally, membrane materials can be divided into natural, synthetic, and biological.

1.3.1.1 Biological and natural membranes

Biological membranes can be easily fabricated, but at the same time it has some limitations as such as small temperature and pH range, and problems with cleaning [3]. While natural membranes can be living membranes or non-living membranes. Living membranes as skin of all mammals is an efficient and high selective membranes that can control release sweat to cool down the temperature of bodies. Lungs are other example of efficient membranes because within the lungs there are small cells that allow passage oxygen from the air to the body and release carbon dioxide in the same stream, and in the same time prevent the nitrogen gas to enter the body regardless of the concentration of it. While, non-living membranes such as in old agriculture communities invented and developed household sieves to separate fin grain from coarse grain and shells. Cheesecloth which made from cotton fiber can be considered as membrane to separate milk from its butter and to make chees [1]. Recently, many researchers around the world interested in fabricating and synthesizing membranes, so the synthetic membranes become very wide field, which will be focused on in the next section.

1.3.1.2 Synthetic membranes

Synthesized membranes can be divide into inorganic, organic, hybrid membranes, and others like polymeric membranes. The application of polymeric organic membranes are restricted in low temperature and not useful to separate chemically inert materials. Inorganic, organic, and hybrid membranes will be briefly reviewed.

1.3.1.2.1 Inorganic membranes

Ceramics, aluminum, palladium, fiber-reinforced carbon, and high-grade steel are examples of inorganic membranes, which are highly recommended for high temperature and separate an active mixture. Inorganic membranes offer some advantages over other membranes, these include:

1. Pore sizes are well defined
2. High heat resistance, as an example ceramic membranes can resist until 350°C
3. Chemically resistant; they are unreactive toward chemical solutions except HF and H_3PO_4
4. Very stable in within wide range of pH, such as ceramic within 1-13 are stable
5. Not affected by biological degradation or microbial attack
6. Exhibit high erosion resistance and exhibit catalytic activities

Generally, inorganic membranes can be classified into ceramic, zeolite, and metallicmembranes. Where the ceramic membranes can be defined as: unbalanced or asymmetric porous made on the support material. These pores can be classified according to International Union of Pure and Applied Chemistry (IUPAC) as: Macropores (> 50

nm), Mesopores (2 to 50 nm), Micropores (<2 nm). On the other hand, inorganic membranes have disadvantages as well such as:

1. Very difficult to get a reproducible product quality
2. It's very brittle materials
3. Much heavier than polymeric membranes [4]

1.3.1.2.2 Organic membranes

Organic membranes are usually based on polymeric materials. There are various types of polymers available around the world, which make the life much easier to select the suitable polymer to solve a given separation problem. Organic membranes can be categorized into Polyamide (PA), cellulosic polymers, Polysulfone (PS), hydrocarbon-based polymers, Fluoropolymers, and Polycarbonates.

The first type of organic membranes is Polyamide (PA) membranes, and from its name the main function group in this membranes is amide group. This type of membranes can be prepared by condensation of dicarboxylic acids with polyamines as shown in Figure 2.

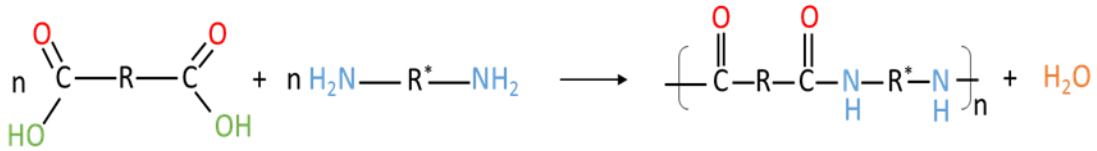

Figure 2: Condensation of dicarboxylic acids with polyamines to produce Polyamide membranes

Additionally, PA membranes can be exist as aliphatic chain which is called as "nylon class" such as nylon 6, 6; nylon 6; and nylon 6, 12. Or it can exist as semi-aromatic chain

and can called “Aramid” where Polyphthalamide is an example of it. However, a semi-aromatic PA membranes are much preferred in wide application due to their chemical, physical and thermal stability with solvents. Also, they have good fatigue and abrasion resistances, but they can be affected with extreme high or low pH condition. These membranes can be used in solvents filtration due to their low porosity. Aliphatic and semi-aromatic PAs can be used as the base polymers for microfiltration membranes.

The second type of organic membranes are those formed from polysaccharides under one condition which is the molecular weight should be up to 1,500,000 g/mole, and in this case these membranes called cellulosic membranes. This type of membranes could be from esters like cellulose nitrate and cellulose acetate, or from ethers such as ethyl cellulose. Wood and cotton are the main source to extracted cellulose. By chemically modified of cellulose, cellulose acetate can be produced. The main propriety of these membranes is hydrophilic structure which make them a suitable for microfiltration and ultrafiltration. Also, it can used for biopharmaceutical processes because it has a low adsorption capability. It is necessary to enhance the chemical stability of these membranes to be suitable for use under high pH condition.

Polyethersulfone (PES) and Polysulfone (PS) are examples of a new type of organic membranes called Polysulfone Which has amorphous structure. PSs membranes are the broadest one with highly porosity and can be symmetric, asymmetric, or a combination of both and it can used for nanofiltration, microfiltration, and ultrafiltration and can be used as the basic support for composite membranes. It shows an excellent thermal stability and high resistance toward ionizing irradiation and hydrolysis over all pH values. Moreover,

it can dissolved in polar solvents like dimethylformamide and dimethyl sulfoxide due to similarity in the polarity between the membranes and these solvents.

Other type of organic membranes that can be formed from polymerization of vinyl monomers such as ethane and propylene to produce polyethylene and polypropylene, respectively called Hydrocarbon-based polymers membranes. Normally, these membranes are rigid and tough membranes. Also, the porosity of these membranes are low and considered as symmetric structural. It can be categorized according the position of R group into:

1. Isotactic: are those with all of the R groups on the same side of the carbon chain
2. Atactic: where R group in randomly distribute around the carbon chain
3. Syndiotactic: the R group regularly distribute in both side of carbon chain [3]

Moreover, Fluoropolymer membranes are those membranes had a carbon and florin atom in the structure [5]. These membranes show very good flow rate due to high porosity and it can be used in the membrane technology. Polytetrafluorethylene (PTFE) is the most famous example of these membranes. PTFE is very thermal stable which can be used up to 260 °C. It is very useful for chemicals and air filtration because it is extreme hydrophobic structural. Also, PTFE chemically compatible with all known solvents.

Polycarbonates membranes referred to the polymer that has the carbonate group in the chain. And the most common example of this polymer is bisphenol A polycarbonate. It can used in many application like in greenhouse, automobile headlights, and others. The characteristic of this material include:

1- Considered as very tough material
2- Amorphous structural
3- transparent
4- Low price
5- Low porosity [3, 6, 7]

1.3.1.2.3 Hybrid membranes

Furthermore, hybrid membranes or called composite membranes which containing different types of materials like combination of polymeric and inorganic material. This type of membranes can work as separating barrier when it coated on the porous support and it will allow certain substances to diffuse and penetrate through it, and by this combination it will have a new properties as the result of interaction between two different types of materials.

There are many other classification and categorization of the membranes, for example: Structure and morphology, geometry and configuration, etc. as mentioned previously. As a result of these varieties, there are several separation mechanism which will be discussed in the next section [3].

1.3.2 Mechanisms of gas permeation through membranes

A very famous physical process that describe the movement from high concentration of molecules to low concentration is called Diffusion process, and can happens for solutions, gases, or liquids. The molecules had various mechanisms to cross the membranes, and these mechanisms depend on the properties of the molecules that will

penetrate and the properties of membranes. Bulk poiseuille, Knudsen diffusion, surface diffusion, Gas translation, and a solid-state diffusion mechanism are examples of these mechanisms.

1.3.2.1 Bulk poiseuille

Bulk poiseuille occurs when the pore size is larger than mean free path (λ) of the molecules where mean free path given by:

$$\lambda = \frac{1}{\sqrt{2}\,\pi d^2\ N/V}$$

Where λ is mean free path, where d is the diameter of molecules, N is the number of molecules and V is the volume of the gas

1.3.2.2 Knudsen diffusion

The Second mechanism is Knudsen diffusion, which occurs when the pore diameter is smaller than free pathway of the molecule and in this scenario; the collision will happen between the molecules and the pore wall rather than collide between the gas molecules themself. This collision is elastic and negligible, so there is no chance to adsorption of gas molecule on the pore wall. Knudsen permeance (Ā) is given by:

$$\bar{A} = \frac{\varepsilon d_p}{\tau L}\left(\frac{8}{9\pi MRT}\right)^{1/2}$$

Where ε is the porosity of the membrane, d_p is pore diameter, L is the thickness of the membrane, τ the tortuosity, R the gas constant, T the absolute temperature M is the molecular weight of the diffusing gas.

1.3.2.3 Surface diffusion

At low temperature, surface diffusion mechanism will occur, in this mechanism, the kinetic energy of gas is smaller than interaction between gas molecule and inner surface, and due to that, the molecule cannot escape from surface potential field. More interesting thing in this mechanism is: the gas can be penetrated through the membranes by: adsorb molecules onto the surface of the membrane at the pore entrance, diffuse through the membrane, and desorb at the pore exit. Langmuir adsorption model describe this mechanism and the equation of it is:

$$\theta = \frac{q}{q_s}$$

Where θ is the fractional occupancy of adsorption sites, q is the amount of adsorbed gas molecules per unit mass of adsorbent [mol・kg-1], q_s the saturation amount of adsorbed molecules [mol・kg-1].

1.3.2.4 Activated knudsen diffusion

Forth mechanism can called: activated Knudsen diffusion model or gas-translational model, and this name came from combination of two mechanisms: Knudsen diffusion model and the surface diffusion model together. In this mechanism, molecules have enough kinetic energy to escape from surface potential, but does not happen because pore wall will present in other side, and this mechanism used with different material such as zeolite membranes and Vycor glass.

$$\bar{A} = \frac{\varepsilon d_p \rho_g}{\tau L} \left(\frac{8}{\pi MRT}\right)^{1/2} exp\left(-\frac{\Delta E}{RT}\right)$$

Where ε is the porosity of the membrane, d_p pore diameter, τ the tortuosity, R the gas constant, T the absolute temperature M is the molecular weight of the diffusing gas, L is the thickness of the membrane, ΔE kinetic energy.

1.3.2.5 Solid-state diffusion

With more decrease in pore size of membranes, the gas molecules will interact strongly with membranes material, and in this cause the solubility need to be considered. And this is the fifth mechanism called "Solid-state diffusion" where the permeability = solubility × diffusivity. Add to that, glassy membranes, metallic membranes, and polymeric membranes mechanisms are three different causes belong to Solid-state diffusion [8, 9]. All mechanisms that discussed previous are shown in Figure 3.

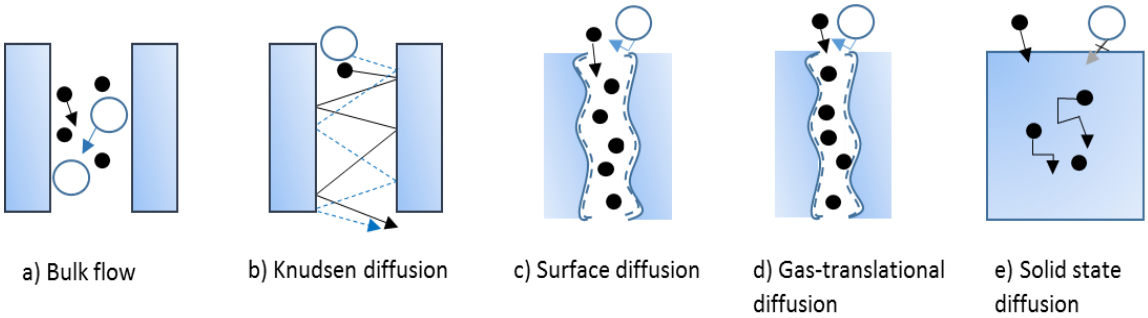

Figure 3: Various Gas Separation Mechanisms

1.4 Membranes used in the present work

1.4.1 Teflon AF

Teflon Amorphous Fluoropolymers (AF) is one type of amorphous glassy copolymers, which has high fractional free volume (FFV) as shown in Figure 4. It consist of two different types of polymer which were tetrafluoroethylene (TFE) and 2,2-bistrifluoromethyl-4,5-difluoro-1,3 dioxole (BDD). DuPont produce two types of Teflon AF by changing the ratios of the copolymer to give Teflon AF 2400 with ratio TFE: 13 mol%; BDD: 87 mol%, and Teflon AF 1600 with ratio TFE: 35 mol%; BDD: 65 mol%.

Where chemical structural of Teflon AF shown in Figure 4 and some physical properties of Teflon AF are shown in Table 1.

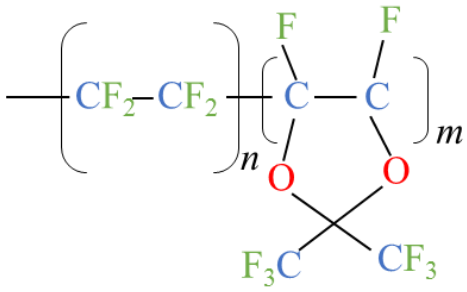

Figure 4: Structural of Teflon AF

Table 1: Some general properties of Teflon AF

Property	**Teflon AF 2400**	**Teflon AF 1600**
Crystallinity	None	None
M_w (kDa)	300	100
T_g (°C)	240 ± 10	160 ± 10
Density (g/cm^3)	1.75	1.82
Fractional Free volume FFV (%)	33.4	30.0
Refractive index	1.29	1.31
Dielectric constant	1.90	1.93
Contact angle with water (°)	105	104
Permeability O_2 (barrer)	1140	170

Gases can diffuse through Teflon AFs by solid-state diffusion mechanism [1]. However, Teflon AF 2400 and Teflon AF 1600 membranes have similar behavior of low free volume glassy polymers (e.g., polysulfone, polycarbonate, etc) which is size sieving. Which means the permeability decreases as the molecular size of the gas molecule increases. Moreover, Teflon AF 1600 is less permeable to gases because it has a lower free volume [10, 11].

The permeability coefficients of helium, hydrogen, carbon dioxide, oxygen, nitrogen, methane, ethane and propane for solution-cast Teflon AF 2400 films are presented in Table 2 [12] which shows the highest permeability to CO_2. Due to excellent thermal, chemical and electrical properties of Teflon AF, it has been used in several applications such as: it used in electronic chip manufacturing to produce deep UV pellicles. Teflon AF can used as inter-layer dielectrics because it has low dielectric constant and poor water absorption. Add to that, the low refraction index of Teflon AF make it excellent material for optical lenses and protective coatings [13].

Table 2: Pure gas permeabilities of Teflon AF 2400 (20 µm thick) at 25°C and a feed pressure of 50 psig

Gas	**Permeability coefficient $\times 10^{10}$ (cm^3 (STP)cm/cm^2 s cmHg**
CO_2	3900
He	3600
H_2	3400
O_2	1600
N_2	780
CH_4	600
C_2H_6	370
C_3H_8	200

1.4.2 Silicone rubber

In 1901, Kipping named a new compound with general formula R_2SiO by silicone. This compound composed of silicon linked with carbon, and oxygen. It is an elastomer material (rubber-like material). Actually Silicone rubber corresponding to polydialkylsiloxanes, with the following general chemical formula in Figure 5.

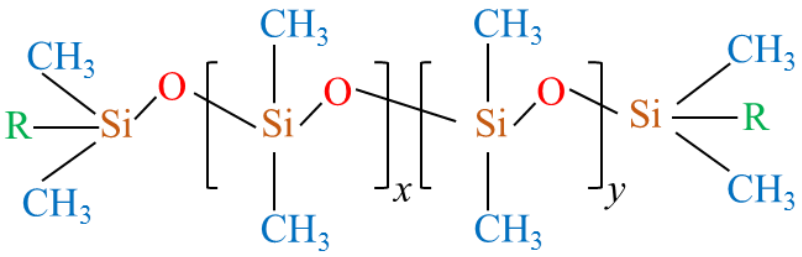

Figure 5: Chemical structure of polydialkylsiloxanes. R = methyl, phenyl, vinyl or trifluoropropyl

The Si–O bond in Silicone Rubber has significantly higher energy than C–C bond in organic compounds, due to that silicones have high thermo oxidation and remarkable thermal resistance. Also, silicones far less readily attacked by radiation (i.e., γ rays and UV radiation and α and β particles) than organic plastics.

There are some general properties of Silicone Rubber membranes, which are: Heat resistance where Silicone Rubber withstands use for over 10,000 consecutive hours even at 200°C and excellent resistance to cold temperatures to -60°C to -70°C. Furthermore, the tear strength of silicone was generally around 9.8 kN/m. Add to that, Compared to organic rubber or plastic films, thin films of silicone rubber have better gas and vapor permeability and selectivity [14] [15]. The permeability, diffusion, and solubility of different gases throughout of silicon rubber shown in Tables 3 and 4 [16].

Table 3: Gas permeabilities in dimethyl-silicone

Gas	$\mathbf{Pr\times\ 10^{10}}\ \frac{cc\ gas\ (RTP)cm}{sec, sq\ cm, cm\ Hg\ \Delta p}$	Gas	$\mathbf{Pr\times\ 10^{10}}\ \frac{cc\ gas\ (RTP)cm}{sec, sq\ cm, cm\ Hg\ \Delta p}$
H_2	65	C_2H_4	135
He	35	C_2H_8	2640
NH_3	590	C_3H_8	410
H_2O	3600	n-C_4H_{10}	900
CO	34	n-C_5H_{12}	2000
N_2	28	n-C_6H_{14}	940
NO	60	n-C_8H_{18}	860
O_2	60	n-$C_{10}H_{22}$	430
H_2S	1000	HCHO	1110
Ar	60	CH_3OH	1390
CO_2	325	$COCl_2$	1500
N_2O	435	Aceton	586
NO_2	760	Pyridine	1910
SO_2	1500	Benzen	1080
CS_2	9000	Phenol	2100
CH_4	95	Toulen	913
C_2H_6	250		

Table 4: Solubility and diffusion coefficients of gases in silicone rubber

Gas	$\mathbf{Pr\times 10^9}$	$D\times\ 10^6\ \frac{cm^2}{sec}$	S $\left[\frac{cc(RTP)}{CC,atm}\right]$
He	35.5	60	0.045
H_2	66	43	0.12
CH_4	94	12.7	0.57
N_2	28.7	15	0.15
O_2	62	16	0.31
Ar	61.3	14	0.33
CO_2	323	11	2.2
C_4H_{10}	~1000	~5	15

As shown in previous Tables, oxygen, methane, nitrogen, and carbon dioxide have close diffusivity values and they are significantly different in permeability. Also, Silicone Rubber has high permeability of Oxygen and Carbon dioxide.

Silicone Rubber used widely in medical application that required high permeability of Oxygen and Carbon dioxide such as: blood oxygenator membrane, and underlying corneal tissues. Furthermore, it can used for heart pacemakers, blood pumps, drug delivery devices, and artificial skin [17]. Moreover, Silicone Rubber can used in industrial field as an example: automobiles, in building and construction, electronics, and now a days used it in aerospace [18].

1.4.3 Track etched membranes

Track etched membranes had other name which is ion track membranes, these membranes can produced by hitting or irradiation of thin film by heavy ions and after that this film will chemically etching. It became procures of nanotechnology in 1990s. In recent years, due to pore structural and narrow pore size distribution make this membranes attractive for some applications in different fields such as: water purification, biological and biochemical sensors, and filtration of medical injections [19, 20]. There are several different types of Track etched membranes. Polycarbonate (PC), polyester (PET), and polyimide (PI) are the types that used in this work [21].

1.4.3.1 Polycarbonate (PC)

Polycarbonate (PC) received that name because it have carbonate group in the polymer. The most popular one in the economical field is 2,2-bis(4-hydroxyphenyl)propane polycarbonate or it can named bisphenol A polycarbonate (BPA-PC) with structural shown in Figure 6.

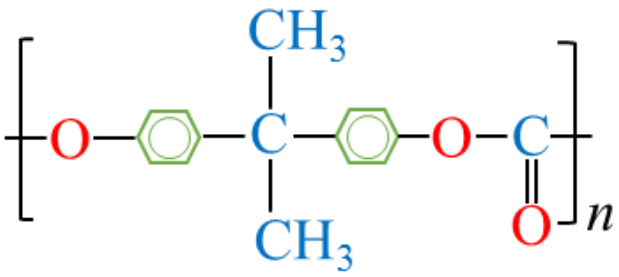

Figure 6: bisphenol A polycarbonate (BPA-PC) structural

There are some interesting proprieties of this polymer which are: it is not dissolve in water or alcohol, but it totally soluble in hydrocarbons. The T_g of it is 150°C which mean it has high heat resistance and it start to decomposed at 400°C. Add to that, this polymer are amorphous and high transparent and it is low flammability. This polymer can used in electrical sensor because it has previous properties and especially in power plugs, safety switches, components for electronic calculator. Moreover, because it transparent material it used in window panes and roofing. Also, due to heat and weather resistance, and high impact strength it can used in Automobile sensors. And there are several other applications such as: information storage, and medical application like sterilizable equipment [22].

1.4.3.2 Poly ester (PET)

When the polymer contains ester as a functional group in the chain, this polymer called poly ester. Polyester can prepared from reaction between dicarboxylic acids and diols. Even there are many different types of ester this term usually referred to polyethylene terephthalate (PET) and the structural of it shown in Figure 7 [23]. This polymer could be exist as amorphous or semi-crystalline. The semi-crystalline of PET has

some characteristics such as: opaque with white color, hardness, toughness, and good strength, while the amorphous one is less stiffness and hardness, and better ductility [24].

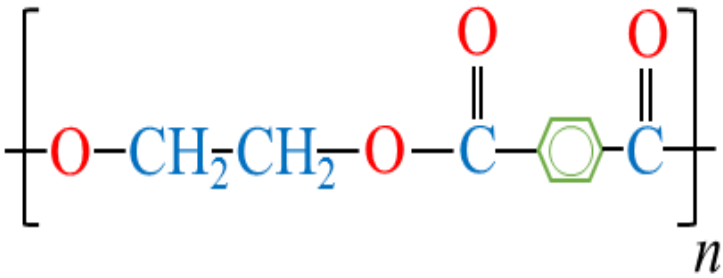

Figure 7: Structure of Polyester PET

Additionally, low moisture absorption, toughness, rigidity, insulate electricity, good mechanical strength, high viscosity, low thermal expansion, and it can be recycled by physical or chemical methods are properties of PET [25, 26]. Polyester polymers are extensively used around the world for different applications as an example of it: in automotive, electrical devices, medical, and used as membranes in different fields. Also, it can used in piping, and storage tanks, for food storage and other consumer products. Moreover, PET found in fire-retarding materials [23, 27].

1.4.3.3 Polyimide (PI)

The Third type is Polyimide (PI), from it is name this polymer can be classified as a hetro-chain polymer because it has an imide group on the chain. The general formula of polyimide was shown in Figure 8 [28]. The permeability and diffusion of different gases in polyimide are shown in Table 5 [29].

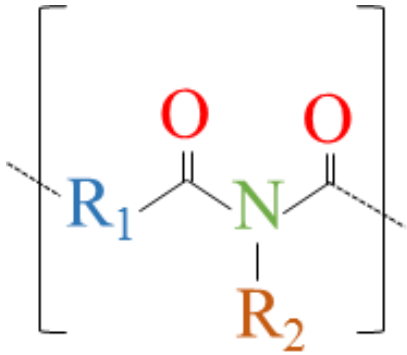

Figure 8: General formula of polyimide

Table 5: Permeability and diffusion of different gases in polyimide

Gases	$\mathbf{Pr\times\ 10^{18}}$ $\frac{m^3\ (STP).m}{m^2.sec.Pa}$	$D\times\ 10^{15}$ $\frac{m^2}{sec}$
H_2	38.4	-
He	44.4	-
CH_4	0.239	15.1
N_2	0.236	66.4
CO	0.490	85.7
C_2H_6	0.0382	0.423
O_2	1.88	396
Ar	0.450	93.1
CO_2	11.1	82.4
C_3H_8	0.00425	0.0736

Polyimide has an excellent and very interesting properties such as chemical and thermal stability, it considerate as a glass polymer where the T_g of most of PI could reach 300°C high permeability of CO_2, high CO_2/CH_4 selectivity, it separate any molecules base on size which called size-sieving, resistance of plasticization phenomena [30]. Furthermore, PI considered as insulator material due to the stability of this material, and from here the medical applications of PI rose for different devices and encapsulation

active implants, also it can used in nano-biosensor device [31]. PI can used in gases separation fields such as: used to separate N_2 and O_2 from Air, to separate hydrogen in ammonia plants, purification of water vapor from natural gas and other applications [32].

1.4.4 Zeolite membranes

When the robust crystalline three-dimensional network of silicate or alumina-silicate with uniform size and shape of pores exist, it will called zeolite. These pores give zeolites ability to separate molecules based of the size (molecules sieving), where the molecules with huge size (bigger than pores size) will exclude it [32-34]. The size of these pores between 0.3 nm to 1.3 nm. Most interesting thing in zeolites is: there are many different types of zeolite around the world, which could be more than 200 types. To make life easily, the International Zeolite Association classified zeolite to mainly three families which are: MFI, LTA and FAU. Zeolites ZSM-5 which used in this work are from MFI family [36].

The properties of zeolites are changing with increase the concentration of silica in the ratio of Si/Al in the framework, for example when the ratio of silica increase the thermal stability will increase from 700°C to 1300°C. Also, zeolites are hydrophilic with low concentration of silica and when it increase the zeolites will be hydrophobic. The cation concentration and ion exchange will decrease when the concentration of silica increase. Moreover, acidity strength of it will increase when the silica increase [36]. Now a days, zeolites have significant application, such as: in the medical field it used it for kidney dialysis machine to prevent ammonia buildup in the body because zeolite can absorb it, it can absorb oxygen from the air with high purity could reach 95% which can

used it for patients whom suffering from emphysema. Zeolite can be used in the agriculture to prove plants with K^+ and NH_4^+ from soil and that will be very useful in long space missions in future. Approximately 500,000 tons of zeolite used to cleaning up the nuclear waste as in Chernobyl. It can used it to separate mixture of linear Alkane and branched Alkane when they pass throw column filled with zeolite. Moreover, zeolite can used as drying agent to separate water from other solvents [38, 39].

1.4.5 Alumina membranes

Inorganic membranes have many advantages over other membranes as mentioned previously [3]. One of the very famous and useful inorganic membrane is Anodic Aluminum Oxide (AAO). At room temperature and normal atmosphere Al metal react with oxygen (present in the air) to form very thin oxide film with thickness 1-2 nm. This thin layer will protect the metal from react with oxygen more and more, but this thick is not enough for traditional application. While thicker layer of oxide could reach it by anodizing process. Anodizing is an electric process where the Al will be anode and the carbon rod will be cathode in the suitable electrolyte such as sodium and ammonium chloride solution. In this situation, the thick layer of Alumina oxide will formed in the surface of Al [40].

AAO is a porous structural. These porous are uniformly distributed, parallel and perpendicular to the surface. Additionally, AAO are very stable at high temperature and in organic solvent. More interesting, the hardness of these membranes will increase with increasing the temperature [41]. The permeability of various gases in AAO are shown in Table 6 [42].

Table 6: Permeability for different gases at 295 K

Gases	$\frac{\text{Premeability (STP) cm}^3\text{. cm}}{\text{cm}^2\text{. s. Pa}}$
H_2	4.4
He	4.9
N_2	4.6
CO_2	4.1
CO	5.0
C_2H_6	4.2
C_3H_8	4.1

There are many applications that can used AAO such as: sodium ion batteries, super capacitors, water splitting by photo electrochemical, water treatment, cleaning pharmaceutical equipment. Also, it can use it in the medical field for drug delivery in intravascular, cultivating liver culture. In sensors field such as humidity sensors are other application of AAO [40, 43, 44].

1.5 Gas analysis techniques

Now days, there are many techniques available for gas analysis such as infrared spectroscope (IR), gas chromatograph (GC), mass spectroscope, NMR and others. These techniques can used for qualitative and quantitative analysis. This section spot the light on some of these techniques which are: Infrared (IR), GC, Mass spectrometer, and Electronic nose.

1.5.1 Infrared spectroscope

Infrared spectroscopy is a powerful tool for qualitative and quantitative gas analysis based on the interaction between infrared radiation and molecules. By absorbing certain portions of light in the infrared region, higher energy states can be excited, resulting in vibrations and rotations of the molecules. Due to the dependence of the absorbance on the wavenumber (ν), different gas components can be distinguished using the absorption spectrum and by this way can used it as qualitative analysis. While in quantitate analysis used Beer's law that gives a linear relationship between the absorbance (A) and the gas concentration (c) [45].

1.5.2 Gas chromatography (GC)

Gas chromatography uses a gaseous mobile phase to transport sample components through either packed columns or hollow capillary columns containing a polymeric liquid stationary phase. GC has developed into a sophisticated technique since the pioneering work of Martin and James in 1951, and is capable of separating very complex mixtures of volatile analytes. In this technique, analyte separation is achieved by optimizing the differences in stationary phase affinity and the relative vapor pressures of the analytes. In practice these parameters are manipulated by changing the chemical nature of the stationary phase and the column temperature. Retention times provide the qualitative aspect of the chromatogram and for determination of the actual amount of the compound, the area or height is compared against standards of known concentration as a quantitative

analysis. Furthermore, GC can used it in natural gas analysis or refineries, gasoline characterization and fraction quantitation, aromatics in benzene [46].

1.5.3 Mass spectrometry (MS)

Mass spectrometry uses the difference in the mass-to-charge ratio (m/e) of ionized atoms or molecules to separate them from each other. Mass spectrometry is therefore useful for quantitation of atoms or molecules, also it used for determining chemical and structural information about molecules. Molecules have distinctive fragmentation patterns that provide structural information to identify structural components [47]. Mass spectrometry can used for determination of the climate gases CH_4, CO_2 and N_2O in air samples and soil atmosphere [48].

1.5.4 Electronic nose technique

An electronic nose (E-nose) is a potential approach to perform odor analysis. A typical E-nose system ordinarily consists of two parts: a gas-sensor array and a pattern recognition unit. The former part generates odor fingerprints from gas-sensor responses with high cross sensitivity while the latter performs data analysis using computational algorithms. With this structure, E-noses can identify complicated gas components with low-cost gas-sensor arrays [49]. The growth of industries and other human activities have led to ever-increasing amounts of pollutants in both outdoor and indoor spaces. This technique used for determine some of the important pollutants such as NO_x, NH_3, SO_x, CO, formaldehyde, toluene, and so on [50].

Chapter 2: Experimental work and set-up

2.1 Materials

Several Track Etched polycarbonate, polyester and polyimide membranes of different thickness, surface treatment and pore densities were purchased from it4ip (Belgium). Track Etched Polycarbonate, and PEEK, PVDF and polyether sulfone membranes (25-mm dia) were purchased from Sterlitech (USA). Track Etched polycarbonate membranes (6-µm thick and 25-mm dia) were also purchased from SPI (USA). Teflon AF membranes (40-µm thick) of different diameters were purchased from Biogeneral Inc. (USA). Silicon rubber film (128-µm thick) was purchased from AAA-ACME (USA). Two Alumina Nanomembranes of different thickness and pore diameter were purchased from Synkera Technologies (USA). Zeolite rods of different types were purchased from Hutong Global Co., LTD (China). The details of all membranes are provided in Table 7.

Acrylic sheets (15 mm, 20 mm, and 30 mm thick) were purchased from Signtrade, UAE. Needle and ball valves, stainless steel (SS) tubes, SS bolts, NBR O-rings, two-part quick epoxy (Devcon®), and two-part Epo-Putty (ALTECO) were purchased from the local hardware stores. Different porous SS discs (6 mm thickness) were purchased from Mott Corp. (USA). Thin epoxy (Epothin ®) was purchased from Buehler.

Hydrogen (99.9992%), nitrogen (99.9992%), helium (99.9992%), neon (99.985%), argon (99.9992%), carbon dioxide (99.99%), methane (99.999%), ethane (99.5%), ethylene (99.95%), propane (99.999%) gas cylinders were purchased from Air products (United Arab Emirates).

Table 7: Specifications of the membranes used in the present work

	Membrane	**Abbreviation**	**Specification**
1	Polycarbonate	PC-1	Dia 25 mm, thickness 6 µm, pore diameter 0.01 µm (Hydrophilic)
2	Polycarbonate	PC-2	Dia 25 mm, thickness 10 µm, pore density 3 × 10^9 cm^{-2}, pore diameter 0.01 µm (Hydrophilic)
3	Polycarbonate	PC-3	Dia 25 mm, thickness 25 µm, pore density 4 × 10^9 cm^{-2}, pore diameter 0.01 µm (Hydrophilic)
4	Poly carbonate	PC-4	Dia 25 mm, thickness 50 µm, pore density 2 × 10^9 cm^{-2}, pore diameter 0.01 µm (Hydrophilic)
5	Polycarbonate	PC-5	Dia 25 mm, thickness 50 µm, pore density 2 × 10^9 cm^{-2}, pore diameter 0.01 µm (Hydrophobic)
6	Polyester	PET-1	Dia 25 mm, thickness 23 µm, pore density 4 × 10^9 cm^{-2}, pore diameter 0.01 µm (Hydrophilic)
7	Polyester	PET-2	Dia 13 mm, thickness 12 µm, pore density 3 × 10^9 cm^{-2}, pore diameter 0.01 µm (Hydrophilic)
8	Poly ester	PET-3	Dia 13 mm, thickness 12 µm, pore density 3 × 10^9 cm^{-2}, pore diameter 0.01 µm (Hydrophobic)
9	Polyimide	PI-1	Dia 25 mm, thickness 25 µm, pore density 1 × 10^9 cm^{-2}, pore diameter 0.01 µm (Hydrophilic)
10	Polyimide	PI-2	Dia 13 mm, thickness 25 µm, pore density 6 × 10^9 cm^{-2}, pore diameter 0.01 µm (Hydrophilic)
11	PEEK-20	PEEK-20	Dia 25 mm, pore diameter 0.02 µm
12	PVDF-20	PVDF-20	Dia 25 mm, pore diameter 0.02 µm
13	Polyether sulfone	PES	Dia 25 mm, pore diameter 0.1 µm
14	Teflon AF®	Teflon AF	Dia 47 mm, thickness 40 µm
15	Teflon AF®	Teflon AF	Dia 25 mm, thickness 40 µm
16	Teflon AF®	Teflon AF	Dia 13 mm, thickness 40 µm
17	Silicon Rubber	SR	Film membrane, thickness 128 µm
18	Nano Alumina	AAO-1	Dia 13 mm, thickness 51 µm, pore density 1 × 10^{11} cm^{-2}, pore diameter 13 nm
19	Nano Alumina	AAO-2	Dia 13 mm, thickness 101 µm, pore density 1 × 10^{11} cm^{-2}, pore diameter 18 nm
20	Zeolite (ZSM-5)	ZSM-5	Dia 3 mm, Length 43 mm, Si/Al ration 50
21	Zeolite (Nay)	Nay	Dia 2.7 mm, Length 26 mm, Si/Al ration 50

2.2. CNC machining

The Minitron D-23 Desktop CNC (Computer Numerical Control) router machine shown in Figure 9 was received from CanCam (Canada). Sheets of 15, 20, and 30 mm were used to fabricate the gas diffusion system by using CNC drill bits of different diameters (i.e. 2, 3, 4 and 6 mm). The CNC utility Vectric software (Version 9.0) was used to draw and design of various parts to be cut by the CNC router. The specifications of the CNC routers are shown in Table 8.

Figure 9: CNC. machine

Table 8: CNC machine specifications

Specification	**Description**
Machining Bed	63.5 cm x 93.98 cm
Weight	150 kg
Color	White/Blue
Power	2.2 kW / 3 HP
Max Speed	24000 RPM
Rapid Speed	315 IMP
Max Cutting Speed	240 IMP

2.3 Experimental setup

2.3.1 Concept design of parallel diffusion system

The concept design of the parallel diffusion system is illustrated in Figure 10. The system is constructed from an inlet reservoir of the pressurized gas sample and six membrane holders arranged in such a way to allow parallel gas diffusion from the common inlet reservoir to the individual confined spaces behind the 6 membranes, respectively. The pressure buildup behind the membranes (i.e., P1 to P6) is recorded by means of six individual pressure sensors (i.e., S1-S6) to provide the diffusion pattern/spectrum of the test gas. The construction details of the parallel diffusion system is provided in the following section.

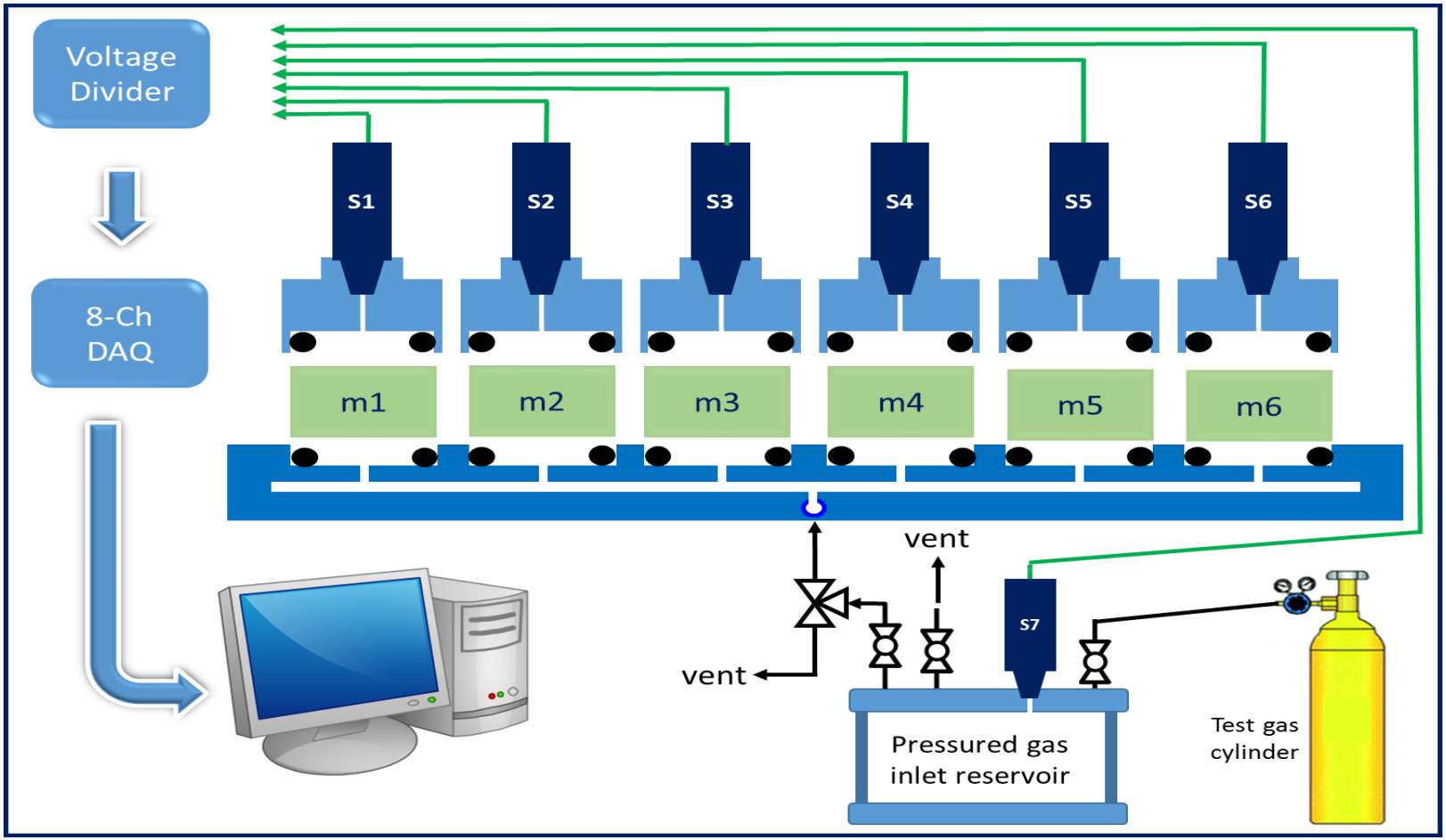

Figure 10: The 6-channel experimental setup for testing the independent parallel gas diffusion through different membranes. The systemis constructed from 6 membrane holders (m1-m6), 7 gas pressure sensors (S1-S7), pressured gas inlet reservoir, ball valves, two-way valve, test gas cylinder, voltage divider, 8-Channel data acquisition card (DAQ), and a PC

2.4 Detailed construction of the gas diffusion system

2.4.1 Construction of the gas distributer/base unit

The gas distributer (which also served as the base of the gas diffusion system) was constructed from two layers, each was cut from a transparent acrylic sheet (20-mm thick). The dimensions and the design of the first (base) layer is shown in Figure 11 (A). The base layer was designed in such a way to serve as (i) gas inlet, (ii) gas distributer (middle orange region) and (iii) foundation for the second layer which hosts six membrane holders. To achieve the desired functions, the base layer consisted of six levels carved at different depths as shown in Figure 11(A), where the zero level refers to the surface of the 20-mm acrylic sheet. More detailed dimensions indicated for the dashed rectangle area in Figure 11(A) was shown in Figure 11(B). The cross sections of the base layer (across lines X and Y) were shown in Figure 11(C).

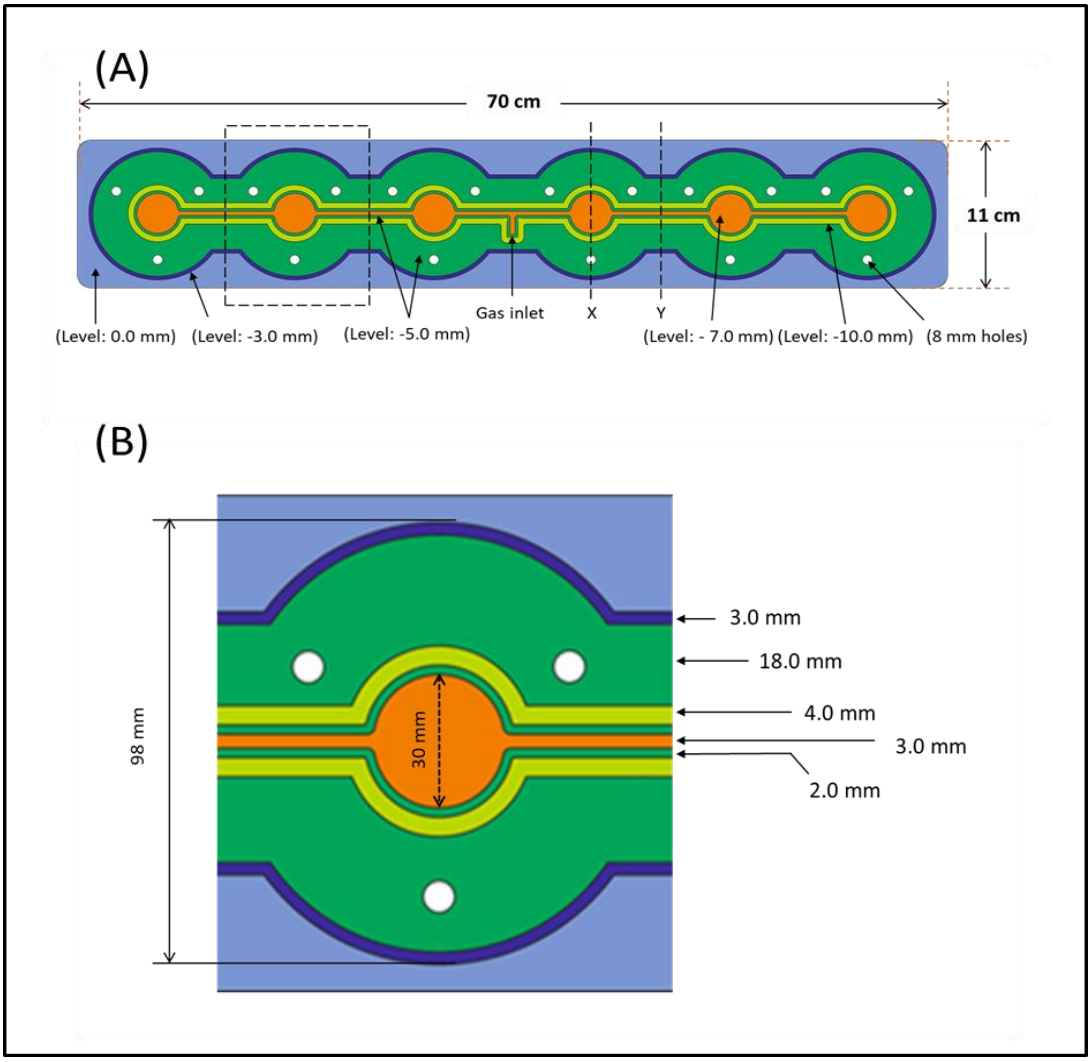

Figure 11: (A) The top view design (of the base layer) for the gas distribution unit.
(B) The width of the six designated regions shown in (A)

The second (top) layer of the gas distribution unit was designed in such a way to connect with the base layer and to form a footprint for the membrane holders.

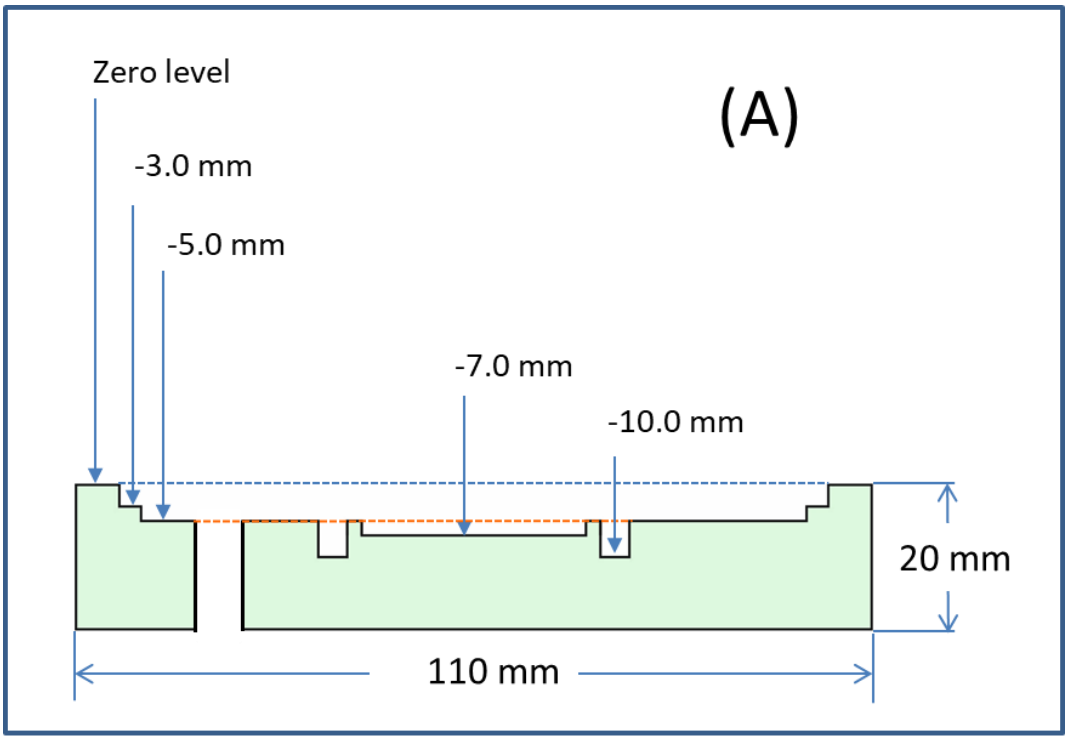

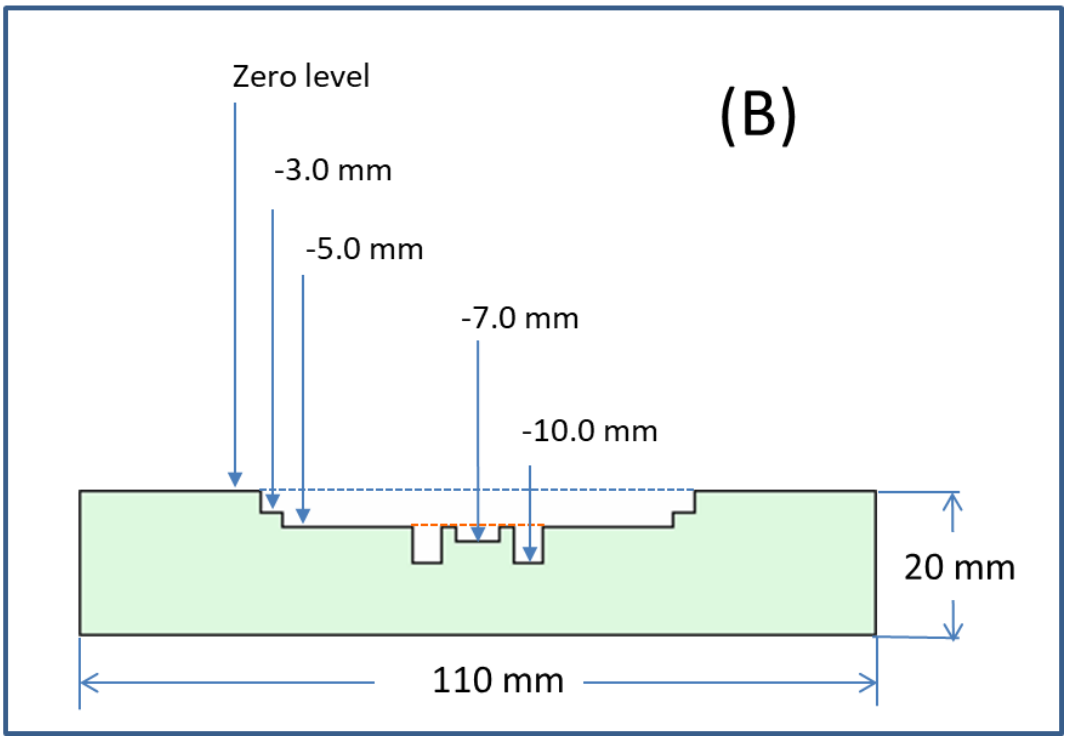

Figure 11: (C) Cross section of the base layer across line X (A) and line Y (B) of the gas distributer shown in Figure 11(A) continued

The construction of the second (upper layer) of the gas distributer unit was shown in Figure 12. Six cavities (6-mm deep and 50-mm diameter, each) were machined on the upper face of this layer to serve as foundation for the 6 membrane holders. Five holes (2-mm diameter each) were drilled through the cavities to allow for gas flow from the base layer to the membrane holders as shown in Figure 12(A). The bottom of this layer was machined in such a way to form a protruded (5-mm height) closed loop as indicated by the dark area in Figure 12(B). The cross section view through line X shown in Figure 12(B) was presented in Figure 12(C).

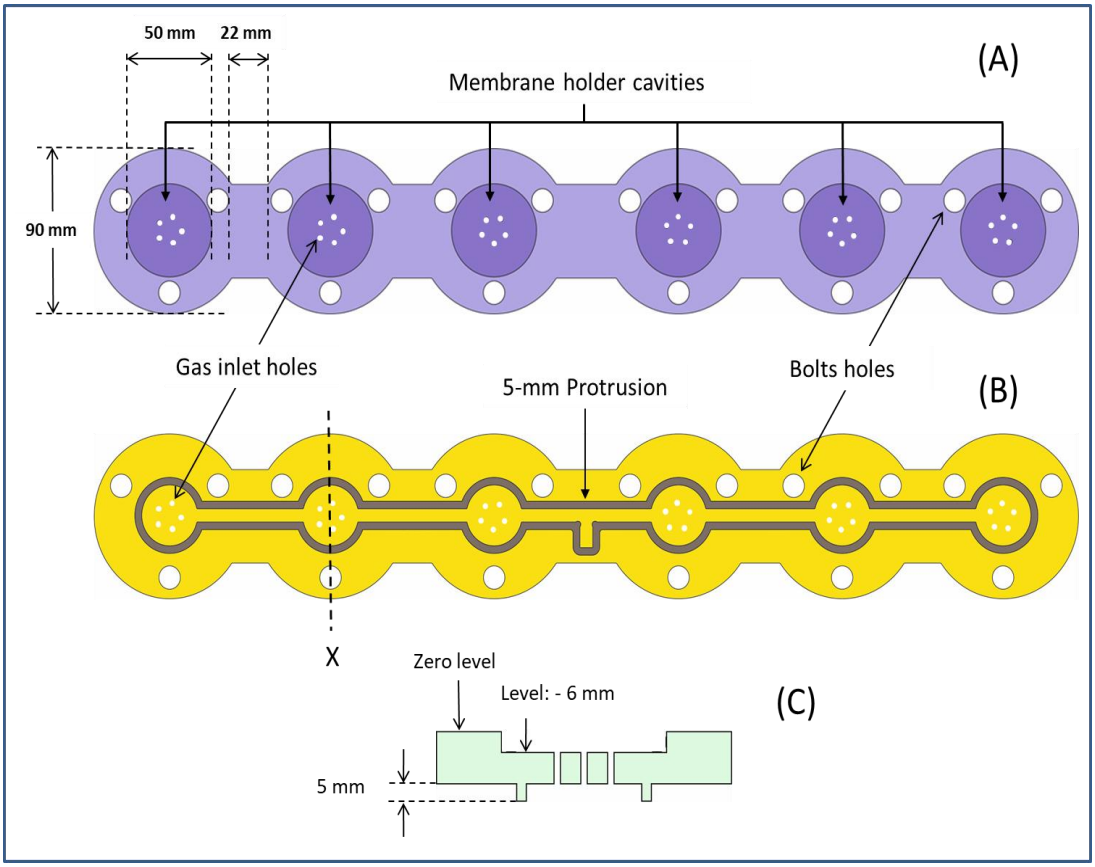

Figure 12: The construction details of the second (upper) layer of the gas distributer unit. Top view (A), bottom view (B) and cross section view (C)

2.4.2 Construction the membrane holders

Two different types of membrane holders (I & II) were designed, fabricated and used throughout the present work. Type-I holders were used for thin membranes (i.e., polycarbonate, polyester, polyimide, Teflon AF, silicone rubber and Alumina). Whereas Type-II holders were used for rod-shaped zeolites. The general constructions of the two holder types were shown Figure 13(A) and 13(B), respectively. Type I is a sandwich holders consisting from two discs, where the membranes secured in placed between two O-rings as shown in Figure 13(A), where the two discs assembled together by SS bolts with insert nuts as shown in Figure 13(A). While Type II holders constructed from a single acrylic disc (50-mm dia, 30-mm height). Either a single or multi-hole (each 5-mm dia and 27-mm depth) were drilled in the center of the disc and filled with thin epoxy. The epoxy was left to partially set for 2 hours, zeolite rods (~3 mm in diameter and ~25 mm in length) was inserted completely in the epoxy and left overnight for complete setting. The zeolite rods was exposed at both sides by very gentle stepwise (0.5 mm) removal of acrylic layer (from the bottom) and the epoxy (from top) by CNC machining using a 4-mm end mill. Photos for Type I and II holders are presented in Figure 14 and 15, respectively.

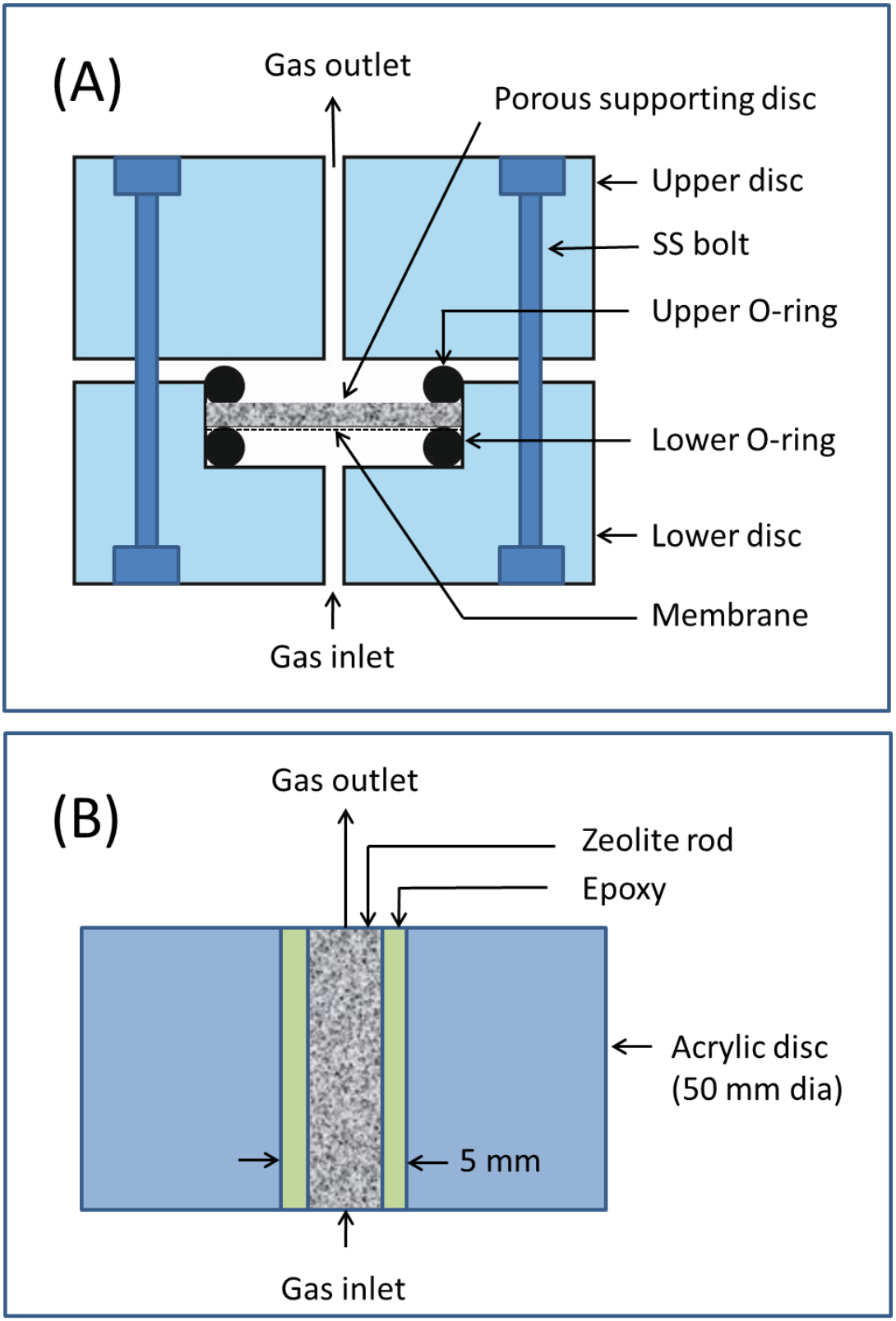

Figure 13: Cross section view of the Type I (A) and Type II (B) holders, respectively

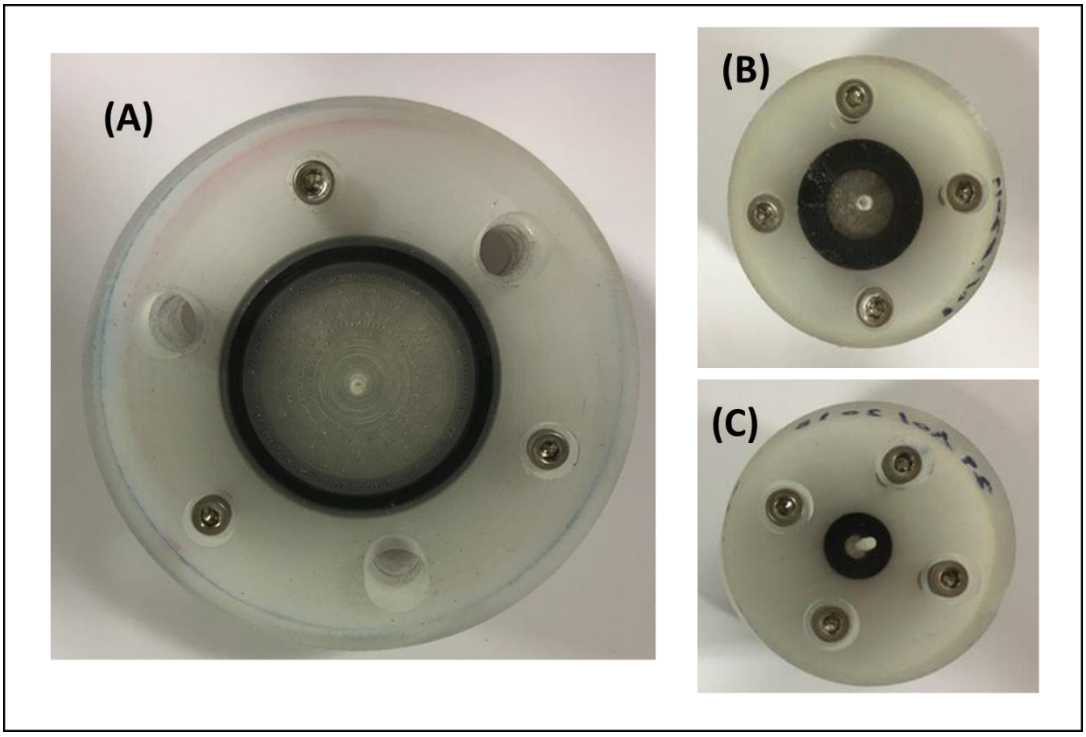

Figure 14: Top views of Type I holders for 47-, 25- and 13-mm dia membranes (A), (B) and (C), respectively

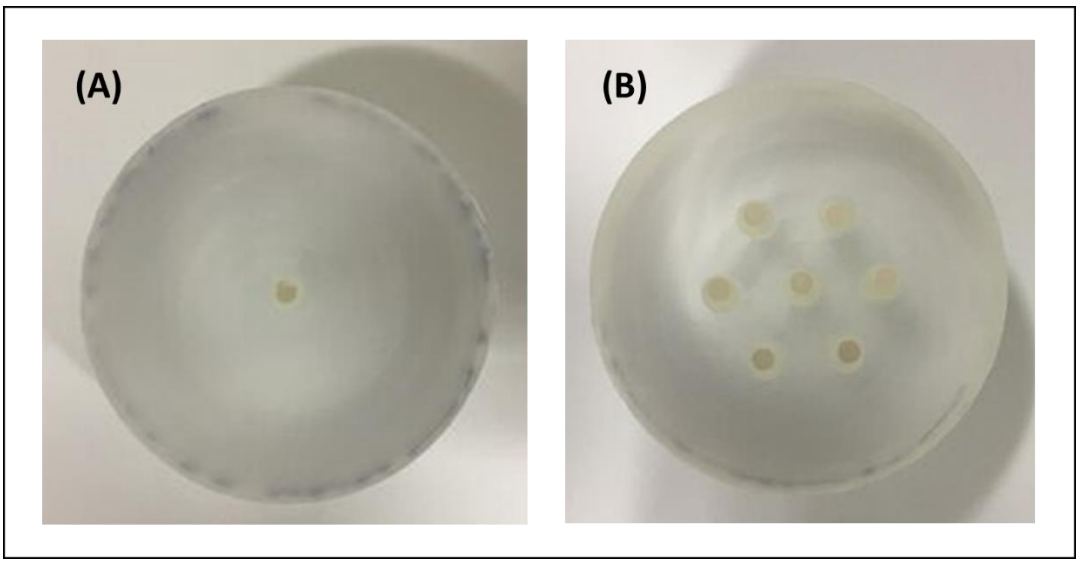

Figure 15: Top views of Type II holders for zeolite single and multi-rod

2.4.3 Construction of pressure sensors holders/ covers

Covers constructed from transparent acrylic disc (30- mm thick). A ¼" NPT thread was machined from the upper side to install the pressure sensor. A central 2-mm dia hole was drilled through the disc center to allow gas transfer to the pressure sensor. Two features were machined in the lower face: (i) the 6-mm O-ring groove and (ii) a 0.5-mm depth central groove to act as a constant volume permeation reservoir. A horizontal vent line connecting the pressure sensor compartment and a ball valve was machine as shown in Figure 16.

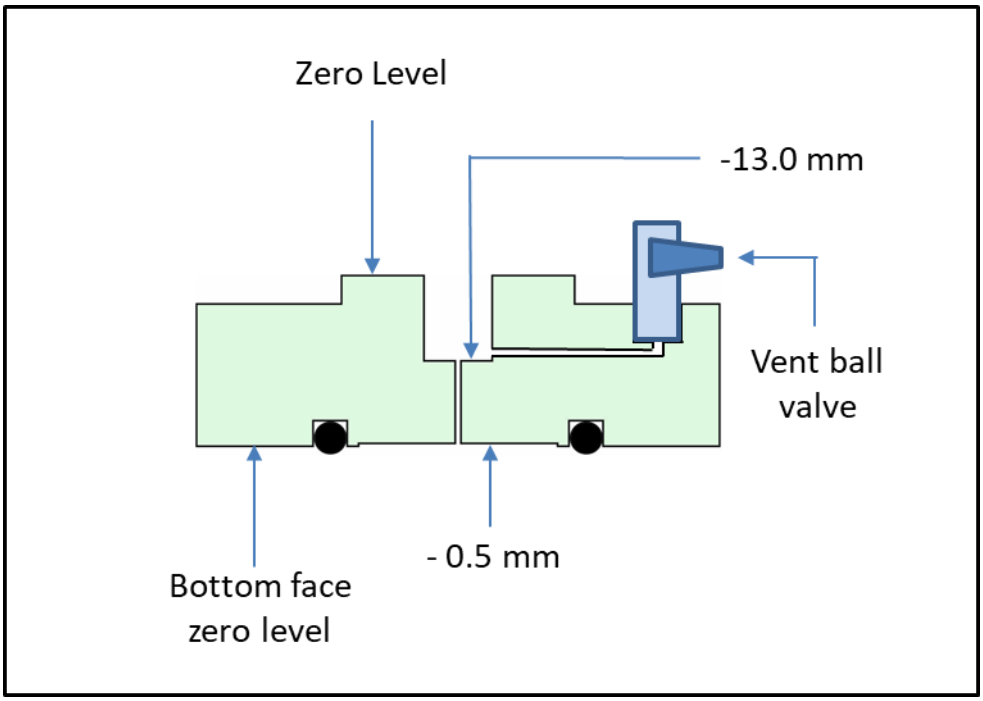

Figure 16: Cross section of pressure sensor holder/covers

2.4.4 Assembled gas diffusion system

An expanded view of one channel of the gas diffusion system (gas distribution, membrane holder, and the pressure sensor holder/cover) was shown in Figure 17 and the assembled view in Figure 18. A photo of the experimental setup was shown in Figure 19.

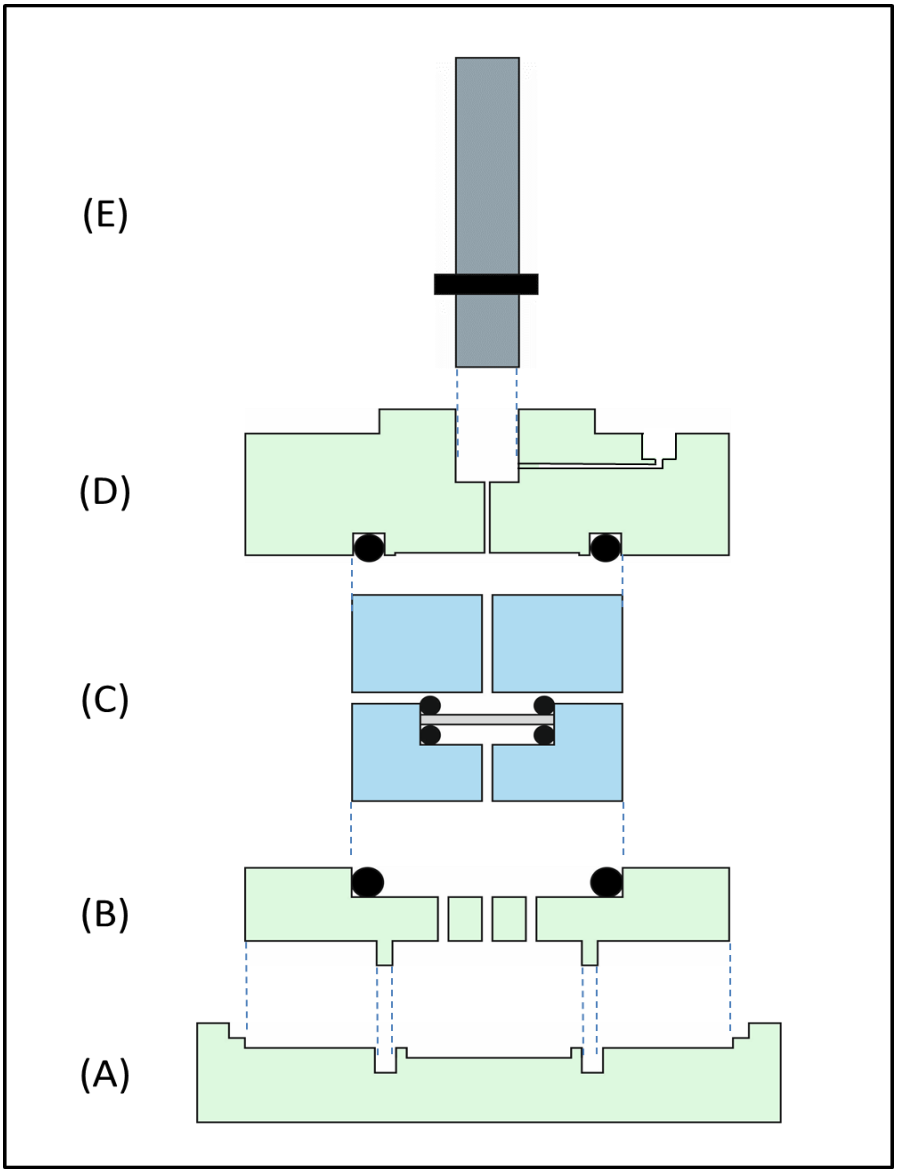

Figure 17: Expanded view of one channel of the gas diffusion system. The figure shows the two layers of the base/gas distributer (A&B), membrane holder (C), the sensor holder/cover (D) and the pressure sensor (E)

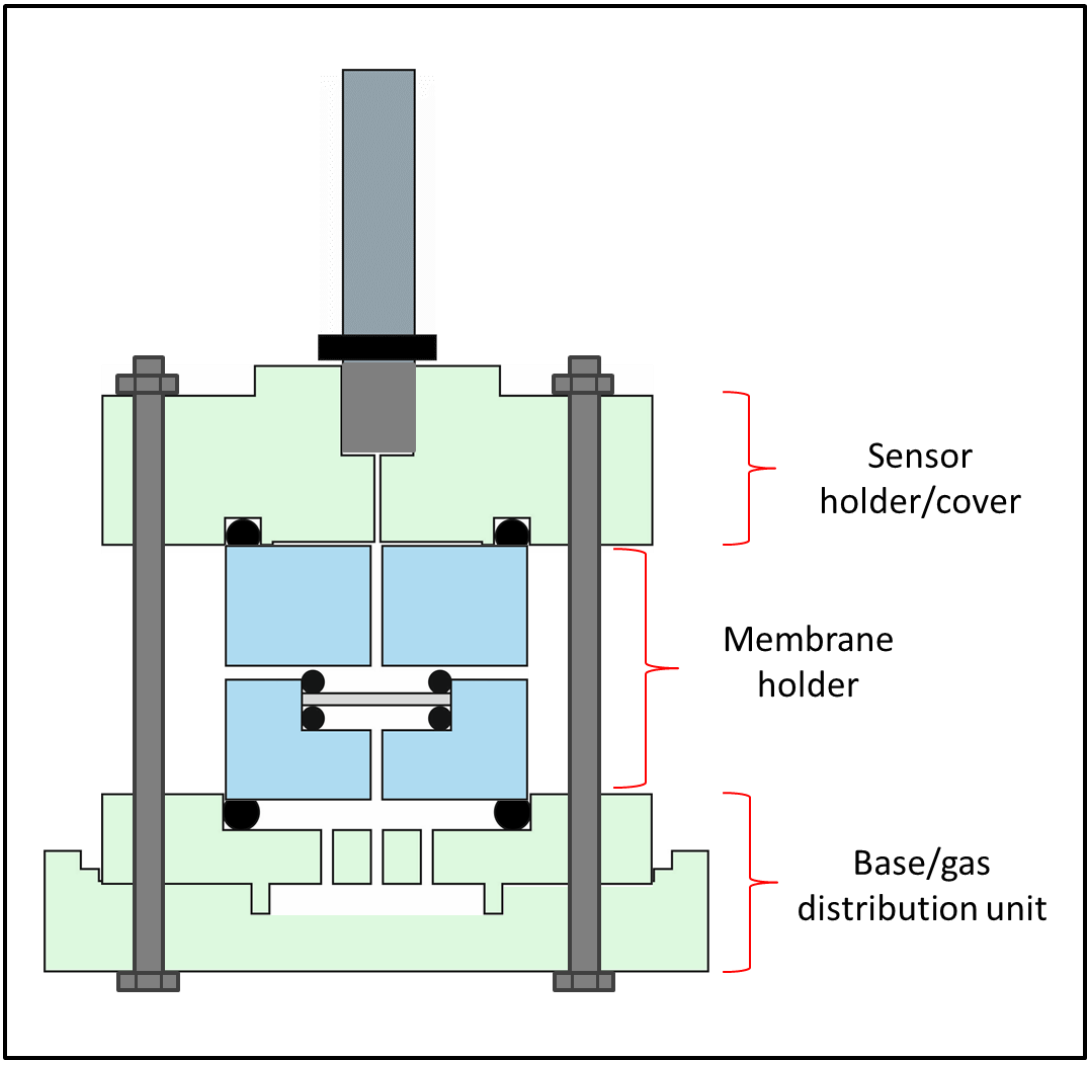

Figure 18: Assembled view of one channel of the gas diffusion system. The figure shows the two layers of the base/gas distributer (A&B), membrane holder (C), the pressure sensor holder/cover (D) and the pressure sensor (E). The gas vent in the holder is not shown for simplicity

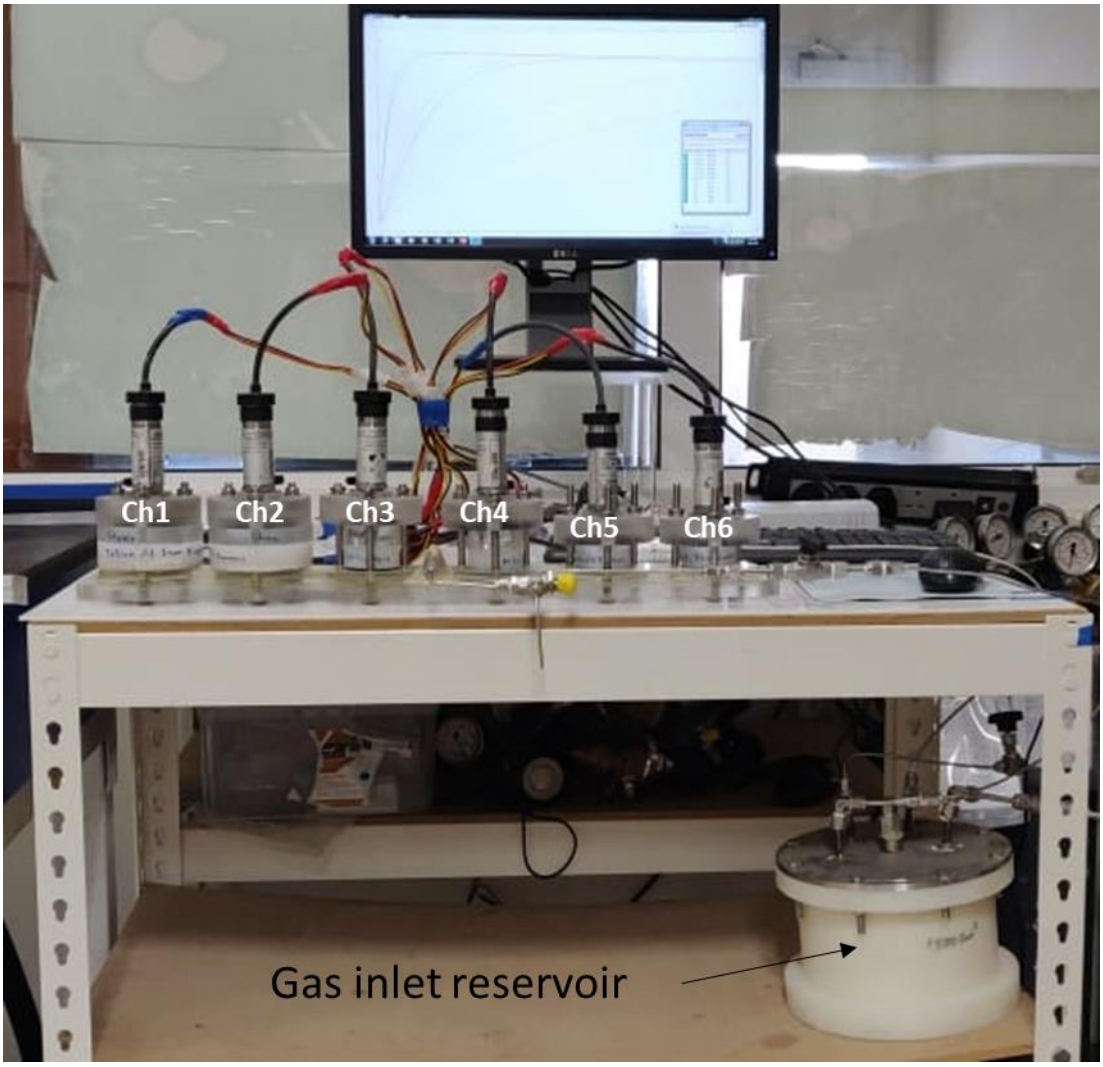

Figure 19: A front view of the 6-CH gas diffusion system and the gas inlet reservoir

2.5 Gas mixing system

An 8-Channel data acquisition card (Model ADC-20) with 2.5 V input voltage was purchased from Pico Technology (UK). Pressure sensors 0-60 PSI and 0-100 PSI (Ashcroft) with 1-5 VDC output and 1/4" NPT male connection, were purchased from Cole Palmer. A 50-50 Voltage divider was custom designed and constructed to reduce the maximum sensor output (i.e. 5 V) to 2.5 V. A 4-CH computer controlled gas mixer (Model MFC-4, Sable Systems, USA) was used to control two Mass Flow Controllers (MFCs) (Sierra Instruments, USA) to prepare gas mixtures of variable compositions.

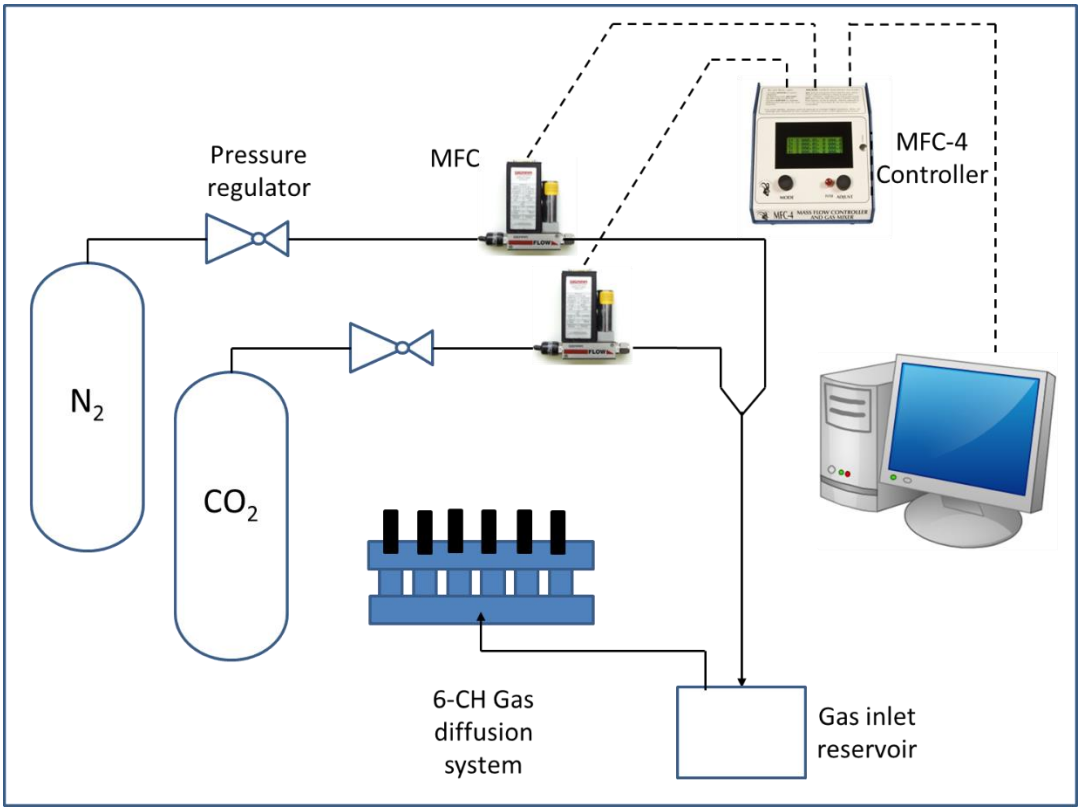

Figure 20: The experimental setup used for gas mixing

2.6 Measurements

The desired test gas (either pure or mixture) was fed into the gas inlet reservoir to the desired inlet pressure. Fine pressure adjustment was achieved by the small vent needle valve. To start the experiment, the inlet ball valve was opened to allow the test gas to expand to the gas distributer and to permeate through the membrane. The vent valves behind the membranes were opened to vent the accumulated gas. This process was repeated at least 3 times to ensure that the gas distributer unit was flushed with the test gas. The inlet pressure in the inlet reservoir was readjusted to the desired pressure. To start a given measurement, the vent valves behind each membrane were closed. Then, the inlet valve was opened to allow the test gas expansion to the gas distributer. The gas pressure accumulation behind the membrane was measured

continuously using pressure sensors (Ashcroft) with 1-5 VDC output, and the pressure readings were recorded using 8-Channel data acquisition card (Model ADC-20) and Pico log software at rate of one sample per second. The pressured build up was allowed to progress for enough time to at least equilibrate with the pressure of the gas inlet reservoir. A typical recording of the pressure buildup behind a given membrane was shown in Figure 21.

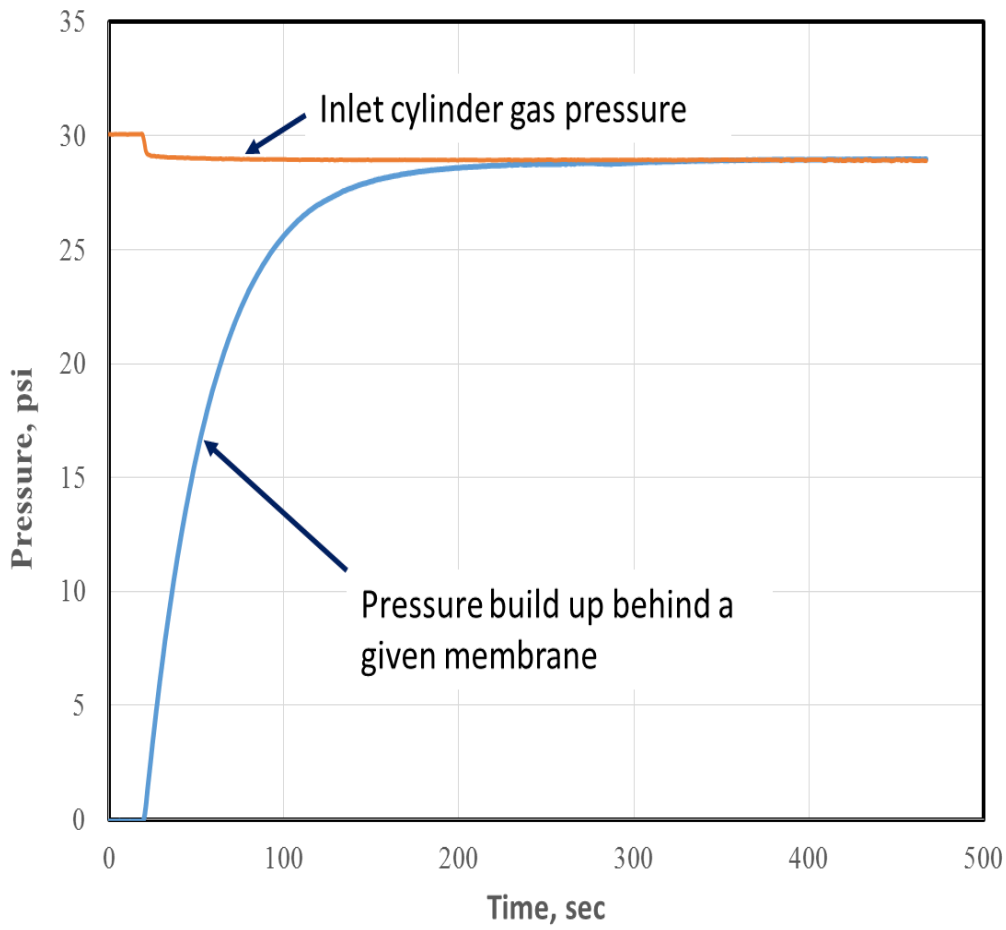

Figure 21: A typical recording obtained for the gas diffusion in a given channel

Chapter 3: Results and discussion

3.1 Construction of the gas diffusion system

Several aspects were rationalized in constructing the gas diffusion system. These included: (i) 6-channel system for rapid testing, (ii) negligible internal volume of the gas distributer compared to the inlet gas reservoir, (iii) to sustain pressures upon to 100 psi, (iv) strict leak tight (<0.1 psi/hour), (v) convenient pressurization and venting of the test gas, (vi) convenient membrane replacement, and (vii) capability of continuous pressure monitoring with high resolution (0.01 psi).

All construction prerequisites were achieved by proper design of a 6-channel system in which 6 membranes holders were linearly arranged on a rectangular base. Thick transparent acrylic sheets (20 mm-thick) was used throughout the construction and proved suitable to achieve safely the required pressure rating. The volume of the gas inlet reservoir was 1500 cm^3 which was significantly larger than the internal volume of the connection line and the base of the gas diffusion which was estimated at approximately 50 cm^3. The total internal volume between the membranes and the gas sensors were estimated as 80 cm^3. Careful construction, proper O-ring sizes and construction successfully led to desired excellent leak tightness. A ball valve installed in the front panel between the gas inlet reservoir and the base unit ensured convenient control of the inlet test gas as shown in Figure 19. Gas venting was somehow less convenient since each channel had to be vented separately through a vacuum line via a ball valve installed on the cover of each membrane holder as shown in Figure 16.

3.2 Characterization of the gas diffusion system

Beside the membrane type, which is obviously the most important variable in the present study, three other variables which could have significant effects on the intended experiments are (i) temperature, (ii) the initial inlet pressure of the test gas and (iii) the volume of the gas inlet reservoir. The first variable (i.e., temperature) was not investigated since the system was meant to operate in an air conditioned lab with temperature (± 2°C). Even for possible future operation under wider temperature fluctuations (e.g., ± 20°C in outdoor), the changes in gas permeabilities for such small temperature variations are negligible [51, 52]. However, the effects of the gas inlet pressures and the volume of the inlet gas inlet reservoir were studied, respectively.

The effect of gas inlet pressure was evaluated at four different inlet pressures, as shown in Figure 22 using polycarbonate membrane (PC-1). As one might expect, the higher the inlet pressure the higher the equilibration pressure value. However, opposite to the first immediate expectation that slower equilibration should be obtained at higher inlet pressures, the time required for pressure equilibration was almost constant regardless of the inlet initial pressure. The same behavior was observed when the volume of the inlet reservoir was reduced from 1500 to 750 cm^3 as shown in Figure 23.

The independence of the rate of gas build-up from the inlet gas reservoir pressure and volume, prompted the need for a mathematical model to fully explain the system behavior and further guide the rest of the work. The pressure build-up profile is similar to the approaching mathematical model. These similarities include (i) start from zero (ii) curves are logarithmic build-up (iii) Asymptotic approach to a limiting value. The

most common example for such model is the well-known RC circuit model [53-55] shown in Figure 24.

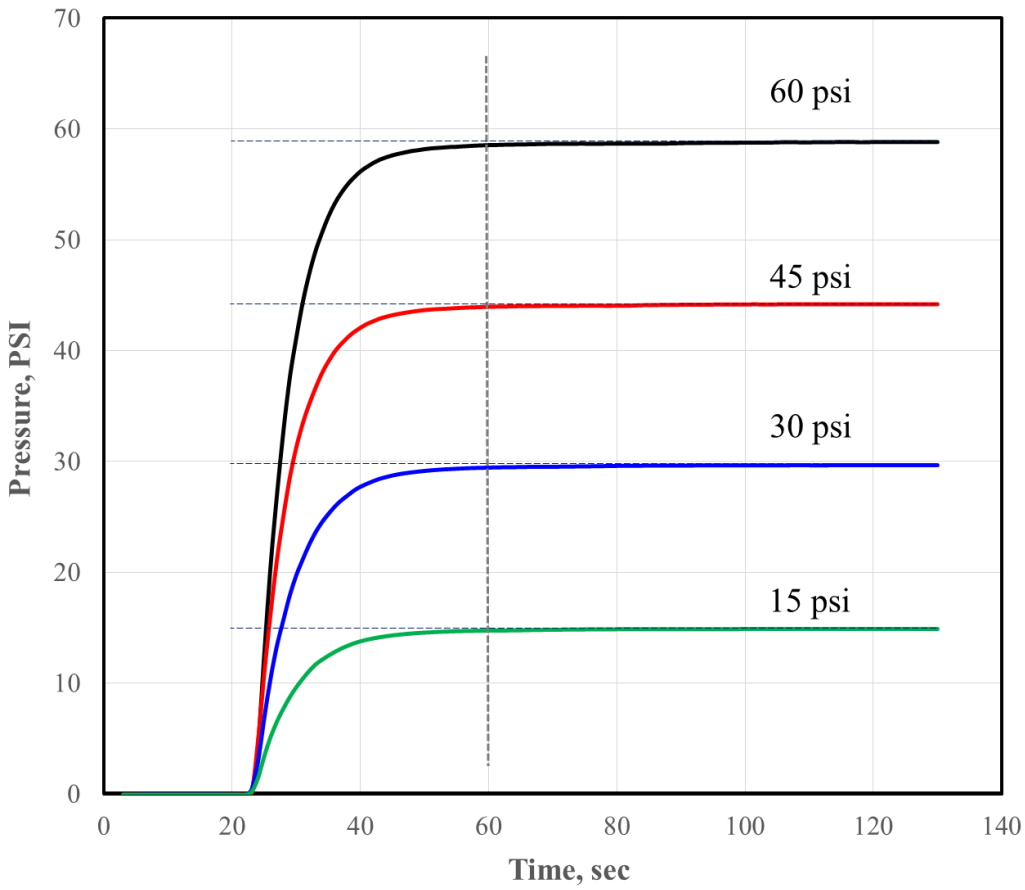

Figure 22: Effect of the initial gas inlet pressure on the equilibration time of nitrogen gas permeation through PC-1 membrane

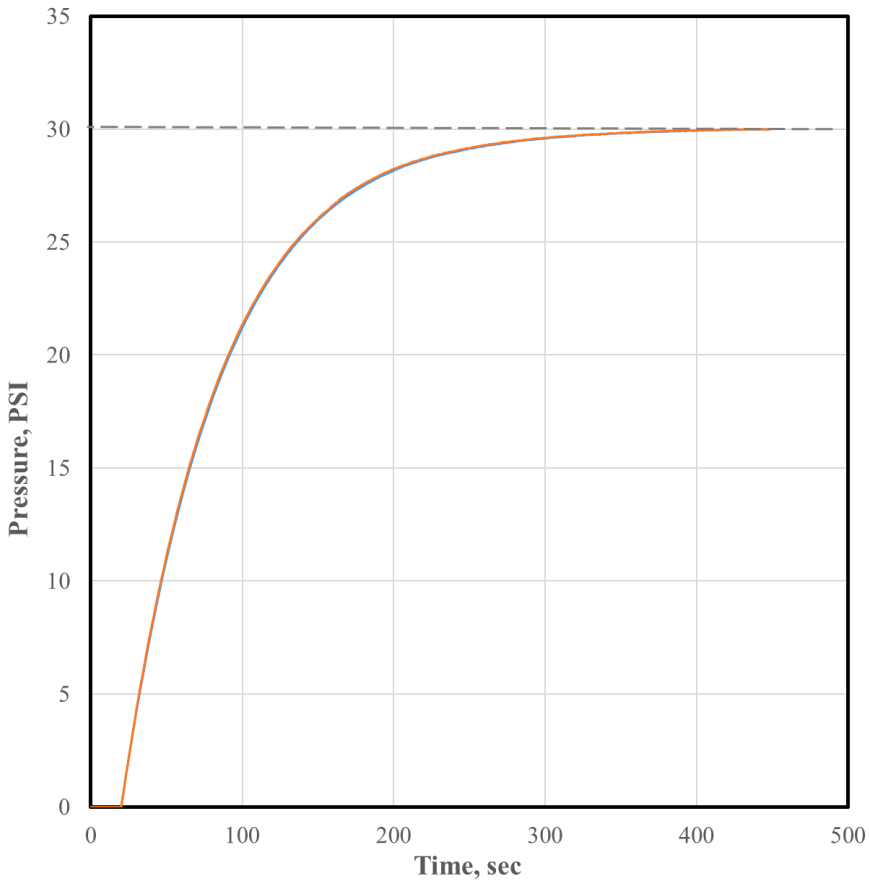

Figure 23: Effect of the volume of the inlet gas reservoir on the rate of Nitrogen gas pressure build-up behind PC-1 membrane. The pressure build-up was identical for two experiments conducted with inlet reservoir of 1500 and 750 cm^3, respectively

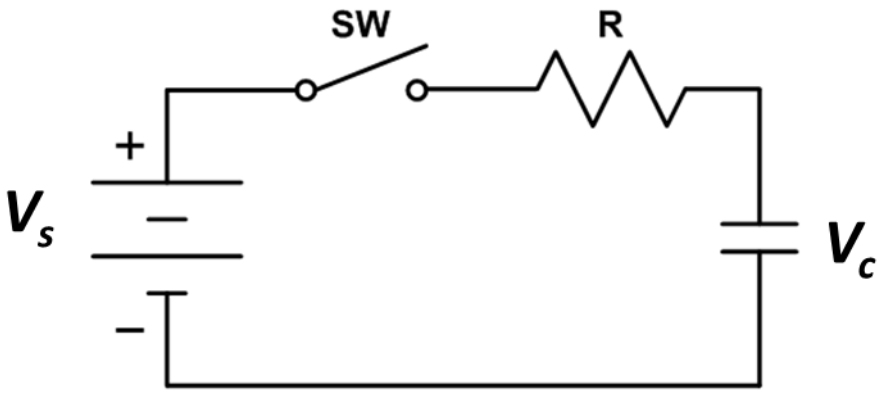

Figure 24: A typical RC circuit

The charging of the capacitor has already been modeled [54] and the voltage across the capacitor (*Vc*) is given by equation 3.1

$$V_c = V_s\left(1 - e^{-t/RC}\right) \quad [3.1]$$

Where:

V_S *is* the voltage of the power supply;

t is the time elapsed since the application of voltage,

RC is the circuit time constant (τ).

The SI units of R and C are given in equation 3.2 and 3.3, respectively.

$$R\ (Ohm) = \frac{kg.m^2}{Coul^2.s} \quad [3.2]$$

$$C(Farad) = \frac{Coul^2.s^2}{kg.m^2} \quad [3.3]$$

Hence, the circuit time constant (τ) has time unit (s). When $t = RC\ (\tau)$, hence:

$$Vc = 0.6321\ Vs. \quad [3.4]$$

By analogy, the present gas pressure build can be described mathematically by equation [3.5]

$$P_m = P_i\left(1 - e^{-t/RC}\right) \quad [3.5]$$

Where the analogous terms could possibly be fined as:

P_m: is the pressure behind the membrane,

P_i: is the initial pressure in the test gas in the inlet reservoir,

t: is the time elapsed since the open of the valve between the inlet reservoir and the gas distributer unit.

R: Membrane resistance to gas transfer.

C: the confined volume between the membrane and the gas sensor.

To verify the assumption that the present system follows the approaching model, the experimental result obtained with the PC-1 membrane and nitrogen test gas was compared with the model prediction. P_m values were calculated using equation 3.5 at different t values and Pi was defined as the equilibration pressure (analogous to the power supply driving force in the RC circuit) and RC (τ) was defined as 0.6321 Pi (analogous to equation 3.4). The excellent agreement between the experimental data and the calculate values was very impressive as shown in Figure 25. Interestingly, the approaching model nicely explained the preliminary observations presented in Figures 22 and 23 since the charging time (time required for pressure equilibration in the present system) is only dictated by RC and is neither dependent on the voltage of the power supply (initial pressure in the present system, Figure 22) nor the size of the power supply (volume of the inlet reservoir in the present system, Figure 23). Given the excellent agreement and the success of the approaching model to explain the initial experimental observations, no further attempts were made to develop an independent model for the present system.

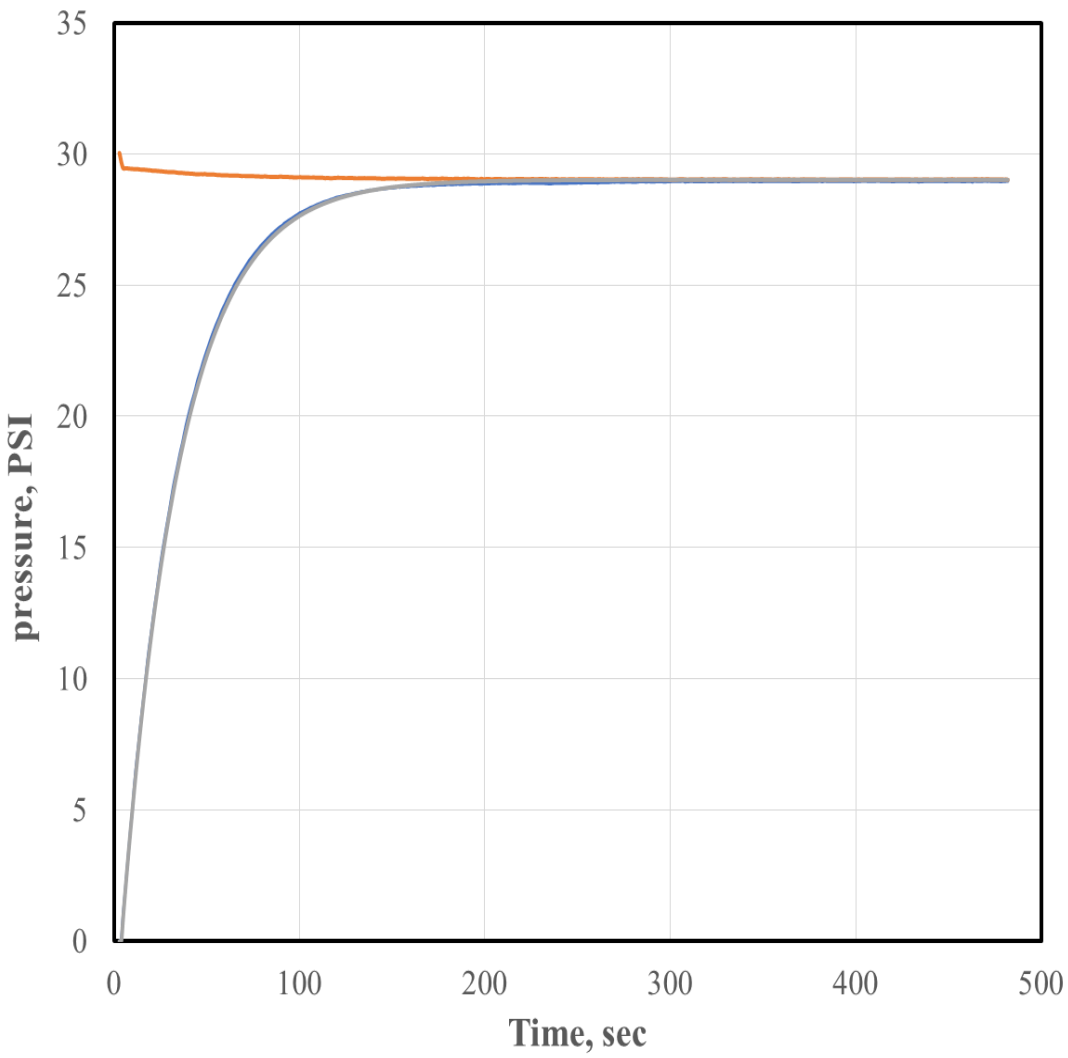

Figure 25: Comparison between the experimental pressure build-up values and modeled values

In addition to the previous overall analogy between the present gas diffusion system and the RC circuit, one more analogy was envisioned between the membrane (which as acts as a resistance element to gas transfer) and the electronic resistor (R) as shown in Figure 26. The rationale behind this analogy is two-fold: (i) to further confirm the validity of the approaching model and (ii) to allow more detailed understanding of the impact of different membrane characteristics such as its thickness, active area, etc.

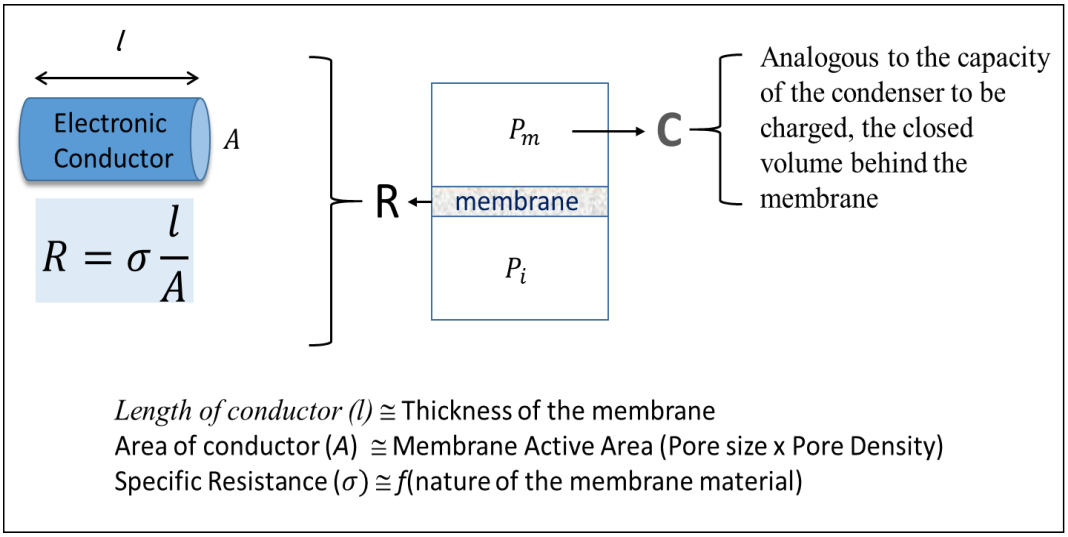

Figure 26: Illustration of the analogy between the membrane and the electronic resistor

One last issue to be resolved before the proposed analogy between the RC circuit and the present gas diffusion system can be safely adopted is the unit of RC. Although it is straightforward to demonstrate that RC has time unit (as shown in Equations 3.2 and 3.3) in the context of the RC circuit, it is not obvious how the multiplication of the membrane resistance (R_m) and the confined volume (C_m) behind the membrane can have time unit. Therefore, a derivation of the unit of R_mC_m was attempted. Gas diffusivity through membranes is defined in Eq. 3.6.

$$\text{Diffusivity D} = \frac{d}{3}\left(\frac{8RT}{\pi M_A}\right)^{\frac{1}{2}} \qquad [3.6]$$

Where;

T = Temperature (K)

R= Universal gas constant ($kg\ m^2\ s^{-2}\ mol^{-1}\ K^{-1}$)

M_A: Molecular weight ($kg\ mol^{-1}$)

d: Kinetic diameter (m)

Therefore, the SI unit of Diffusivity (D) can be reduced to m^2/s as shown in equations 3.7 and 3.8.

$$D = m\left(\frac{m^3.kg.m^{-1}.S^{-2}.K.mol}{mol.K.kg}\right)^{\frac{1}{2}} \quad [3.7]$$

$$D = m\,(m^2.S^{-2})^{\frac{1}{2}} = \frac{m^2}{S} \quad [3.8]$$

The membrane resistivity (σ_m) can be defined by Eq. 3.9

$$\text{Membrane resistivity } (\sigma_m) = \frac{1}{D} = \frac{S}{m^2} \quad [3.9]$$

Given the analogy described in Figure 26, the membrane resistance (R_m) can be defined similarly in terms of the membrane resistivity, length and cross section as shown in Eq. 3.10.

$$\text{Resistance } (R_m) = \sigma \times \frac{L}{A} = \frac{S}{m^2} \times \frac{m}{m^2} \quad [3.10]$$

Then, Resistance (R_m) = $\frac{S}{m^3}$

Capacitance (C_m): Confined Volume behind the membrane (m^3)

Therefore,

$R_m C_m = \frac{S}{m^3} \times m^3$

Therefore, the $R_m C_m$ has time unit and numerically equals to the time required for the pressure behind the membrane to reach 63.21% of the equilibrium value, regardless of the initial gas pressure and the volume of the gas inlet reservoir.

Having confirmed the validity of the overall analogy between the RC circuit and the present gas diffusion setup, the next logical step was to validate the analogy between the membrane resistance (R_m) to gas transfer and the resistor (R) to electric current, presented in Figure 26. The details of such validation is presented in the following section.

3.2.1 Validation of the analogy between membrane resistance (R_m) and electric resistance (R)

3.2.1.1 Membrane thickness vs. the length of the electric conductor

It is well known that the electric resistance (R) is directly proportional to the length of the electric conductor. Hence, the time constant of the RC circuit (τ) should also proportional to the length of the conductor for a given capacitance (note that $\tau = RC$). If the proposed analogy is valid, one might expect that the experimentally measured time constant (τ_m) should also proportional to the length through which the gas permeate through the membrane. This length can vary significantly with membrane tortuosity [56, 57], but in all cases it should proportional to the geometric length of the membrane (hereafter, will be defined as the membrane thickness). Ideally, to determine experimentally the relation between the membrane time constant (τ_m) and the membrane thickness, a series of identical membranes which differ only in their thickness, are required. Unfortunately, such membranes are not available. Instead, 1, 2, 3, 5 and 7 PC-1 membranes were stacked in series in Ch 2, 3, 4, 5 and 6, respectively of the gas diffusion system. Whereas, channel 1 was used as a blank (i.e., no membrane installed). It was assumed that the overall membrane thickness is a sum of the individual membranes stacked in series. The pressure build-up values in the 6 channels were measured simultaneously for N_2 test gas and the obtained results were presented in Figure 27. The membrane time constant (τ_m) values were determined at 63.21% of the final equilibrium pressure value and plotted against the number of membranes (which refers to the membrane thickness). The obtained excellent linearity ($R^2 = 0.9883$) shown in Figure 28 strongly conforms to the predicted analogy between the linear dependence of R and R_m on the length of the conductor and membrane

thickness, respectively. An additional attempt was made to test this analogy using other intact membranes (instead of stacked several membranes) to safely generalize this conclusion. Zeolite ZSM-5 rods proved as suitable candidate for this purpose. Several ZSM-5 membranes for different thicknesses were fabricated and similarly tested using N_2-test gas. The obtained impressive linearity between the measured (τ_m) and the membrane thickness (presented in Figure 29) not only confirmed the analogy but also confirmed the safe generalization to different membrane types.

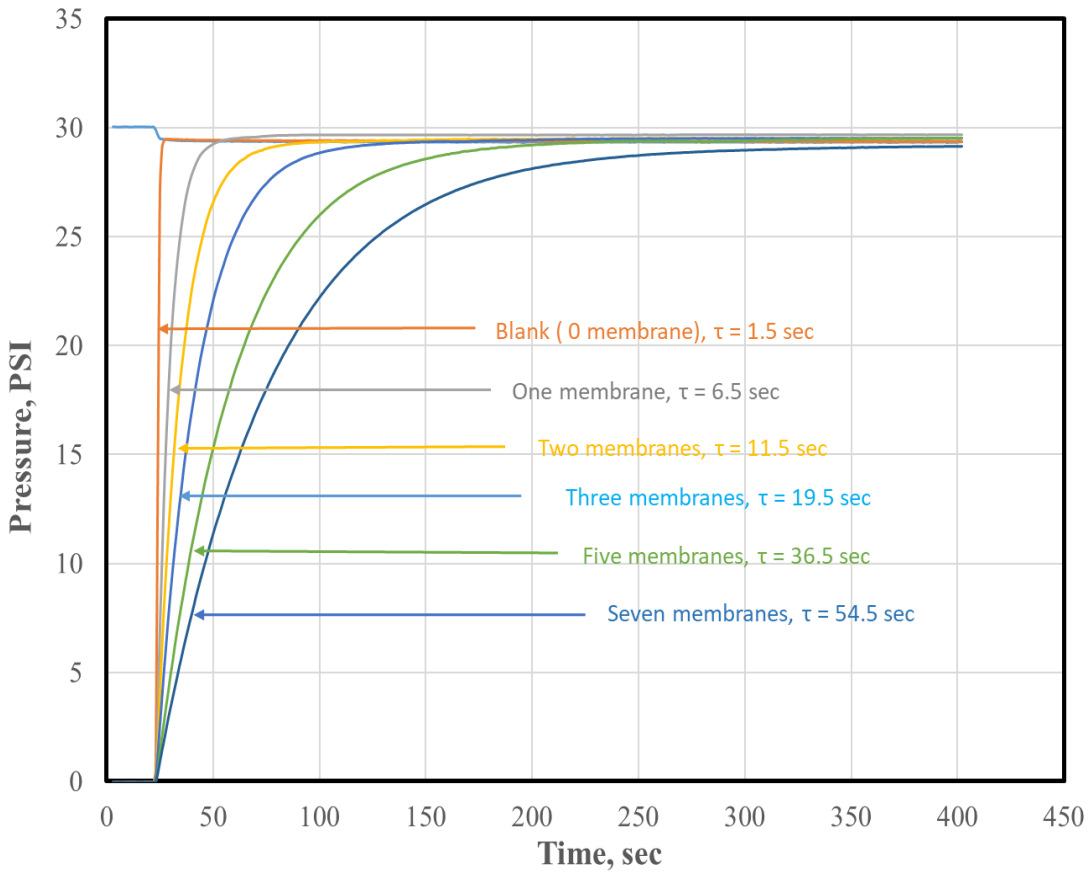

Figure 27: Effect of the number of PC-1 membranes on the rate of the pressure build-up using Nitrogen test gas at initial pressure 30 psi

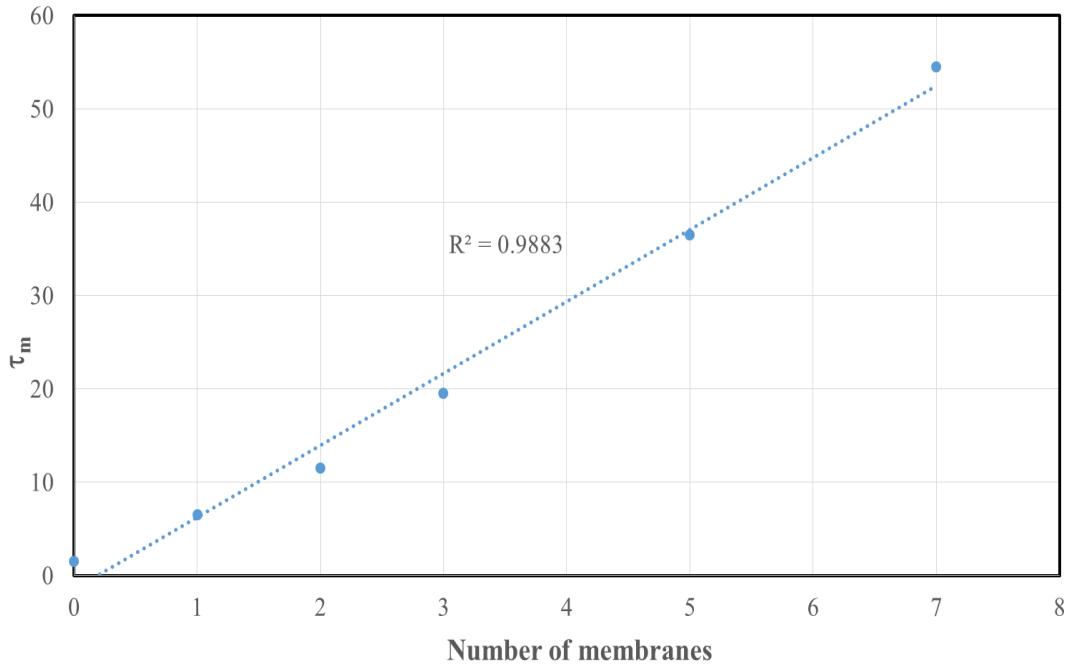

Figure 28: The plot of the membrane time constant (τ_m) vs the number of PC-1 membranes based on the results presented in Figure 27

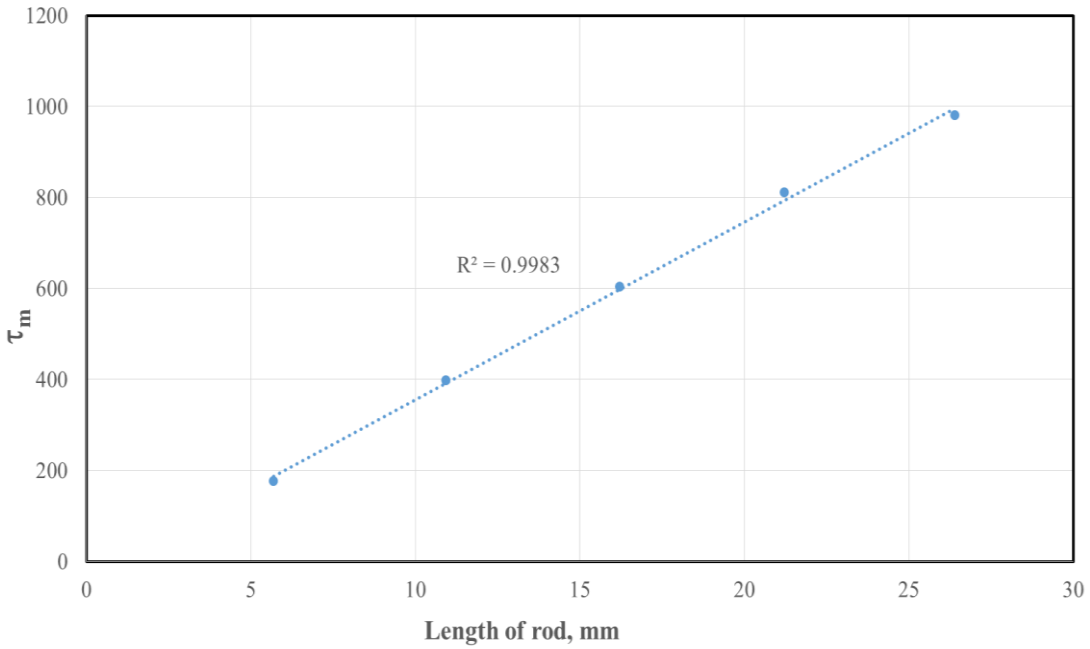

Figure 29: The plot of the membrane time constant (τ_m) vs the number of ZSM-5 membrane thickness. The rest of the conditions are similar to those presented in Figure 27

3.2.1.2 Membrane active area vs. the cross section of an electric conductor

The second component of the R_m and R analogy is the inverse dependence on cross section. To demonstrate such inverse dependence of R_m (and hence R_mC_m given that C_m is constant) on the membrane active area, series of ZSM-5 membrane holders were prepared with 1, 3, 5, 7 and 9 rods, respectively, and the τ_m was determined using N_2-test and the present 6-channel gas diffusion system. The obtained results were presented in Figure 30. It is evident that τ_m decreases with the number of rods used in the membrane holder, which is proportional to the total active area (A_m). For better quantitative confirmation, a plot of τ_m vs. (1/no. of rods) was presented in Figure 31. The excellent linear regression confirms the validity of the assumption that $R_m \alpha (1/A_m)$, which is completely analogous to $R \alpha (1/A)$ as depicted in Figure 26.

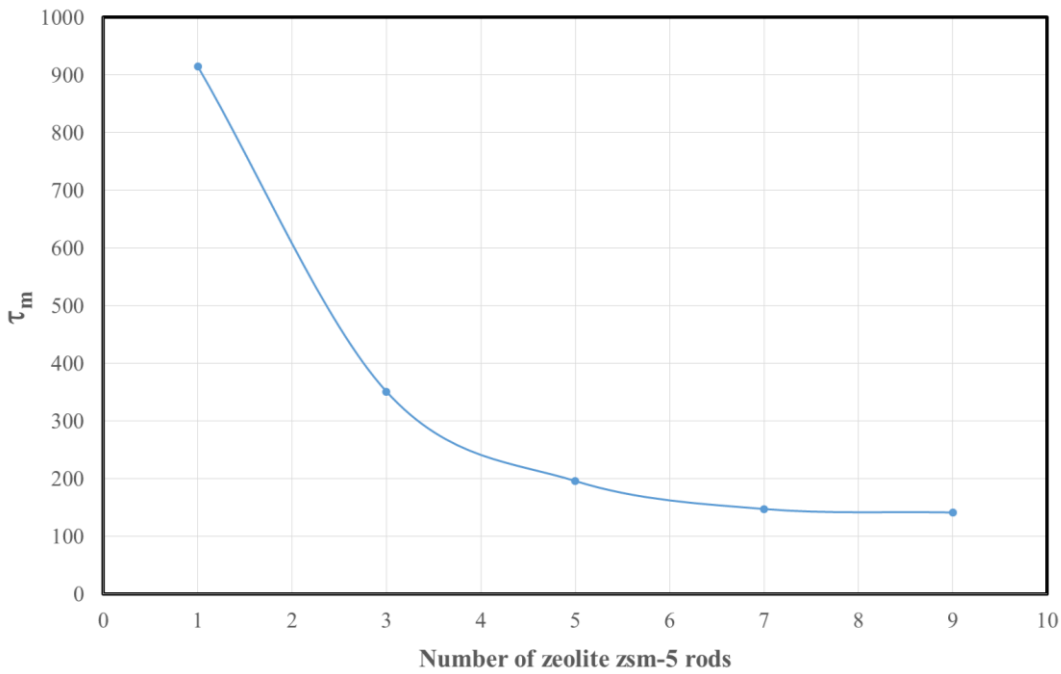

Figure 30: The dependence of τ_m on the number of zeolite rods used in the constructing the ZSM-5 membrane holder. The rest of the conditions are similar to those presented in Figure 27

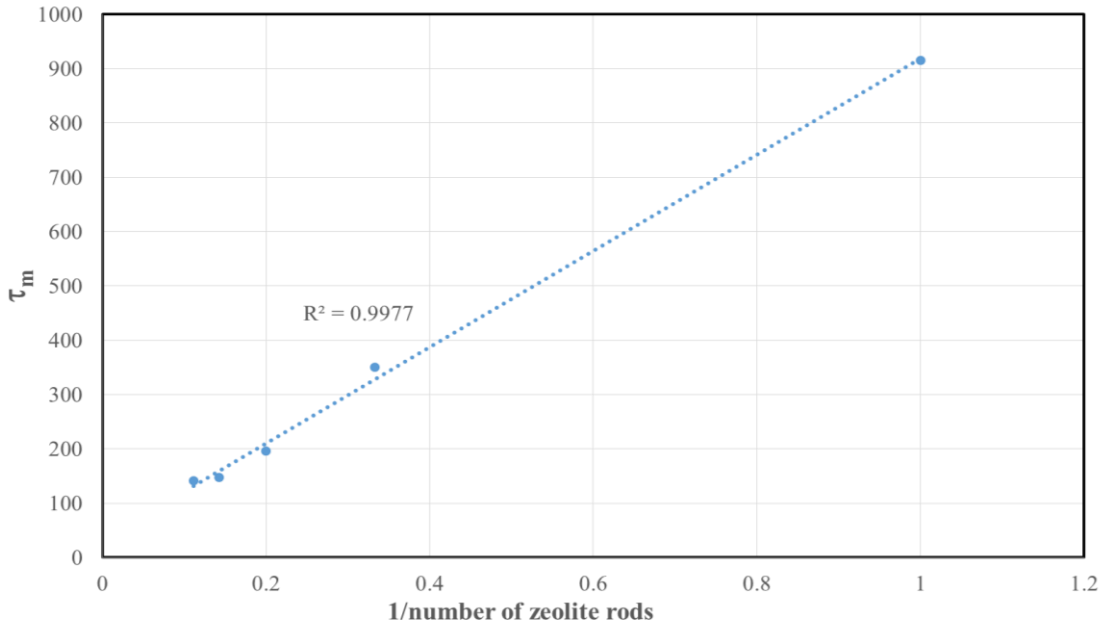

Figure 31: Plot of τ_m versus (1/number of zeolite rods). The conditions are similar to those presented in Figure 27

3.2.1.3 Membrane specific resistance (resistivity, σ_m) vs. the specific resistance (resistivity,σ)

Despite the role of the membrane geometric parameters (i.e., thickness and area) in determining the overall membrane resistance, the membrane specific resistance (resistivity, σ_m) remains the most essential parameter which in its own can be determined by several factors such as membrane material, pore size, pore density, etc. To complete the study of the proposed R_m and R analogy, additional experiments were conducted using membranes of identical geometric values but differ in one intrinsic property such as pore density (shown in Figure 32), surface treatment (shown in Figures 33 A &B) and membrane material (shown in Figure 34). Opposite of σ which is only determined by the intrinsic properties of the electric conductor, σ_m is also sensitive (albeit to different extents) to the permeating gas type as shown in Figure 35. Actually, the sensitivity of σ_m to the gas type forms the bases of the hypothesis of the

present work. It is evident that any change to the membrane intrinsic properties typically lead to change in σ_m.

In conclusion, the analogy between R_m and R has been validated using each of the relevant variables, i.e., the length, cross section and resistivity as depicted in the Figure 26.

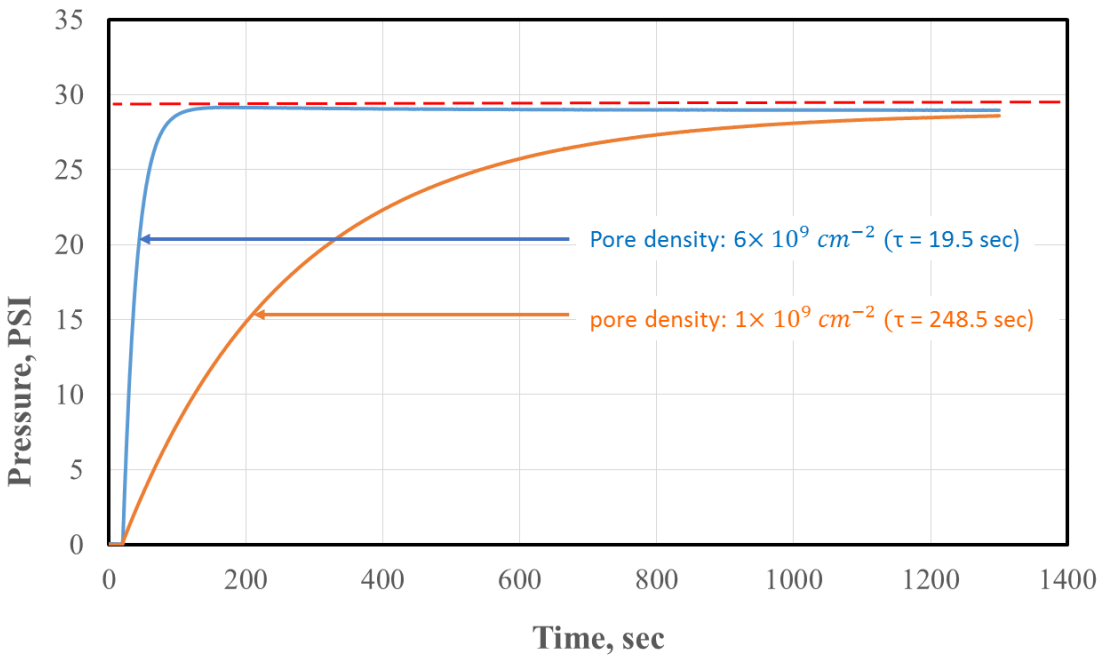

Figure 32: Polyimide 25 µm hydrophilic with pore density $6 \times 10^9\ cm^{-2}$ (τ = 19.5 sec), and Polyimide 25 µm hydrophilic with pore density $1 \times 10^9\ cm^{-2}$ τ = 248.5 sec)

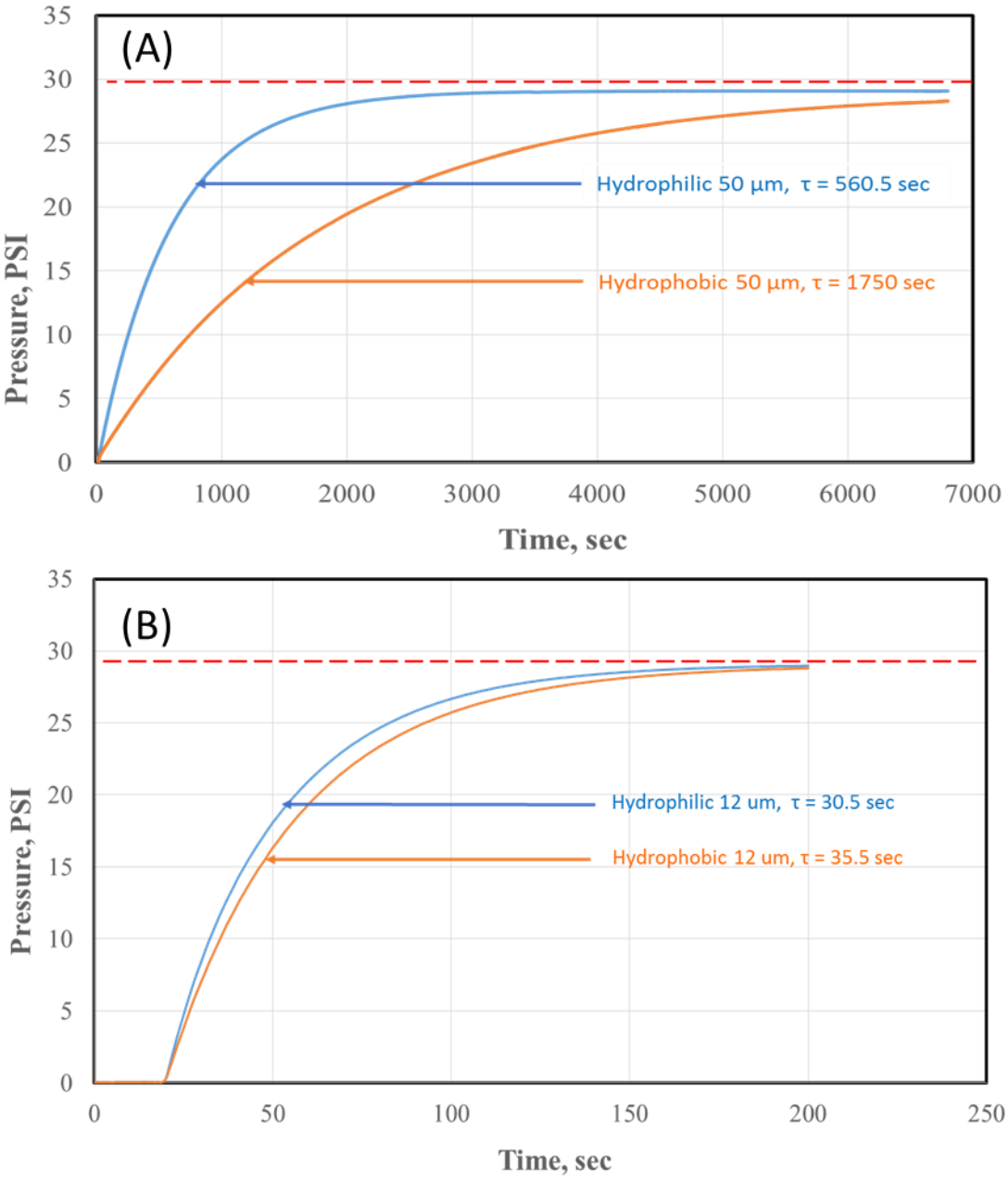

Figure 33: Effect of different types and treatment of membrane. (A) Effect of membrane treatment of 50 µm-thick polycarbonate membranes on the rate of N_2-gas permeation and hence the pressure build-up. (B) Effect of membrane treatment of 12 µm-thick polyester membranes on the rate of N_2-gas permeation and hence the pressure build-up. The rest of the conditions are similar to those presented in Figure 27

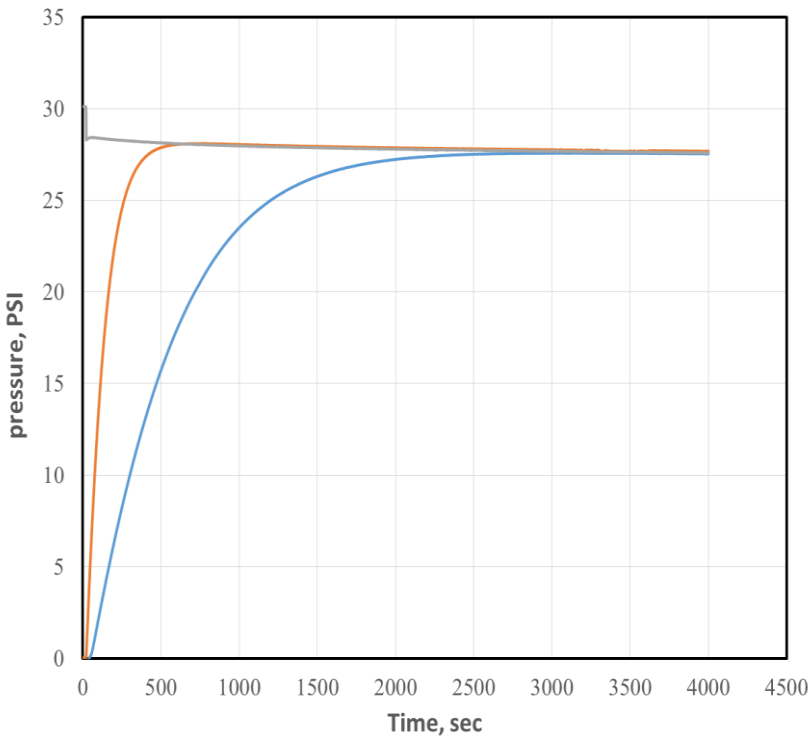

Figure 33: Effect of membrane type on the rate of Ethane-gas permeation and hence the pressure build-up. The rest of the conditions are similar to those presented in Figure 27

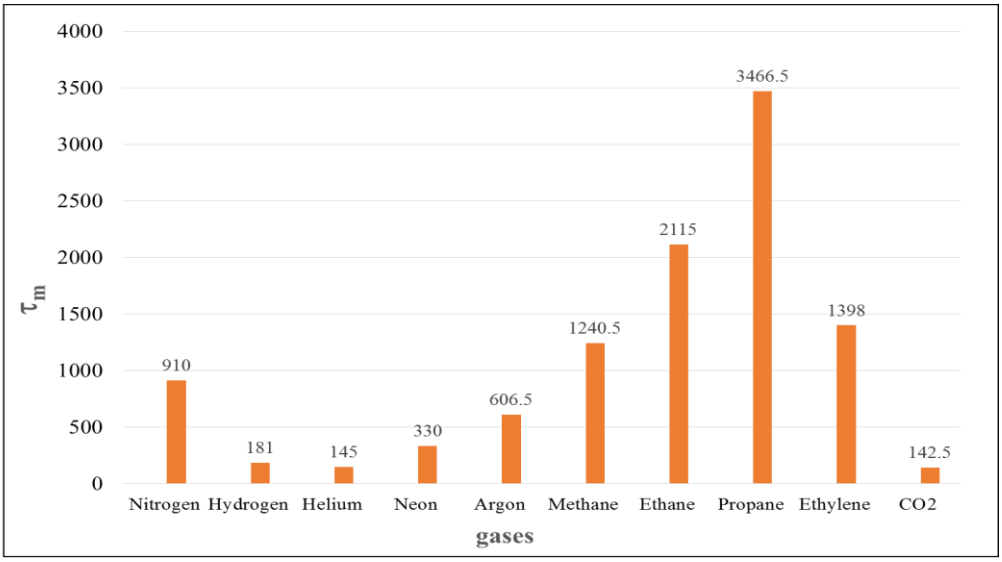

Figure 34: Illustration of the sensitivity of the membrane resistivity (σ_m) to the permeating gas type. Changes in σ_m lead to changes in R_m (given that $R_m = \sigma_m \times (l/Am)$ and hence the time contact τ_m (given that $\tau_m = R_m C_m$). The rest of the conditions are similar to those presented in Figure 27

3.2.2 Validation of the analogy between the confined volume behind the membrane (C_m) and the capacitance (C) of the capacitor in RC circuits

It is straightforward to qualitatively acknowledge that the larger the capacitance (C) value of the capacitor in an RC circuit, the longer the needed time for the electric current to charge the capacitor. This qualitative visualization is confirmed by the model [54] which predicts that the charging time depends only on the time constant, i.e., RC. To finalize the detailed analogy between the RC circuit and the present gas diffusion system, it was hypothesized that the confined volume behind the membrane and the gas sensor (i.e., the volume to be charged by the permeating gas from the pressurized gas inlet reservoir) is equivalent to the capacitance (C) of the capacitor in an RC circuit. Hereafter, this confined volume is denoted as C_m. To test this hypothesis, a series of pressure sensor holders were machined with different depths to create different confined volume (*cf.* Figure 16.) and used in parallel to monitor the pressure build-up of N_2-test gas permeation through PI-1 membrane. The obtained τ_m values were plotted against the depth of the confined volume as shown in Figure 36. The excellent linear regression between τ_m (at fixed R_m because of fixed membrane type) and the volume behind the membrane proves the validity of the proposed analogy between C_m and the confined volume.

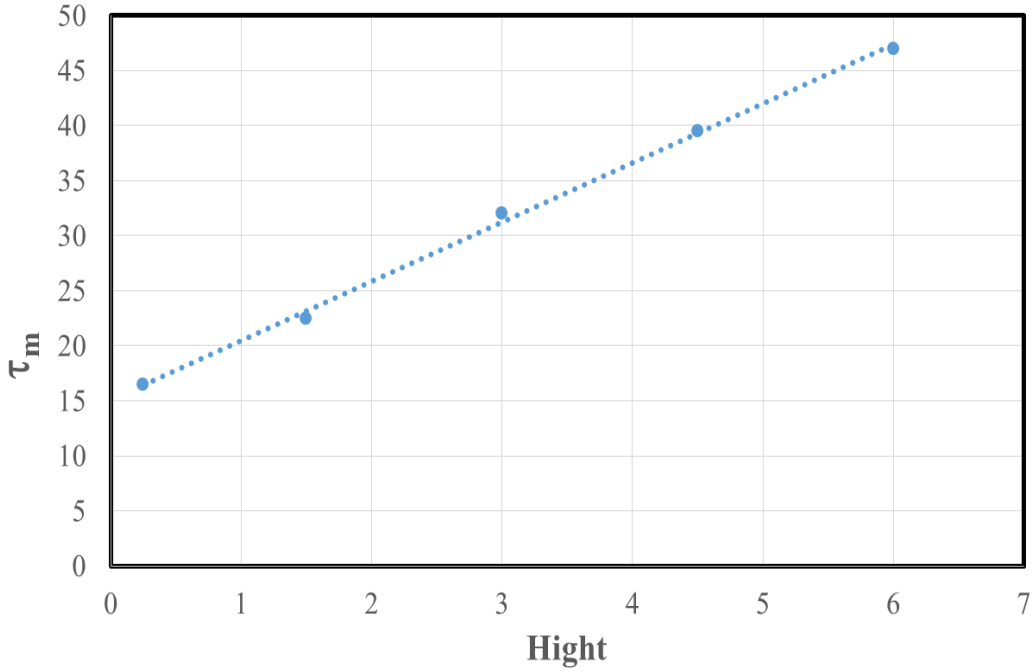

Figure 35: The effect of the depth of the cavity behind the membrane (which determines the confined volume) on τ_m. The rest of conditions are similar to those presented in Figure 27

3.3 Application of the present gas diffusion system

3.3.1 Qualitative analysis of different gases

In Figures 37 to 45, the obtained τ_m for ten different gases (i.e. nitrogen, hydrogen, helium, neon, argon, methane, ethane, propane, ethylene, carbon dioxide) were plotted for a given membrane respectively for Teflon AF, silicon rubber, polycarbonate hydrophilic 50 µm, polycarbonate hydrophobic 50 µm, zeolite zsm-5, zeolite Nay, six membranes of polycarbonate hydrophilic 6 µm over each other, alumina 51 µm, and alumina 101 µm. Visual inspection of Figures 37 to 45 confirm the appropriateness of each of the selected membranes to exhibit variable selectivities to different gases.

Plotting of τ_m for each gas at different membranes are shown in Figures 46 to 55. Visual inspection of these figures clearly confirms the uniqueness of the pattern obtained for each gas. Such patterns could be tentatively named as "diffusion spectrum". It is worth mentioning that the bar graphs of the presented diffusion spectrum has outlook similar to the well-established mass spectra.

For more complex database for larger number of gases (and mixtures, e.g. crude natural gas, and purified natural gas), an algorithm could be developed for gas (or mixture) identification from its diffusion spectrum.

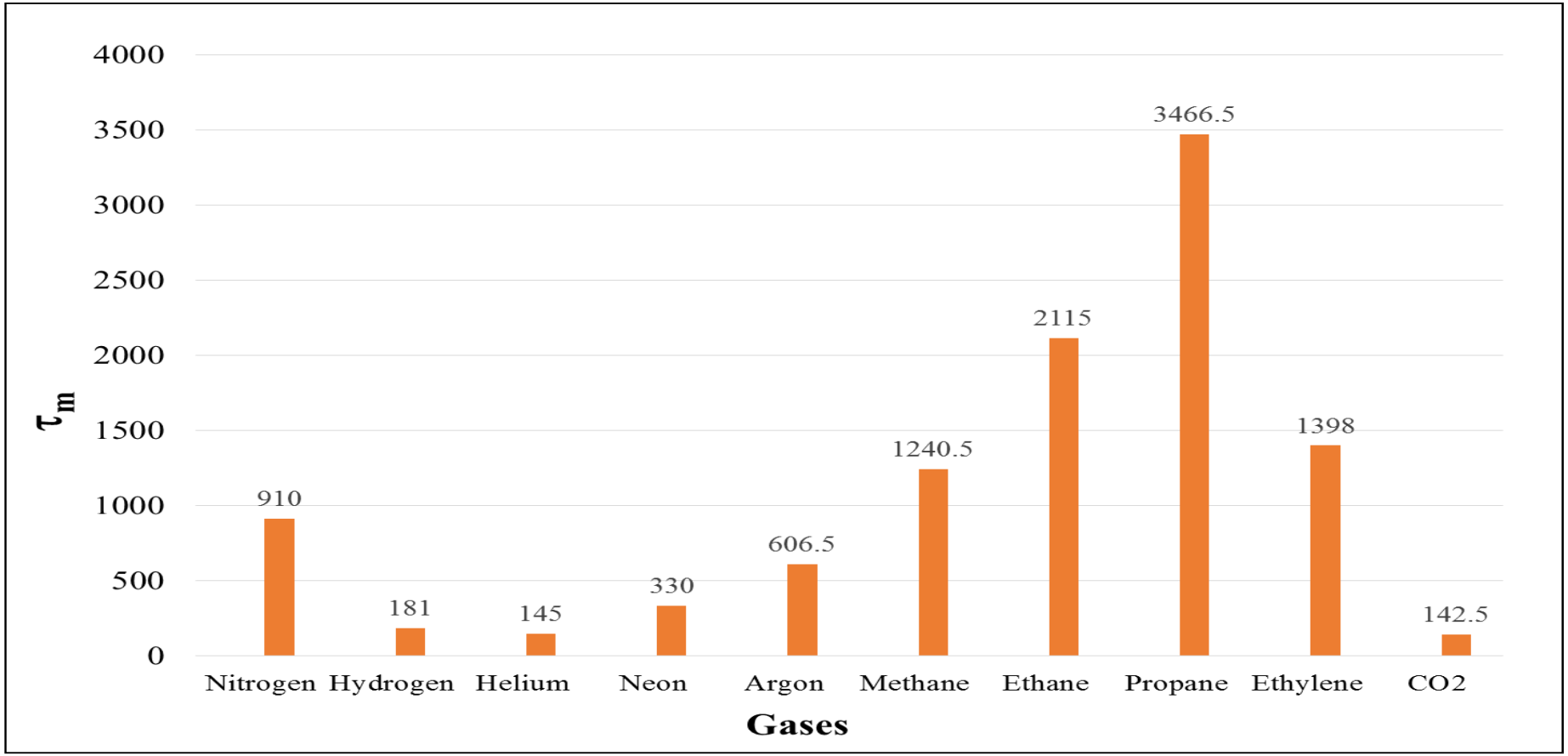

Figure 36: Teflon AF with different gases

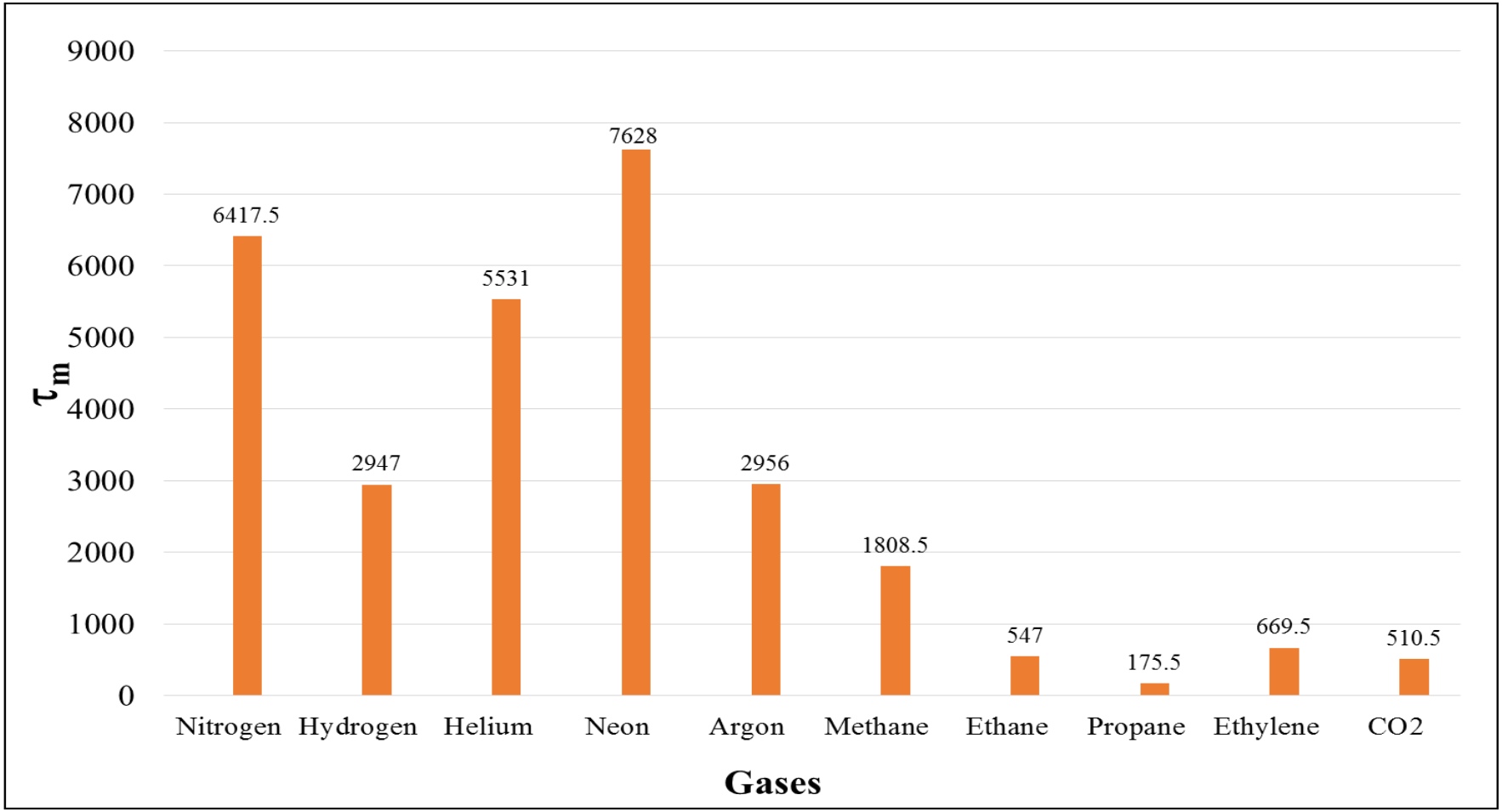

Figure 37: Silicon Rubber with different gases

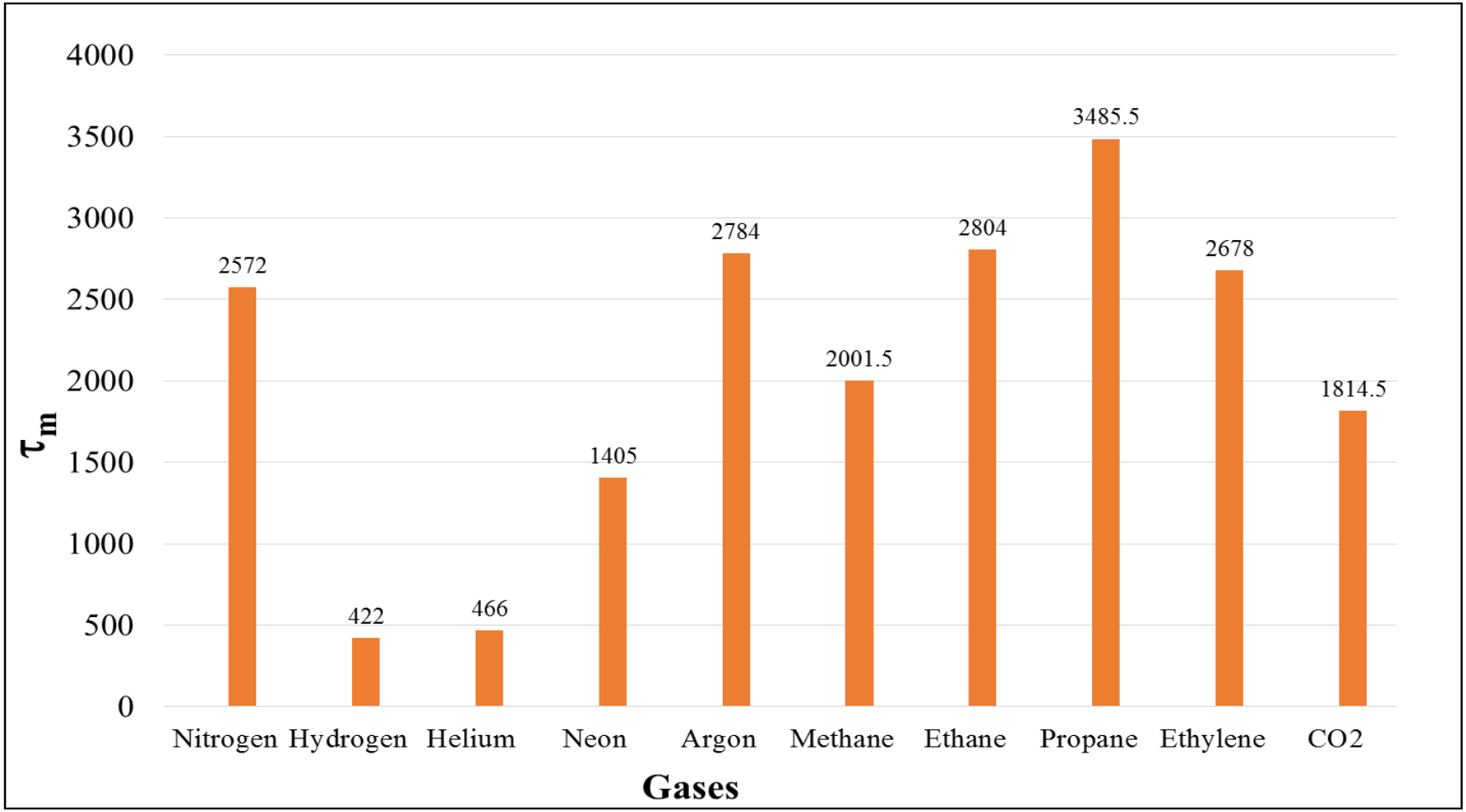

Figure 38: Polycarbonate hydrophilic 50 µm with different gases

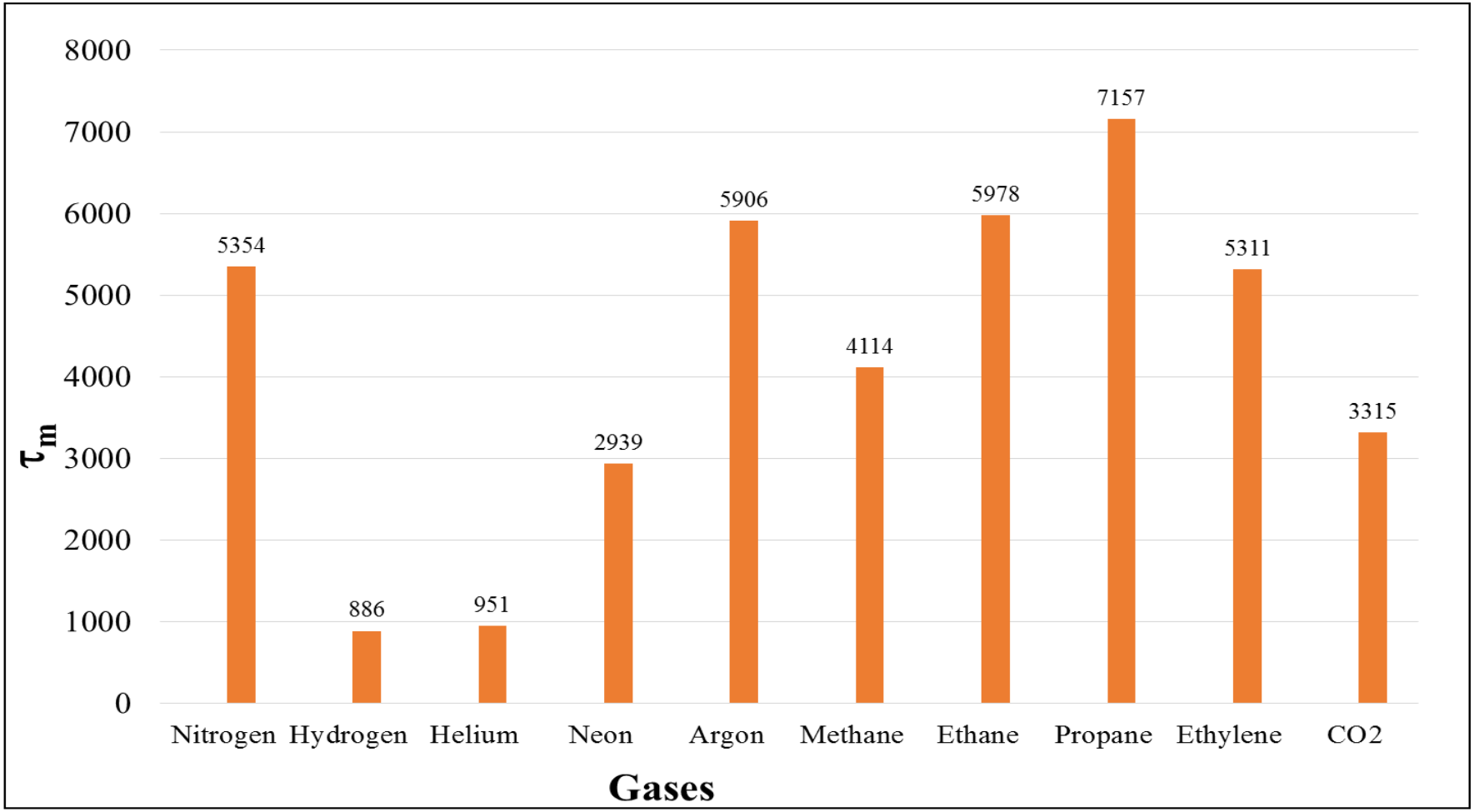

Figure 39: Polycarbonate hydrophobic 50 µm with different gases

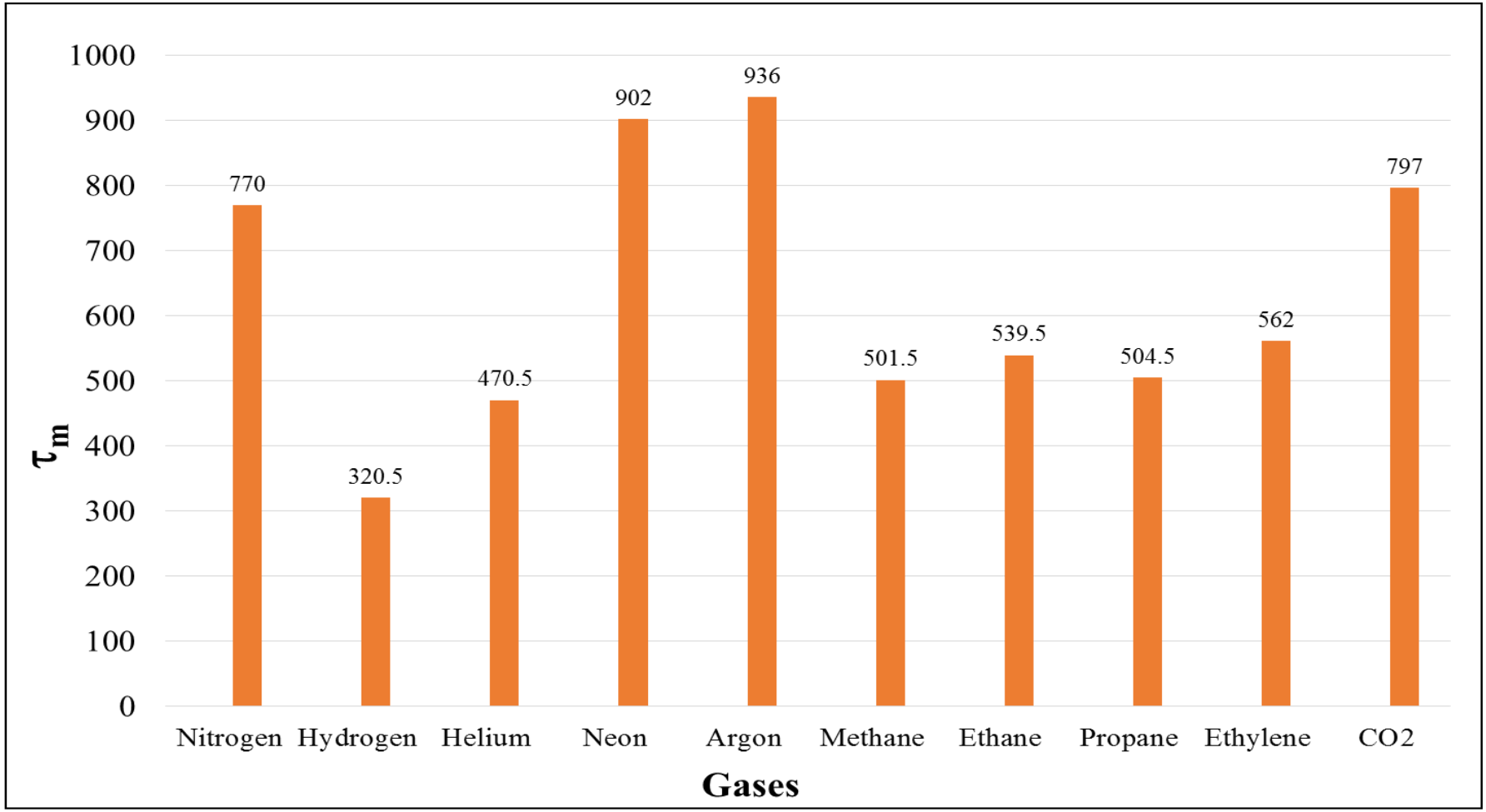

Figure 40: Zeolite zsm-5 with different gases

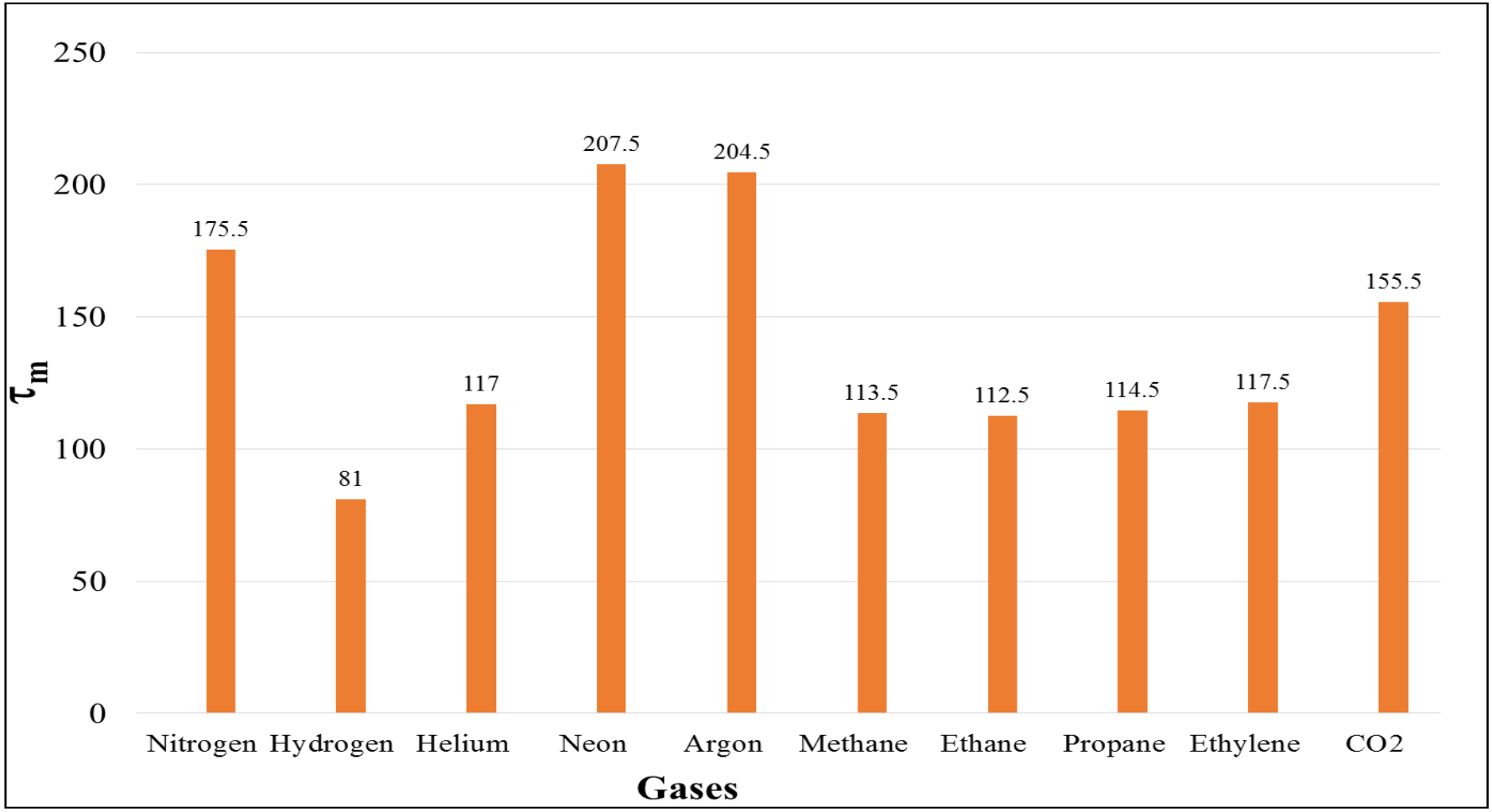

Figure 41: Zeolite Nay with different gases

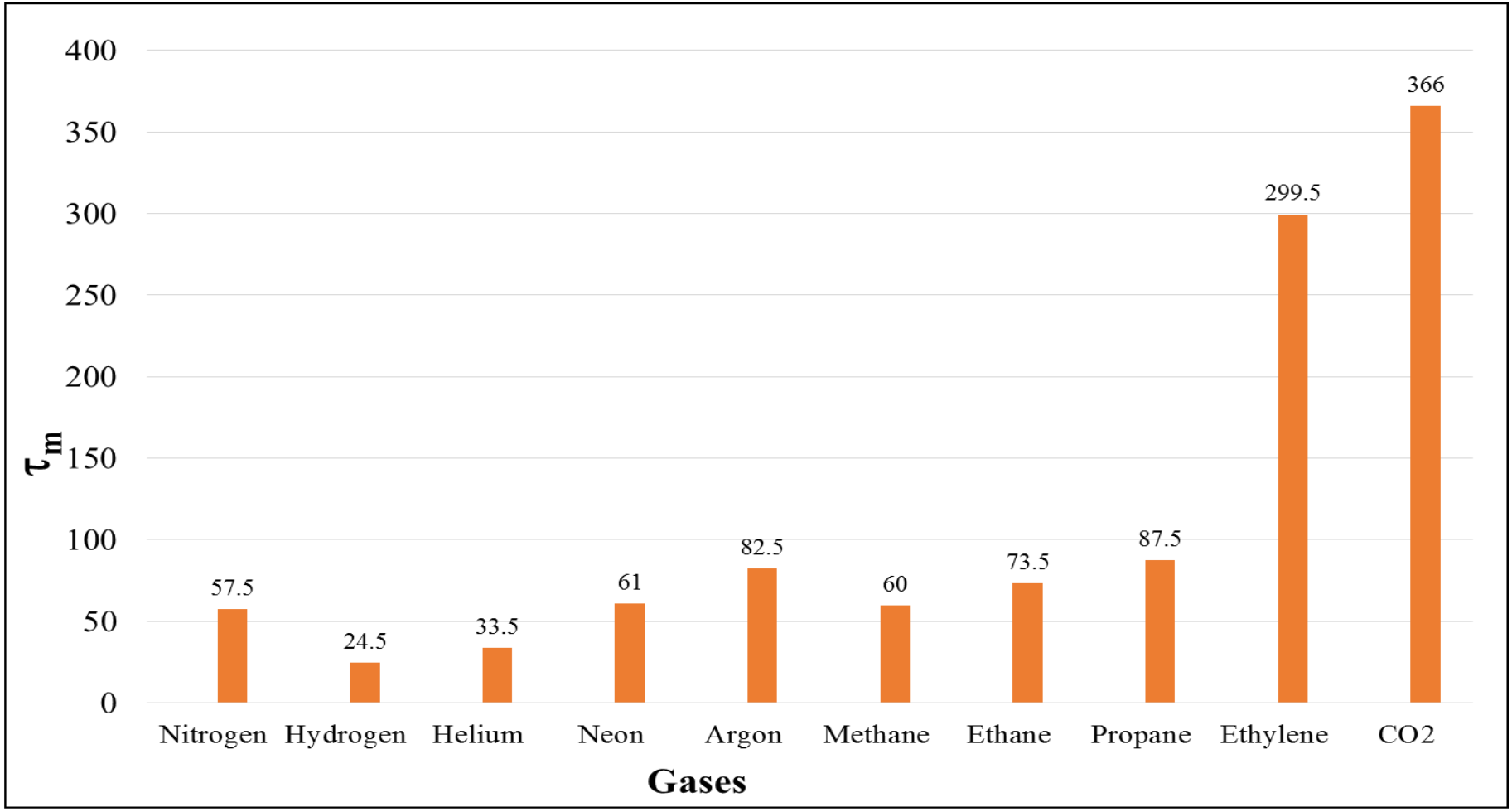

Figure 42: Six membranes of polycarbonate hydrophilic with different gases

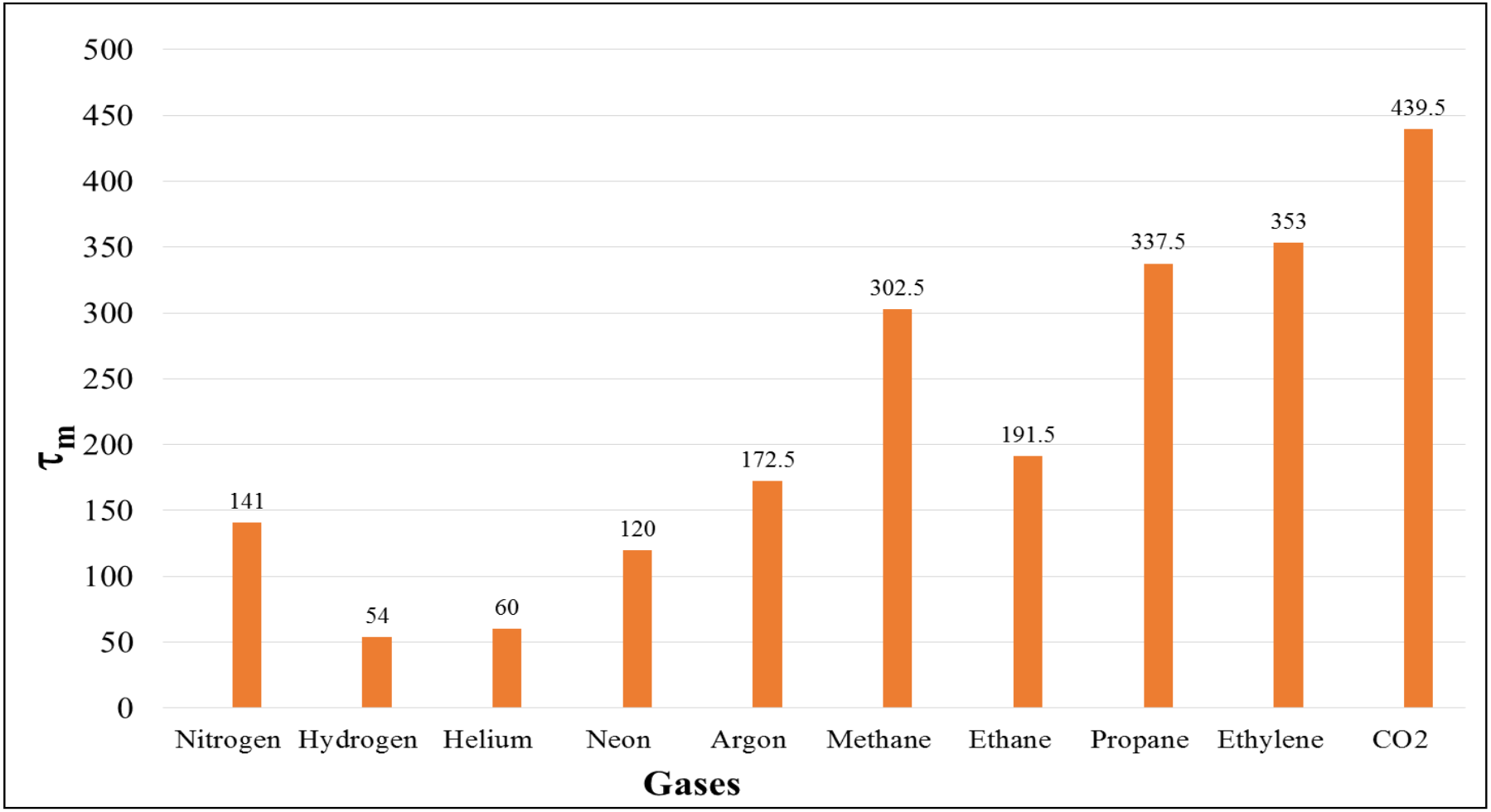

Figure 43: Alumina 51 µm with different gases

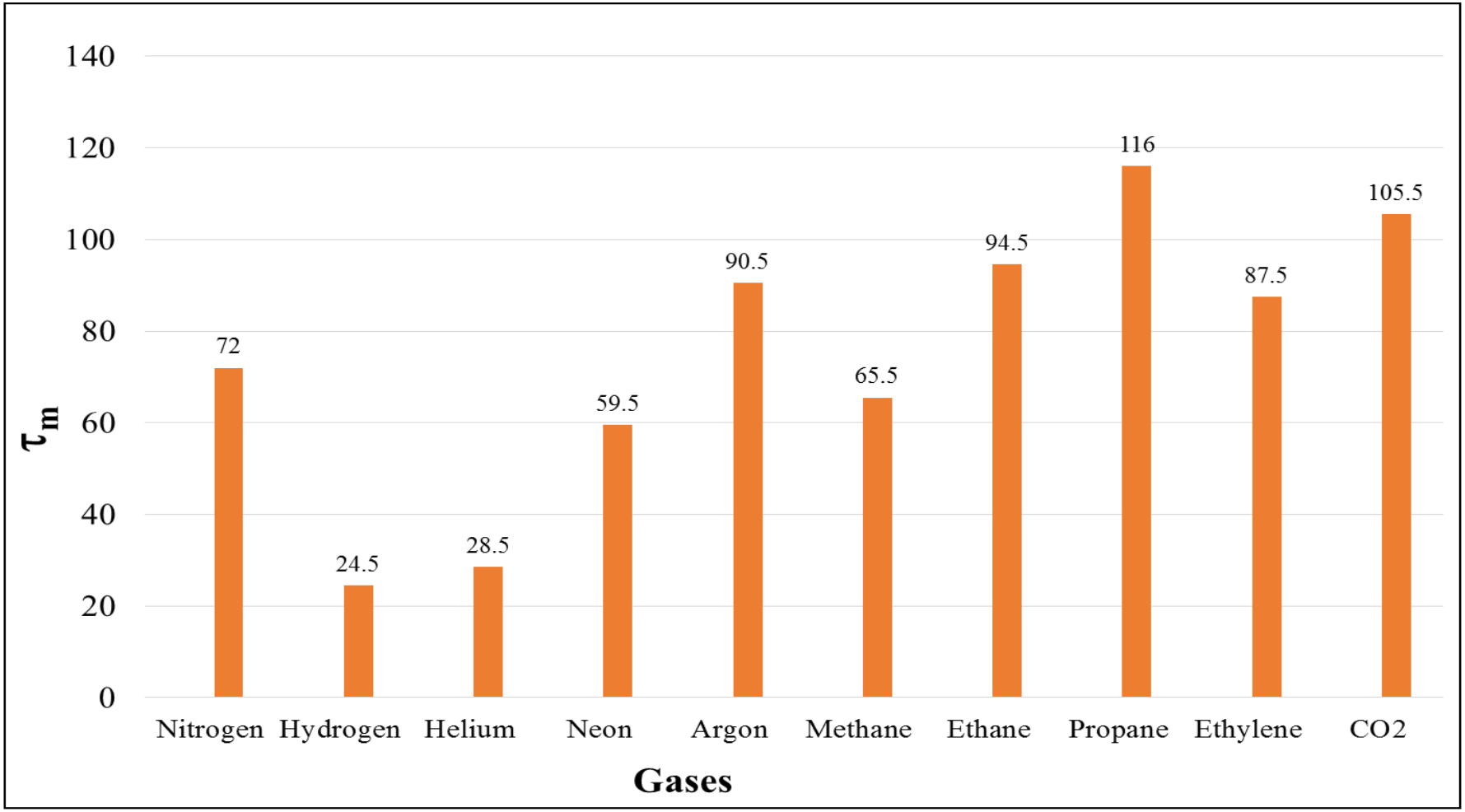

Figure 44: Alumina 101 µm with different gases

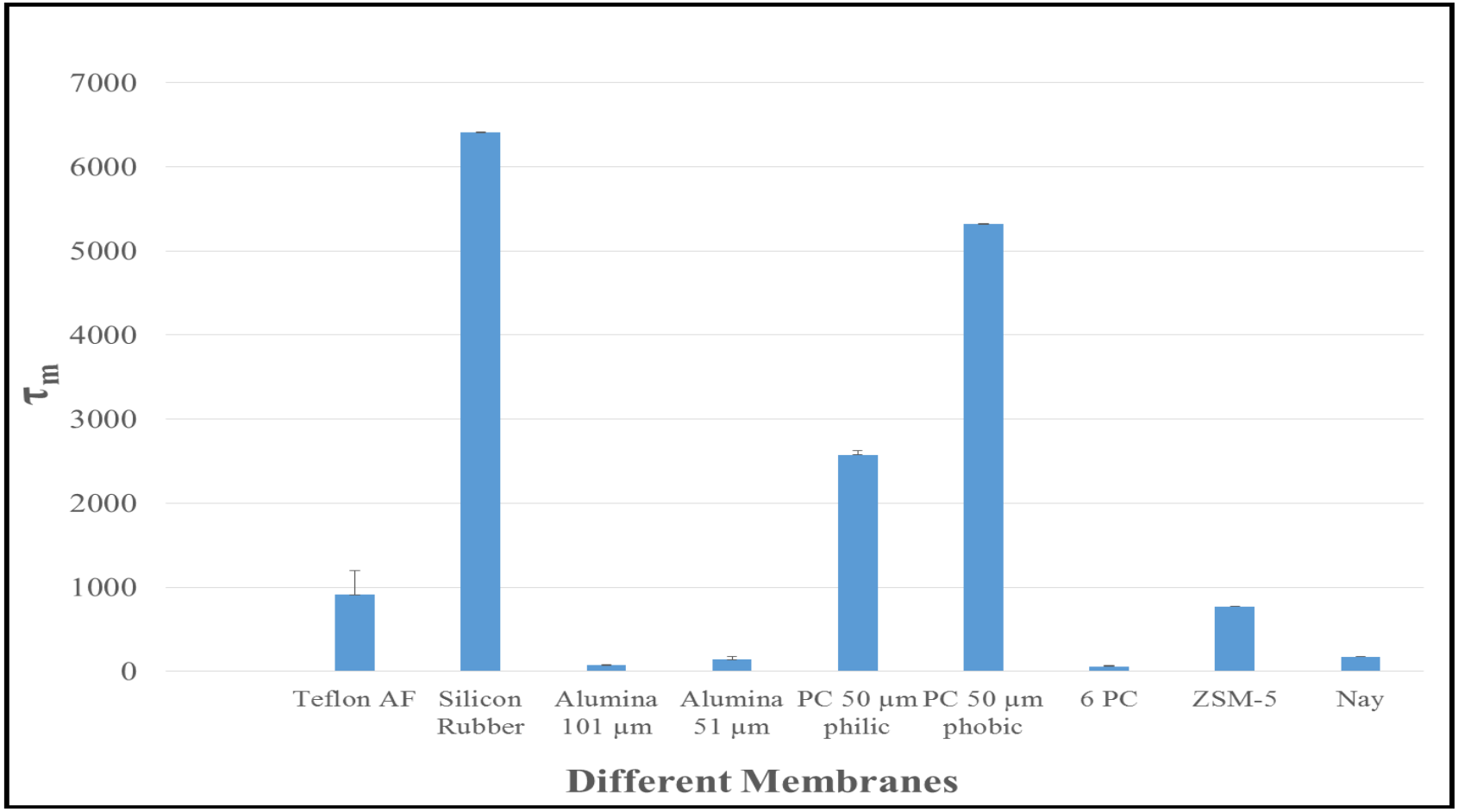

Figure 45: Nitrogen gas with different membranes

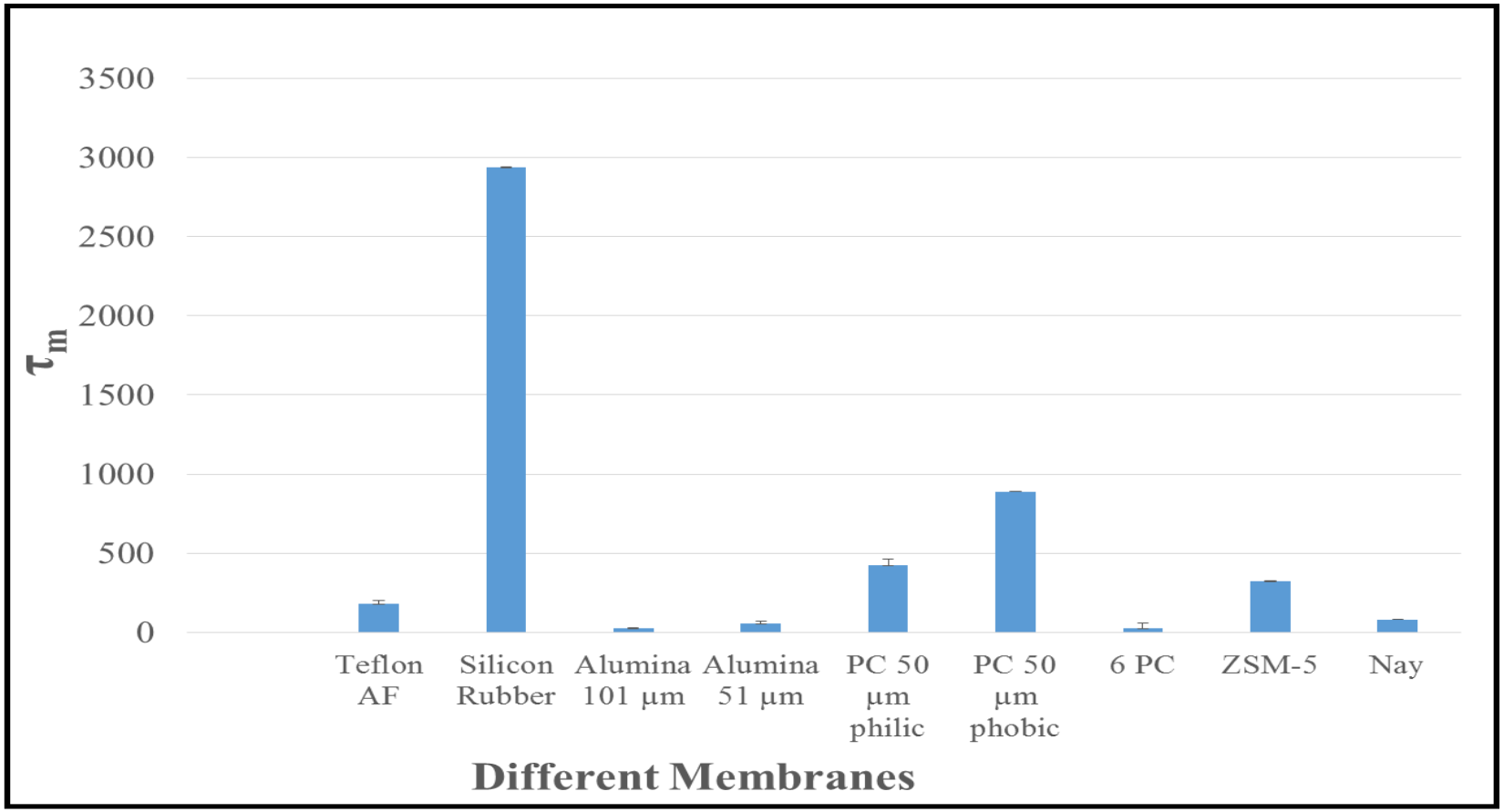

Figure 46: Hydrogen gas with different membranes

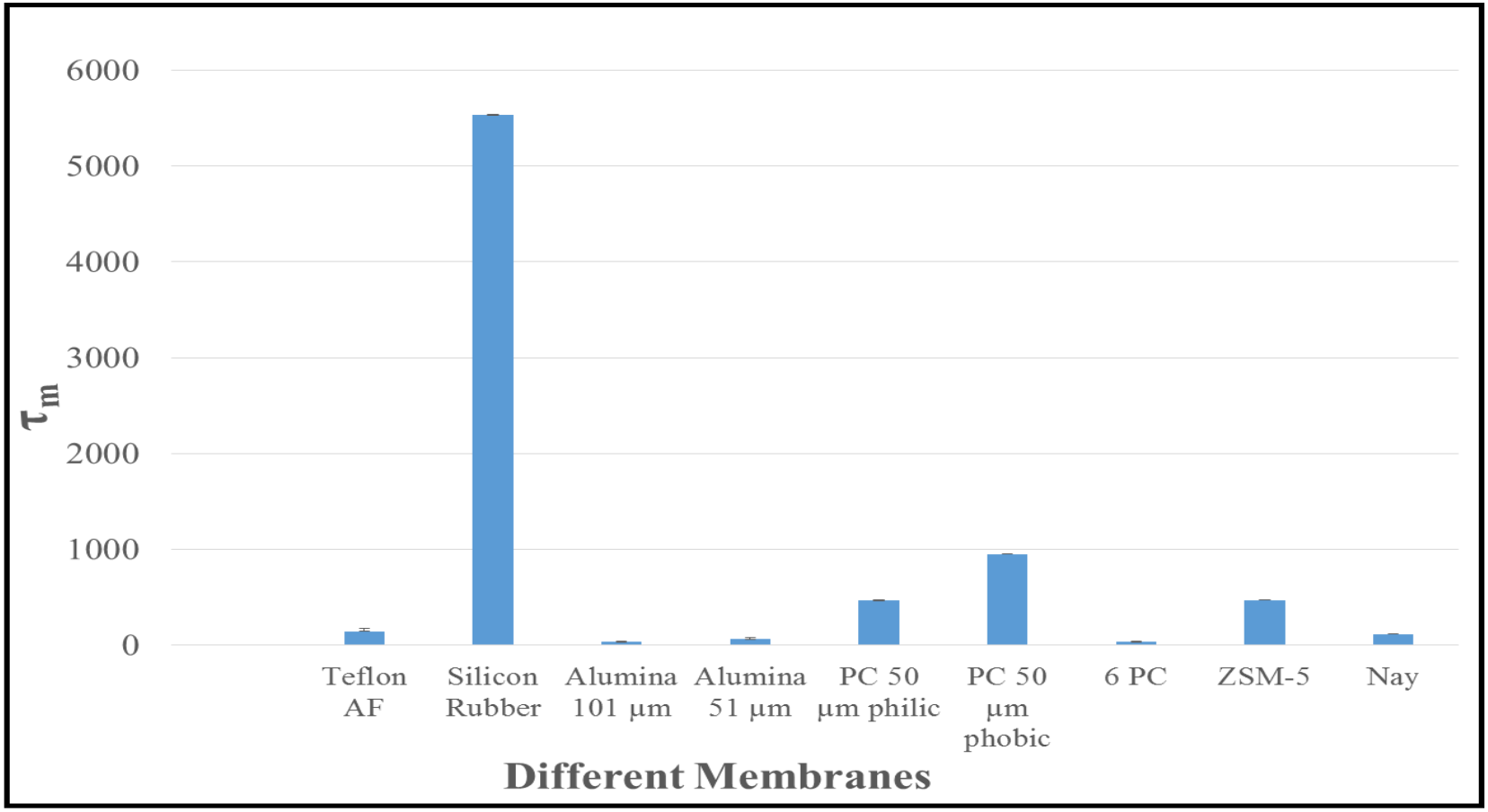

Figure 47: Helium gas with different membranes

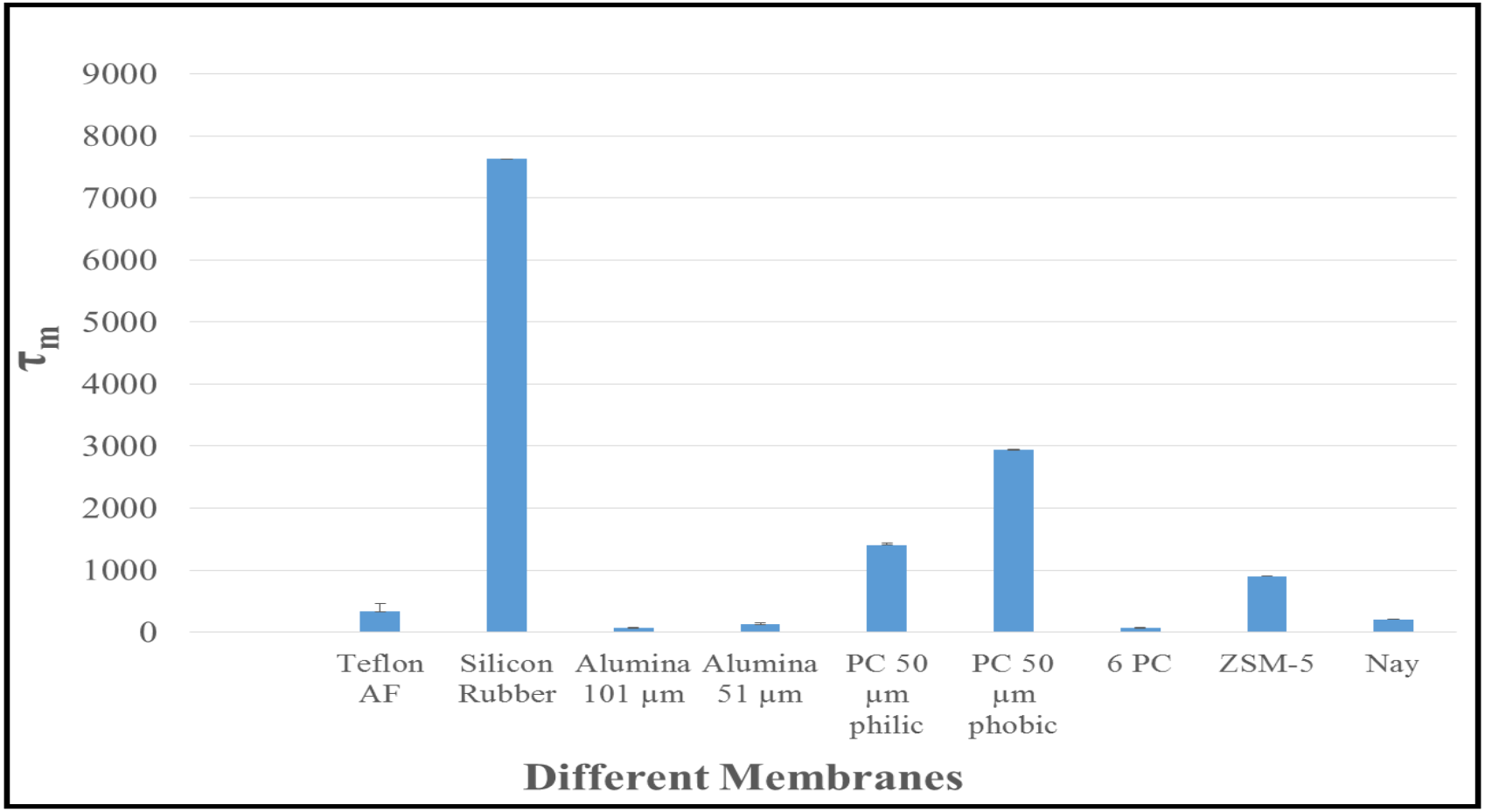

Figure 48: Neon gas with different membranes

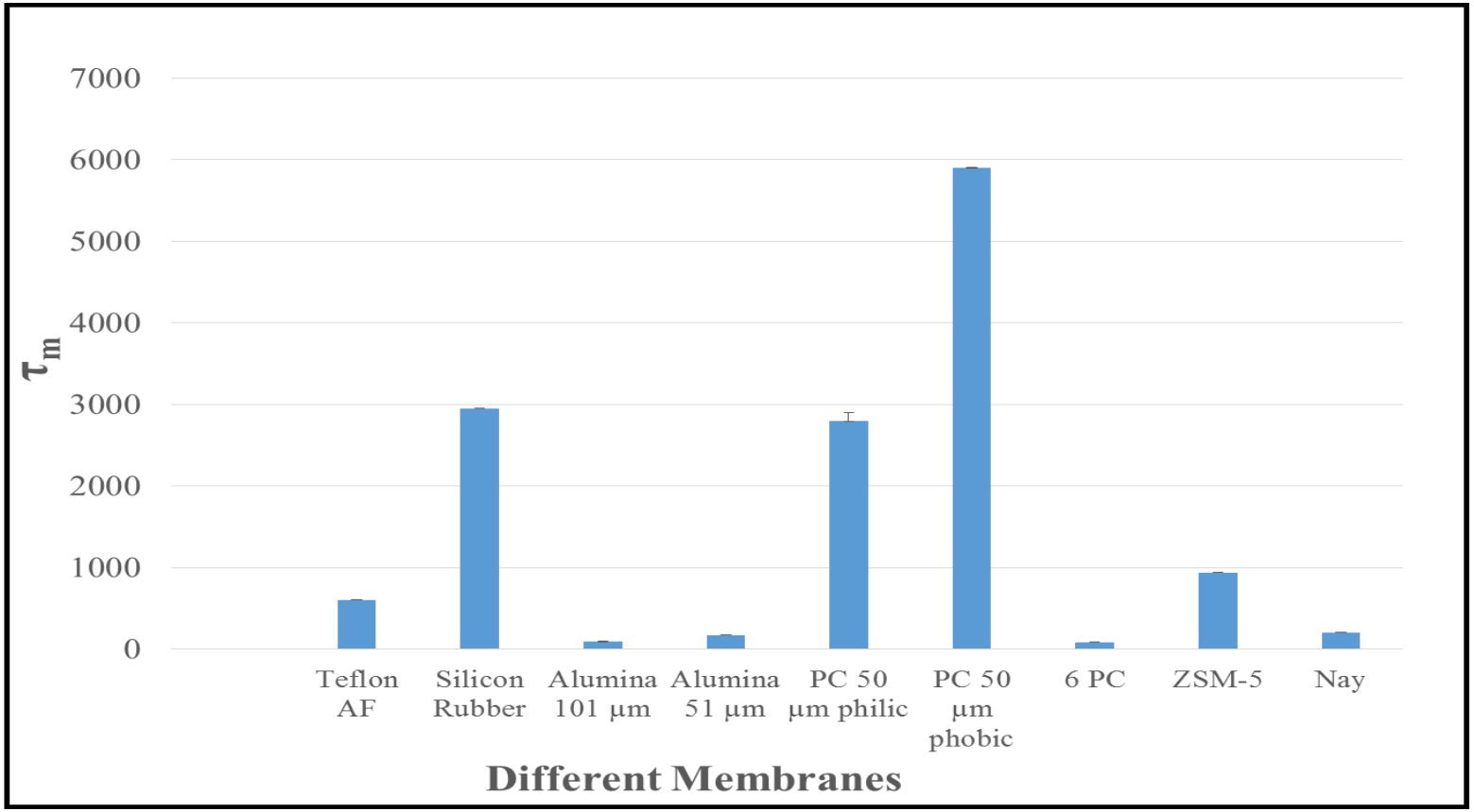

Figure 49: Argon gas with different membranes

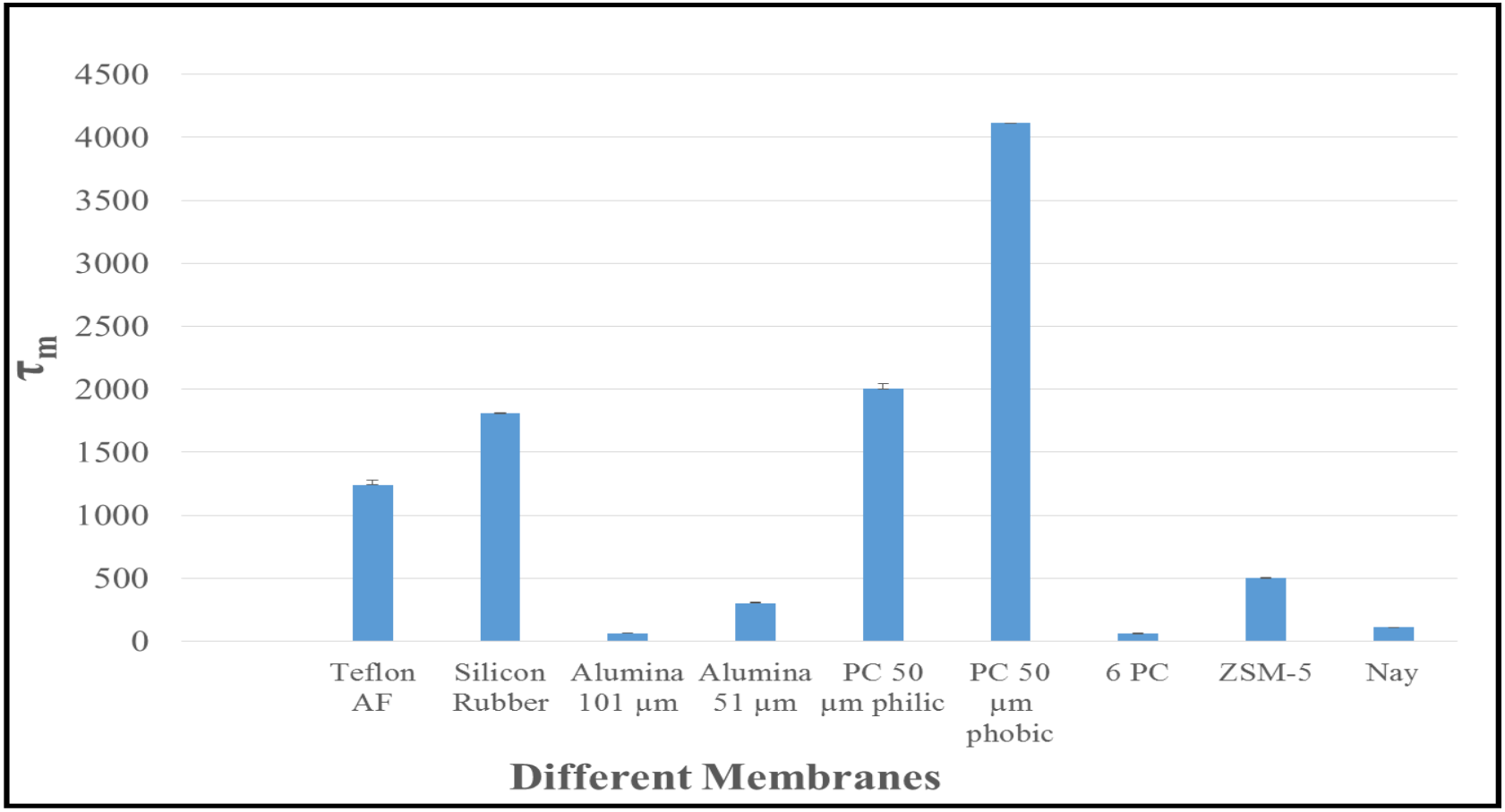

Figure 50: Methane gas with different membranes

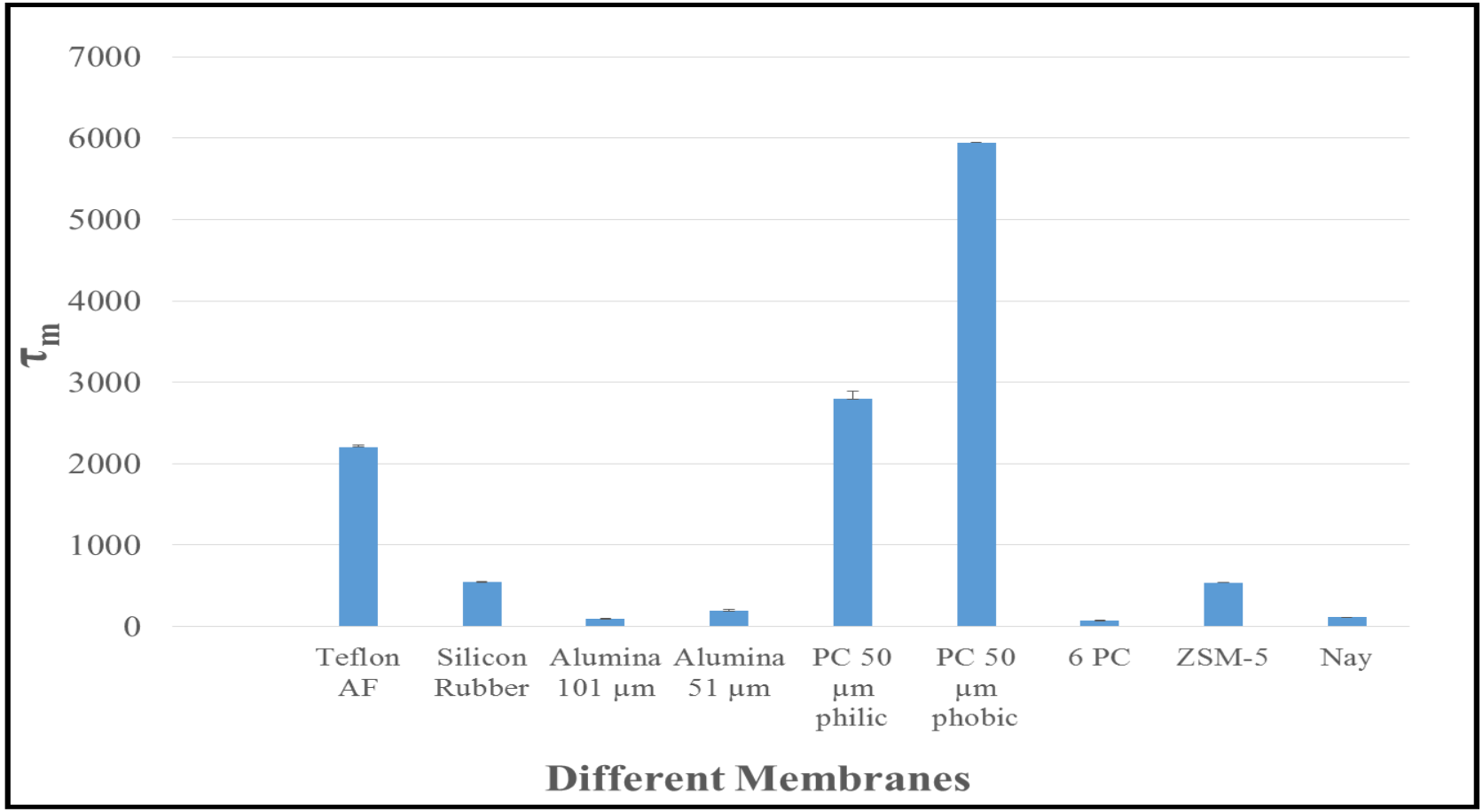

Figure 51: Ethane gas with different membranes

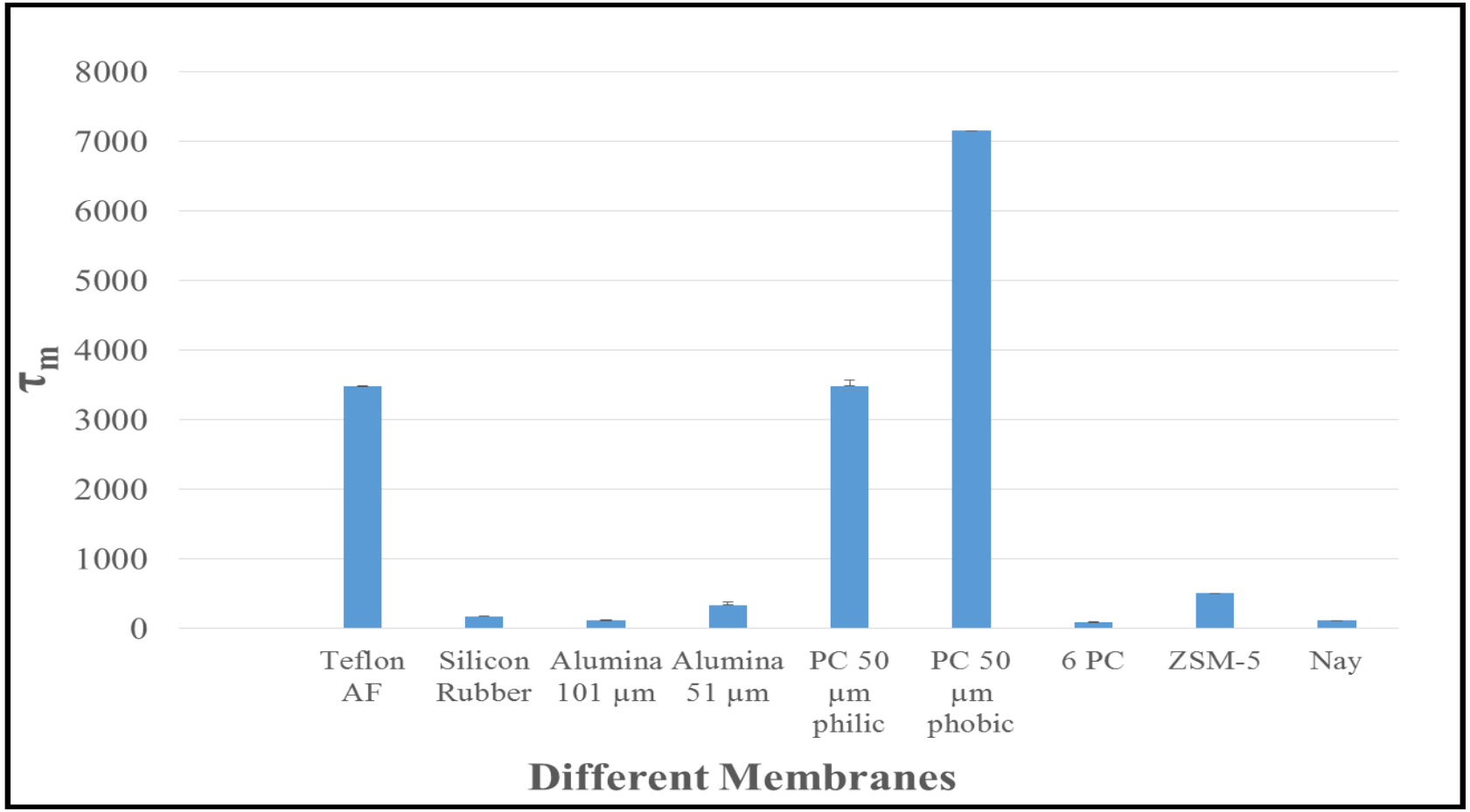

Figure 52: Propane gas with different membranes

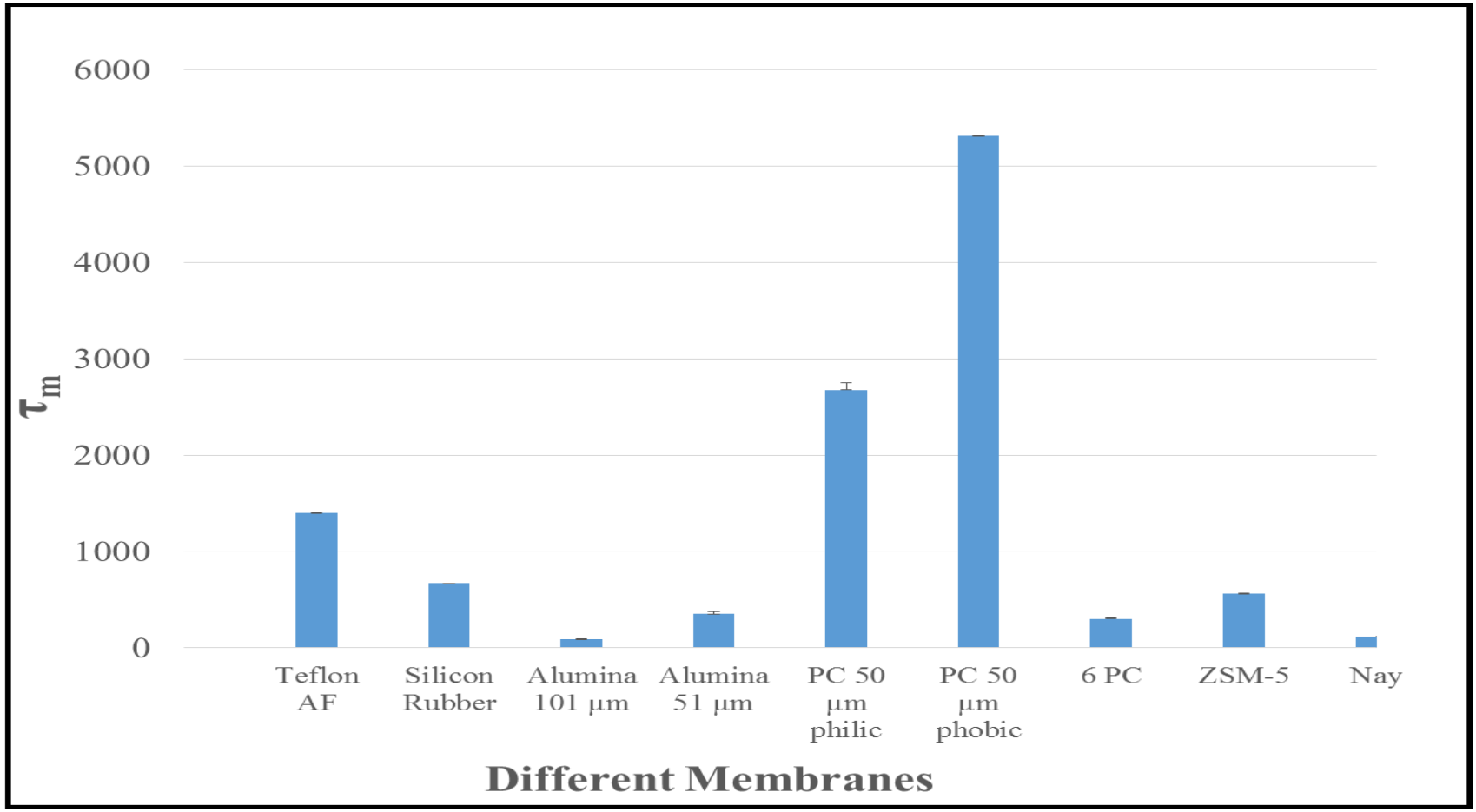

Figure 53: Ethylene gas with different membranes

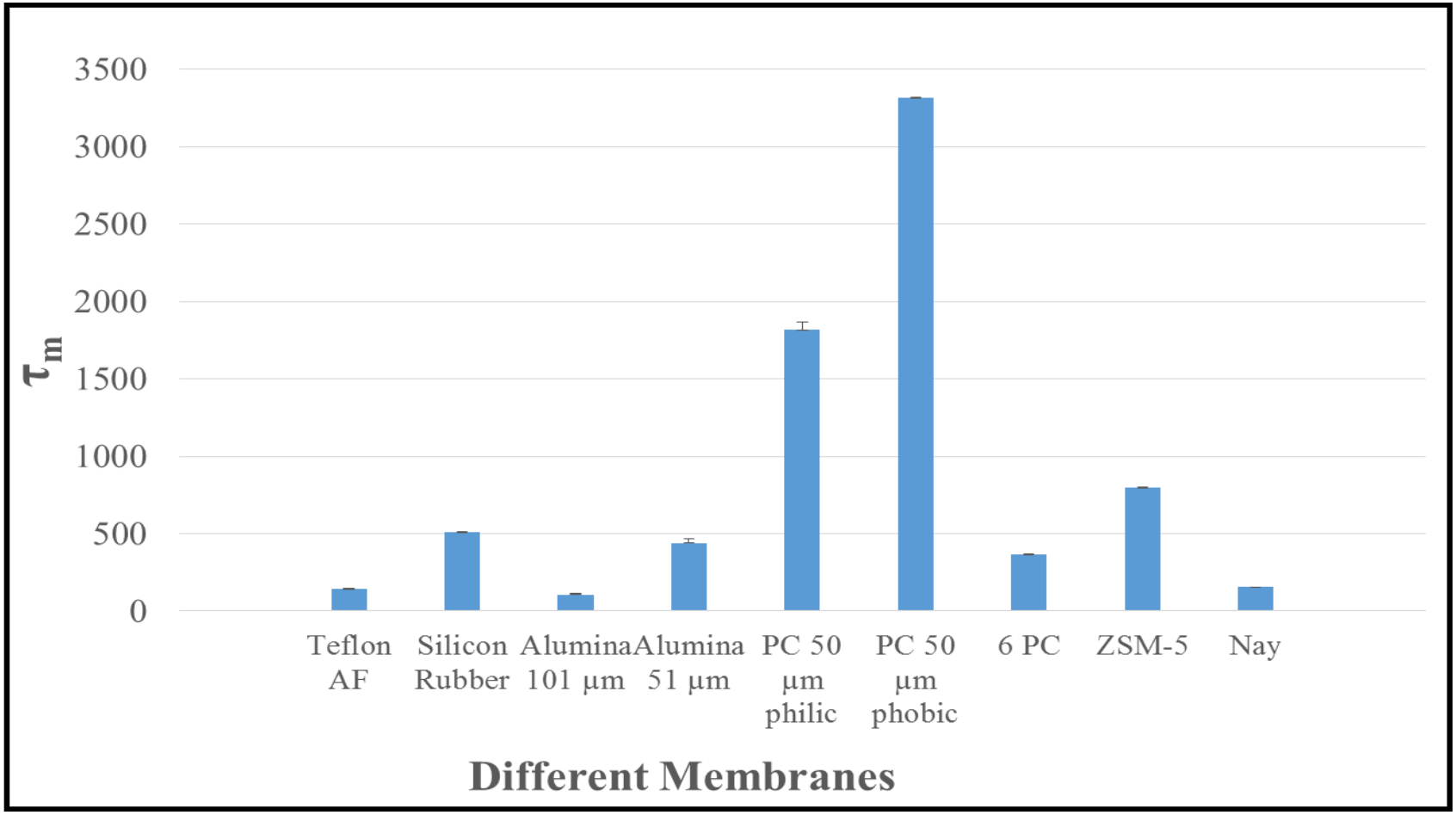

Figure 54: Carbon Dioxide gas with different membranes

3.3.2 Quantitative analysis of N_2-CO_2 binary gas mixture

Preliminary attempt was made to explore the possibility of using at least one channel of the described gas diffusion system in semi-quantitative analysis of binary gas mixtures. The membrane of choice should be a membrane that exhibits wide variation in the permeation rates of the two individual gases constituting the binary mixture. For CO_2 and N_2 binary mixtures, Zeolite ZSM-5 membrane (Figure 41) will not be a suitable option at all since the two gases have almost identical permeation rates. Hence, the rate of permeation of 10% CO_2-90% N_2 mixture will be almost identical to that of 90% CO_2-10% N_2 (i.e., extremely low sensitivity). Whereas, silicone rubber membrane should exhibit highest sensitivity since N_2 and CO_2 have the largest ratio between the permeation rates of the two gases as shown in Figure 38. On the other hand, polycarbonate membrane (shown in Figure 40) for example, is expected to show lower sensitivity than Silicone rubber owing to the smaller ratio between the permeation rates of CO_2 and N_2.

Figure 56 shows the obtained calibration plot of τ_m against the % of CO_2 in the mixture. Apparently, τ_m showed substantial sensitivity to the gas mixture composition, with significant non-linearity though. More extensive future investigation is needed to explore the potential of the present gas diffusion system in quantitative analysis and by enhancing the sensitivity and the linearity. This investigation will include other binary mixtures and membranes. Also, the initial rate of the permeation plots could be used as the measurable signal instead of τ_m.

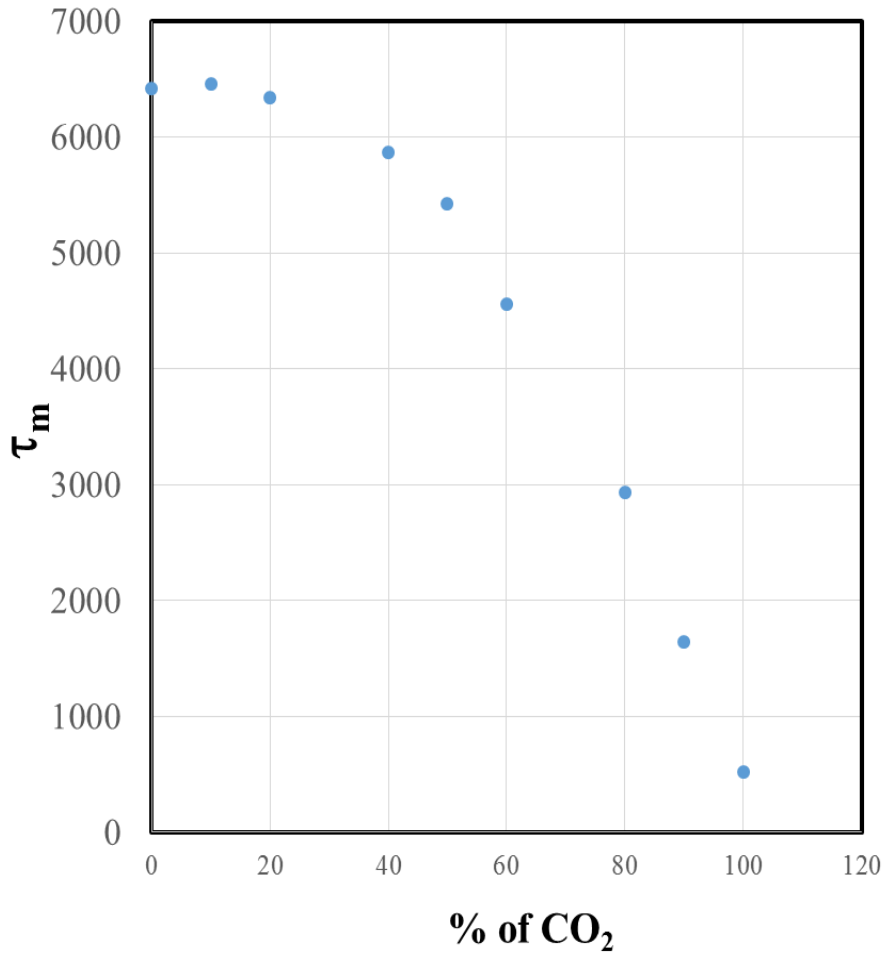

Figure 55: Silicone Rubber vs. mixtures of N_2 and CO_2

Chapter 4: Conclusions and future work

In the present thesis, the following was successfully demonstrated:

(i) Detailed construction and characterization of a 6-channel parallel gas diffusion system.

(ii) Extensive validation of the hypothesized analogy between the RC-circuit and the present gas diffusion system.

(iii) Extensive validation of the hypothesized analogy between the membrane resistance and the electrical resistor in an RC circuit.

(iv) Proving the initial hypothesis of using parallel gas diffusion system in the qualitative identification of gases with good sensitivity (at least among the 10 tested gases).

(v) Preliminary results on the potential application of the presented gas diffusion system in the semi-quantitative determination of binary gas mixtures.

The proven excellent potential of the described system strongly suggests further refinement to construct a portable version. The concept design of the intended portable version is shown in Figure 57. The major intended changes include the following:

1- Utilization of micro-pressure sensors (ideally based on wireless data transmission).

2- Using a single cover (which also act as holder for the pressure sensors) for all channels.

3- Integration of the gas inlet reservoir with the membrane holder and sensors in a single unit.

4- Utilization of solenoid valves instead of manual valves to control the test gas inlet and venting.

5- Use of ~ 100 mL glass syringe for manual test gas pressurization in the inlet reservoir. This is essential for ambient gas testing.

The future version of the gas diffusion system should pave the road for more extensive applications such as quick assessment of the mixture composition or finger printing of gases.

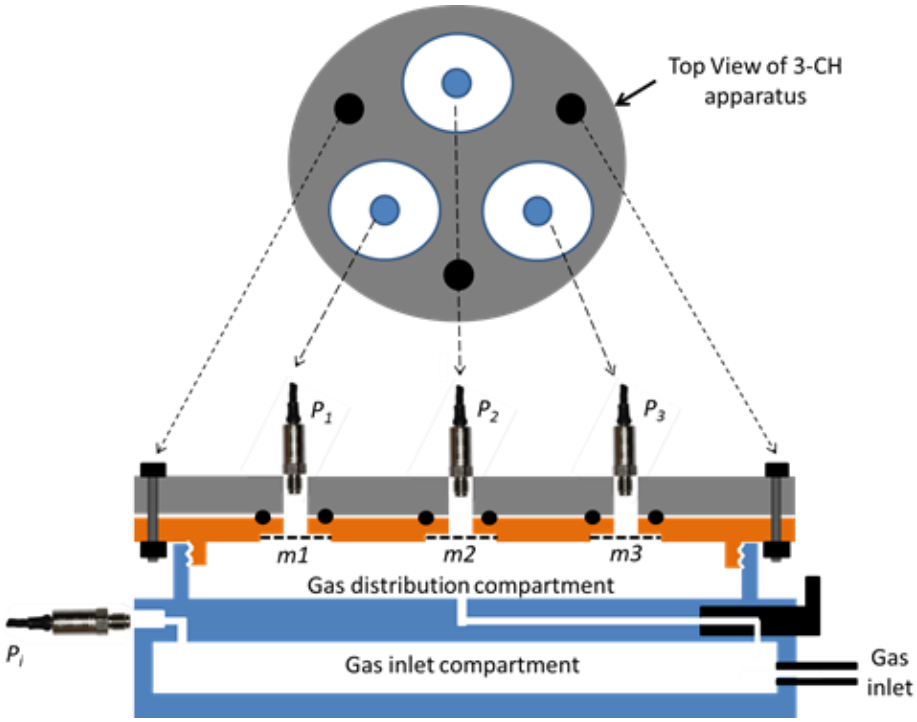

Figure 56: The proposed compact design of the gas diffusion system

References

[1] M. A. A. El-Ghaffar and H. A. Tieama, "A Review of Membranes Classifications, Configurations, Surface Modifications, Characteristics and Its Applications in Water Purification," pp. 1–26, 2017.

[2] X. Chen and J. Shen, "Review of membranes in microfluidics," *J. Chem. Technol. Biotechnol.*, vol. 92, no. 2, pp. 271–282, 2017.

[3] "Chapter 3 - Membrane Classification and Membrane Operations," pp. 1–28, 2016.

[4] N. Kosinov, J. Gascon, F. Kapteijn, and E. J. M. Hensen, "Recent developments in zeolite membranes for gas separation," *J. Membr. Sci.*, vol. 499, pp. 65–79, 2016.

[5] L. W. McKeen, "Fluoropolymers," in *Film Properties of Plastics and Elastomers*, Elsevier, pp. 255–313, 2012.

[6] S.-J. Park and M.-K. Seo, "Element and Processing," in *Interface Science and Technology*, vol. 18, Elsevier, pp. 431–499, 2011.

[7] D. Kyriacos,"Polycarbonates," in *Brydson's Plastics Materials*, Elsevier, pp. 457–485, 2017.

[8] S. T. Oyama, M. Yamada, T. Sugawara, A. Takagaki, and R. Kikuchi, "Review on Mechanisms of Gas Permeation through Inorganic Membranes," *J. Jpn. Pet. Inst.*,vol. 54, no. 5, pp. 298–309, 2011.

[9] T. Li, Y. Wu, J. Huang, and S. Zhang, "Gas sensors based on membrane diffusion for environmental monitoring," *Sens. Actuators B Chem.*, vol. 243, pp. 566–578, 2017.

[10] H. Zhang and S. G. Weber, "Teflon AF Materials," in *Fluorous Chemistry*, vol. 308, I. T. Horváth, Ed. Berlin, Heidelberg: Springer Berlin Heidelberg, pp. 307–337, 2011.

[11] H. Zhang, "Teflon af composite materials in membrane separation and molecular recognition in fluorous media," Ph.D dissertation, College of Art and Science, Pittsburgh Univ., pp. 1–25, 2013.

[12] I. Pinnau and L. G. Toy, "Gas and vapor transport properties of amorphous perfluorinated copolymer membranes based on 2,2-bistrifluoromethyl-4,5-difluoro-l,3-dioxole/tetrafluoroethylene," Journal of Membrane Science, pp. 1–9, 1995.

[13] H. Teng, "Overview of the Development of the Fluoropolymer Industry," Applied sciences, pp. 1–17, 2012.

[14] S. C. Shit and P. Shah, “A Review on Silicone Rubber,” *Natl. Acad. Sci. Lett.*, vol. 36, no. 4, pp. 355–365, 2013.

[15] Z. Wang, J. Tan, Y. Wang, Z. Liu, and Q. Feng, “Chemical and mechanical degradation of silicone rubber under two compression loads in simulated proton-exchange membrane fuel-cell environments,” *J. Appl. Polym. Sci.*, vol. 136, no. 33, pp. 1–13, 2019.

[16] W. L. Robb, “Thin silicone membranes-their permeation properties and some applications,” *Ann. N. Y. Acad. Sci.*, vol. 146, no. 1 Materials in, pp. 119–137, 1968.

[17] A. Rahimi and A. Mashak, “Review on rubbers in medicine: natural, silicone and polyurethane rubbers,” *Plast. Rubber Compos.*, vol. 42, no. 6, pp. 223–230, 2013.

[18] D. T. Vaimakis-Tsogkas, D. G. Bekas, T. Giannakopoulou, N. Todorova, A. S. Paipetis, and N.-M. Barkoula, “Effect of TiO2 addition/coating on the performance of polydimethylsiloxane-based silicone elastomers for outdoor applications,” *Mater. Chem. Phys.*, vol. 223, pp. 366–373, 2019.

[19] S. Kaur and J. Amrita, “Track Etched Membranes for Electronic Applications,” International Journal of Science and Research (IJSR), pp. 1–4, 2015.

[20] I. V. Korolkov, A. A. Mashentseva, O. Güven, Y. G. Gorin, and M. V. Zdorovets,“Protein fouling of modified microporous PET track-etched membranes,” *Radiat. Phys. Chem.*, vol. 151, pp. 141–148, 2018.

[21] W. Starosta, “Radiation use in producing track-etched membranes,” *Inst. Nucl. Chem. Technol.*, pp. 1–32, 2015.

[22] V. Serini, “Polycarbonates,” in *Ullmann’s Encyclopedia of Industrial Chemistry*, Wiley-VCH Verlag GmbH & Co. KGaA, Ed. Weinheim, Germany: Wiley-VCHVerlag GmbH & Co. KGaA, pp. 1–10, 2000.

[23] N. Onar Camlibel, “Polyester - Production, Characterization and Innovative Applications”, 1st ed. [S.l.]: IntechOpen, pp.1-4, 2018.

[24] L. W. McKeen, “Polyesters,” in *Permeability Properties of Plastics and Elastomers*, Elsevier, pp. 89–106, 2012.

[25] D. A. Beeva, V. A. Borisov, A. K. Mikitaev, M. Kh. Ligidov, A. A. Beev, and E. B. Barokova, “Controlling the Barrier Properties of Polyethylene Terephthalate. A Review,” *Int. Polym. Sci. Technol.*, vol. 42, no. 7, pp. 45–52, 2015.

[26] M. Han, “Depolymerization of PET Bottle via Methanolysis and Hydrolysis,” in *Recycling of Polyethylene Terephthalate Bottles*, Elsevier, pp. 85–108, 2019.

[27] N. S. Korivi, “Preparation, characterization, and applications of poly(ethylene terephthalate) nanocomposites,” in *Manufacturing of Nanocomposites with Engineering Plastics*, Elsevier, pp. 167–198, 2015.

[28] G. Q. Chen, “Water vapor permeation through glassy polyimide membranes and its impact upon carbon dioxide capture operations,” pp. 1–8, 2012.

[29] K. Haraya, T. HAKUTA and, and H. Yoshitome, “of Gases through a New Type Polyimide,” *Process Res. Dev. Div. Natl. Chem. Lab. Ind.*, pp. 1–5, 1986.

[30] E. P. Favvas, F. K. Katsaros, S. K. Papageorgiou, A. A. Sapalidis, and A. Ch. Mitropoulos, “A review of the latest development of polyimide based membranes for CO_2 separations,” *React. Funct. Polym.*, vol. 120, pp. 104–130, 2017.

[31] A. Georgiev, D. Dimov, E. Spassova, J. Assa, P. Dineff, and G. Danev, “Chemical and Physical Properties of Polyimides: Biomedical and Engineering Applications,” in *High Performance Polymers - Polyimides Based - From Chemistry to Applications*, M. Abadie, Ed. InTech, pp. 1–21, 2010.

[32] X. Chen, N. Tien-Binh, S. Kaliaguine, and D. Rodrigue, “Polyimide membranes for gas separation: Synthesis, processing and properties,” in *Polyimides: Synthesis, Applications and Research*, pp. 1–72, 2016.

[33] Shiyu Xu, “Characterisation of mesostructured films and single zeolite nanosheets,” Ph.D dissertation, College of Science and Engineering, Manchester Univ., pp.11-14, 2018.

[34] T. Maesen and B. Marcus, “Chapter 1 The zeolite scene—An overview,” in *Studies in Surface Science and Catalysis*, vol. 137, Elsevier, pp. 1–9, 2001.

[35] J. D. F. Ramsay and S. Kallus, “Zeolite Membranes,” in *Membrane Science and Technology*, vol. 6, Elsevier, pp. 373–395, 2000.

[36] P. Ye, “Zeolite Membrane Separation at Low Temperature,” pp. 1–12, 2016.

[37] S. Kulprathipanja, Ed., *Zeolites in industrial separation and catalysis*. Weinheim: Wiley-VCH, 2010.

[38] C. Rhodes, “The Properties and Applications of Zeolites,” *Sci. Prog.*, vol. 93, pp. 223–84, 2010.

[39] Z. Yuan, X. Zhu, M. Li, W. Lu, X. Li, and H. Zhang, “A Highly Ion-Selective Zeolite Flake Layer on Porous Membranes for Flow Battery Applications,” *Angew. Chem. Int. Ed.*, vol. 55, no. 9, pp. 3058–3062, 2016.

[40] H. O. Ali, “Review of porous anodic aluminium oxide (AAO) applications for sensors, MEMS and biomedical devices,” *Trans. IMF*, vol. 95, no. 6, pp. 290–296, 2017.

[41] R. G. Beri, M. K. Kushwaha, and N. Grover, “A Review on Studies of Mechanical Properties of Anodized Alumina Oxide,” International Research Journal of Engineering and Technology (IRJET), pp. 1–5, 2017.

[42] K. Itaya, S. SUGAWARA, K. ARAI, and S. SAITO, “Properties of porous anodic aluminum oxide films as membranes,” *J. Chem. Eng. Jpn. - J CHEM ENG JPN*, vol. 17, pp. 514–520, 1984.

[43] H. Zhao, L. Liu, and Y. Lei, “A mini review: Functional nanostructuring with perfectly-ordered anodic aluminum oxide template for energy conversion and storage,” *Front. Chem. Sci. Eng.*, vol. 12, no. 3, pp. 481–493, 2018.

[44] H. P. Hsieh, R. R. Bhave, and H. L. Fleming, “Microporous alumina membranes,” *J. Membr. Sci.*, vol. 39, no. 3, pp. 221–241, 1988.

[45] M. Köhler, M. Schardt, M. Rauscher, and A. Koch, “Gas Measurement Using Static Fourier Transform Infrared Spectrometers,” *Sensors*, vol. 17, no. 11, pp. 1–11, 2017.

[46] “Theory_and_Instrumentation of GC Introduction.” [Online]. Available:https://www.chromacademy.com/lms/sco10/Theory_and_ Instrumentation of GC Introduction.pdf. [Accessed: 02-Aug-2019].

[47] Timo Kröger, and Nina Paaso, “Method Development of Gas Analysis with Mass Spectrometer,” *POSIVA.*, pp. 1-101, 2006.

[48] D. Ekeberg, G. Ogner, M. Fongen, E. Joner, and T. Wickstrøm, “Determination of CH4, CO2 and N2O in air samples and soil atmosphere by gas chromatography mass spectrometry, GC-MS,” *J. Environ. Monit. JEM*, vol. 6, pp. 621–3, 2004.

[49] T. Liu, D. Li, J. Chen, Y. Chen, T. Yang, and J. Cao, “Gas-Sensor Drift Counteraction with Adaptive Active Learning for an Electronic Nose,” *Sensors*, vol. 18, p. 4028-4034, 2018.

[50] R. Ghosh, J. W. Gardner, and P. K. Guha, “Air Pollution Monitoring Using Near Room Temperature Resistive Gas Sensors: A Review,” *IEEE Trans. Electron Devices*, vol. 66, no. 8, pp. 3254–3264, 2019.

[51] N. K. Acharya, P. K. Yadav, and Y. K. Vijay, “Study of temperature dependent gas permeability for polycarbonate membrane,” *Indian J. Od Pure Appl. Phsics*, pp. 1–3, 2003.

[52] X. Li, X. Yan, and Y. Kang, “Effect of temperature on the permeability of gas adsorbed coal under triaxial stress conditions,” *J. Geophys. Eng.*, vol. 15, no. 2, pp. 386–396,2018.

[53] “Introduction to RC Circuits [Analog Devices Wiki].” [Online]. Available: https://wiki.analog.com/university/courses/engineering_discovery/lab_2. [Accessed: 03-Aug-2019].

[54] A. Moorjani, D. Straus, and J. Zelenty, “A model of voltage in a resistor circuit and an rc circuit,” pp. 1–15, 2010.

[55] M. A. Z. Raja, A. Mehmood, S. A. Niazi, and S. M. Shah, “Computational intelligence methodology for the analysis of RC circuit modelled with nonlinear differential order system,” *Neural Comput. Appl.*, vol. 30, no. 6, pp. 1905–1924, 2018.

[56] B. Ghanbarian, A. Hunt, R. P. Ewing, and M. Sahimi, “Tortuosity in Porous Media: A Critical Review,” *Soil Sci. Soc. Am. J.*, vol. 77, pp. 2–19, 2013.

[57] B. Tjaden, D. J. L. Brett, and P. R. Shearing, “Tortuosity in electrochemical devices: a review of calculation approaches,” *Int. Mater. Rev.*, vol. 63, no. 2 pp. 47–67, 2018.